Springer Tracts in Mechanical Engineering

Zbyszko Kazimierski
Jerzy Wojewoda

Externally Heated Valve Engine

A New Approach to Piston Engines

Springer

Springer Tracts in Mechanical Engineering

About this Series

Springer Tracts in Mechanical Engineering (STME) publishes the latest developments in Mechanical Engineering - quickly, informally and with high quality. The intent is to cover all the main branches of mechanical engineering, both theoretical and applied, including:

- Engineering Design
- Machinery and Machine Elements
- Mechanical structures and stress analysis
- Automotive Engineering
- Engine Technology
- Aerospace Technology and Astronautics
- Nanotechnology and Microengineering
- Control, Robotics, Mechatronics
- MEMS
- Theoretical and Applied Mechanics
- Dynamical Systems, Control
- Fluids mechanics
- Engineering Thermodynamics, Heat and Mass Transfer
- Manufacturing
- Precision engineering, Instrumentation, Measurement
- Materials Engineering
- Tribology and surface technology

Within the scopes of the series are monographs, professional books or graduate textbooks, edited volumes as well as outstanding PhD theses and books purposely devoted to support education in mechanical engineering at graduate and postgraduate levels.

More information about this series at http://www.springer.com/series/11693

Zbyszko Kazimierski · Jerzy Wojewoda

Externally Heated Valve Engine

A New Approach to Piston Engines

Springer

Zbyszko Kazimierski
Institute of Turbomachinery
Lodz University of Technology
Lodz
Poland

Jerzy Wojewoda
Division of Dynamics
Lodz University of Technology
Lodz
Poland

ISSN 2195-9862 ISSN 2195-9870 (electronic)
Springer Tracts in Mechanical Engineering
ISBN 978-3-319-28354-8 ISBN 978-3-319-28355-5 (eBook)
DOI 10.1007/978-3-319-28355-5

Library of Congress Control Number: 2015958913

Printed on acid-free paper

This Springer imprint is published by SpringerNature
The registered company is Springer International Publishing AG Switzerland

Preface

The main aim of the book is to present development in heat air engines. We attempt to apply an idea of external heating to the piston engine manufactured with well known technology for internal combustion engines. External heating, i.e., delivery of energy from outside in order to create mechanical energy inside the engine, is an extensively developed range of engineering applications, especially in the light of a possibility to use a much wider scope of potential "fuels" than those which can only be burnt inside the engine cylinder. In fact, we intend to use any kind of heat from solar, through burning different fuels to heat generated in the nuclear process. On the other hand, externally heated engines still developing since 1800s exhibit a very complicated and difficult mechanical construction in exploitation, with many wear problems. We propose to employ the standard internal combustion piston engine design which is fed with heat from an external heater to warm up the working fluid which, in turn, employs simple thermodynamic laws interchanging its potential energy into the mechanical one. As in internal combustion piston engines, the working fluid expanding over the moving piston triggers mechanical rotations with torque in the rotating crankshaft, providing thus drive for any machinery.

The idea of air engine which originates from the original Stirling design is entirely different from it. It combines the proven technology of internal combustion engines together with their lubrication system and can be an effective solution not only in the future when most mineral fuels run out but even nowadays as it eliminates problems with lubrication of the mechanism, the main disadvantage of present solutions. Additionally, it can use the cheapest working fluid, the atmospheric air, instead of costly helium or hydrogen. Stability of the heat generation process outside the engine is another advantage of the proposed engine. The work is generated by expansion of hot and compressed air in a cylinder located between two heat exchangers, having extreme temperature and pressure values. A compression ratio considered is about 1:10 although higher values can be reached.

The idea comes back to 1995 and was invented by Lech Brzeski and Zbyszko Kazimierski. An engine, in both 2-stroke and 4-stroke cycles, working in a closed

heat cycle is in some way equivalent to internal combustion engines as energy is generated in similar working loops although heat cycles are different. The idea was confirmed by an experimental model in early 2000s when further development of another prototype stopped due to a lack of financial support. Thus, all our efforts were directed to increase theoretically the heat exchange level which was the main problem detected during tests. We present some ideas which can increase dramatically an amount of heat delivered to the working fluid in the work cycle. In parallel, we have also developed new versions of the engine which have yielded even higher performance characteristics in our simulations and remain within feasible engineering solutions even if some devices are added.

The 4-stroke version of the engine appears to be a very attractive proposition as it applies only a single cylinder. Even such a solution is able to realize a complete thermodynamic cycle. When expanded to a multicylinder design, the advantages are obvious. All proposed 2-stroke versions apply either 2 separate cylinders or a design with double-action pistons. The simulation results show impressive numbers of the power and efficiency generated by the engine – it can reach 50 kW per 1 liter of the working volume at the efficiency equal to about 40 %.

Therefore, we compare these numbers with those available for other, effectively working externally heated engines, where a choice of installations of modern Stirling devices is obvious. The results are promising, especially if air and not helium is applied.

We can expect many possible applications of such a source of mechanical energy worldwide and not only, as space applications are possible as well. In the future, when availability of mineral fuels is limited, such engines can replace internal combustion solutions.

Lodz
November 2015

Zbyszko Kazimierski
Jerzy Wojewoda

Acknowledgement

Professor Lech Brzeski who passed away in 2006 was one of the main inventors of the EHVE. The authors of this book are immensely grateful for His contribution.

The authors would also like to express their thanks to Ms Malgorzata Jozwik for Her efforts in preparing the text for publication.

Contents

Nomenclature

α	Crankshaft angle (rad, deg)
α_A	Heat transfer coefficient (W/m^{2}K)
A	Surface of heat exchange area (m^2)
A_{CE}	Surface of the expander piston (m^2)
A_{CC}	Surface of the compressor piston (m^2)
A_j	Cross-section area of the governed valves (m^2)
c_j	Damping at the j-th valve (Ns/m)
c_p	Specific heat at constant pressure (J/kg K)
c_v	Specific heat at constant volume (J/kg K)
δ_{ME}	Overlapping angle of the valves (rad)
$\Delta\alpha_j$	Increase in the valve angle (rad)
d	Diameter (m)
D	Cylinder diameter (m)
d_j	Diameter of the j-th valve (m)
e_T	Total internal energy (J/kg)
η	Efficiency (%)
η_C	Cycle efficiency (%)
η_{PH}	Efficiency with the pre-heater present (%)
h_B	Enthalpy in the blower (J/kg)
h_{C0}	Clearance under the piston at its lowest position (m)
h_{E0}	Clearance over the position of the expander piston at its upper point (m)
$h_{j,max}$	Maximum lift of the j-th valve (m)
h_{SBi}	Enthalpy isentropic increase of blowers (J/kg)
i_T	Total enthalpy (J/kg)
κ	Isentropic expansion index
k_j	Spring stiffness of the j-th valve (N/m)
L	Mechanical work (J)
l	Length of tubes (m)
λ	Heat conductivity coefficient (W/m K)
$\dot{m}_i$	Mass flow rate (kg/s)
M_v	Mass transported through a valve (kg)

$\dot{m}_{g,i}$	Mass stream of the working fluid in the *i*-th cell (kg/s)
$\dot{m}_T$	Mixing air streams (kg/s)
m_j	Mass of the *j*-th valve (kg)
μ	Dynamic viscosity (kg/m s)
n	Number of heat exchanger tubes (–)
n_H	Number of heater tubes (–)
n	Rotational speed (rpm)
Nu	Nusselt number (–)
n	Unit normal vector
ω	Angular velocity of the crankshaft (rad/s)
Π_B	Output to input pressure ratio for a blower (–)
p	Pressure (Pa)
P	Power (W, kW)
Pr	Prandtl number (–)
$\dot{q}_A$	Surface heat flux density (J/sm^2)
$\dot{q}_V$	Volume heat flux density (J/sm^2)
Q	Heat (J)
$\dot{Q}_A$	Heat stream through the surface area (W)
$\dot{Q}_V$	Heat stream through the volume (W)
ρ	Density (kg/m^3)
R	Specific gas constant (J/kg K)
Re	Reynolds number (–)
s	Stroke (m)
s	Specific entropy (J/kg K)
SC	Settling chambers
S	Entropy (J/K)
t	Time (s)
u	Velocity of the surface (m/s)
T	Temperature (K)
t_{pe}	Period of the engine work (s)
V	Volume (m^3)
v	Absolute velocity (m/s)
w	Relative velocity (m/s)
ζ	Coefficient of losses for the mass flow (–)
B_s	Blowers – B_1, B_2, B_{H1}, B_{H3}, B_{Cl2}, B_{Cl4}
Cl_j	Collectors of the cooler – Cl_2, Cl_4
H_j	Collectors of the heater – H_1, H_4

Subscripts

B	Blower
c	Valve closing
C	Compressor
Cl	Cooler

CS	Averaged compressor mass flow rate
Cs	Crank shaft
E	Expander
ES	Averaged expander mass flow rate
f	Friction
FW	Flywheel
G	Heater radiators
H	Heater
iso	Isochoric
o	Valve opening
PH	Pre-heater
PR	Piston rod
RV	Rotary valve
wCL	Cooler wall
wH	Heater wall

Chapter 1
Introduction

The Externally Heated Valve Engine, further on referred to as the EHVE, and its continuous development are described here. External heating, i.e., when heat energy is delivered from outside, was an important task in designing machines able to generate mechanical energy in different applications. The idea of the EHVE aims at a possible use of any kind of heat coming from, e.g., burning fuels or wastes through solar to nuclear energy. Additionally, as most of historical and present devices applying external heating are technologically complicated, we have decided to apply a typical, well developed piston engine with internal combustion in the EHVE design, which may result in easier implementation of the EHVE. Such a technology involving a piston-cylinder set in connection with a standard crankshaft does not need to resign from typical oil lubrication, which is the main disadvantage of other machines using external heating.

Historically, the very first engine employing external heating was built by Robert Stirling in 1816. He was a Scottish minister who invented the first working closed-cycle air engine. It gave the beginning to a class of engines using hot air, further on developed by other designers. Later, in 1884 Fleeming Jenkin proposed that all such engines should therefore generically be referred to as Stirling engines. The idea has been developed till now with many successful applications [1, 2].

There are numerous works in which experimental results on Stirling or similar externally heated engines using different fuels or even alternative sources of energy are published, e.g., [3–20]. Depending on the particular design, they were intended to reach very different performance levels. The presented applications include some demonstration devices [14], waste heat recovery [21–25], general purpose installations [7, 26], solar heated engines [27], marine applicable [5, 28] and even projects potentially possible to work in the outer space like [29]. Examples of reviews of many published elsewhere solutions can be found in [27, 30, 31]. An interesting summary of the performance of some existing machines is presented in [32]. There are also some experimental results, e.g., [33], which provide a foundation for comparisons to other engines with external heating.

Z. Kazimierski and J. Wojewoda, *Externally Heated Valve Engine*,
Springer Tracts in Mechanical Engineering, DOI 10.1007/978-3-319-28355-5_1

Air-powered engines like the EHVE, which works in a modified Joule cycle, are still developed theoretically, see [34], or practically, e.g., [35].

The working fluid in most modern Stirling engines is helium due to their heat transfer properties, although they are usually very expensive both in manufacturing and maintenance. Their crankshafts have very complex designs and heat regenerators have to be used. Application of internal heat exchangers makes lubrication inside the engine practically impossible. Typical Stirling engines use the pressure ratio of the value approximately equal to 2, whereas the maximal pressure is higher than in the EHVE as it does not need any regenerator.

An early design of the EHVE comes from 1995 and is described in [36], with its later developments reported in [37] and [38]. The working fluid in the EHVE is the cheapest gas available – atmospheric air. All of the EHVE designs allow the ratio of applied pressures, i.e., maximal to minimal values, to be approximately 10, like for internal combustion engines. The maximal pressure designed for the EHVE is approximately 100 bar but along with improvement in the sealing system, it can become higher. Any exchange or replenishment of such a fluid is easy.

Heat energy is delivered to the engine through its heaters, the mechanical energy is produced when the hot fluid expands under high pressure in a cylinder called an expander. Then, it is transferred to the engine cooler for cooling at low pressure. In very early versions of the EHVE, two small heaters were applied, later versions used a larger, single heater with blowers forcing the flow through it. Both the heater and the cooler are heat exchangers that are the outside parts of the EHVE. Taking into account this fact, we assume that the latter are counter-current devices. A simple calculation method where all unknown values are time-dependent only is presented later in this book.

The engines discussed in [36, 37] are similar to that described by Kovacs [39]. The similarity arose by chance, in fact both ideas were developed independently with no knowledge on the other work. However, there are no data or even a type of applied heaters in [39]. For this reason, this engine has not been considered here.

The valve control and the flow of the working fluid inside the EHVE use the well-known technology of internal combustion engines. The first design involving a piston located in a single cylinder is presented in Chap. 2. The engine is composed of four essential parts: an expander, a compressor, a heater and a cooler. The heater in this version consists of two small devices, the cooler uses water as a cooling fluid. This is a 2-stroke engine. The expander is placed over the piston, whereas the compressor – below it. Two of four engine valves are of self-acting type.

Let us remind the main advantage of the EHVE which is the fact that it uses air as the working fluid, a conventional crankshaft and a standard oil lubrication system. The method of general calculations is explained in detail in Chap. 2. The experiments were performed on this version of the EHVE, but its construction was changed slightly. A compact, but difficult to manufacture engine cylinder was altered to a 2-cylinder design given in Chap. 3. The main conclusion that followed from the experimental results was a low level of heat amount delivered to the prototype. Theoretically, the heat transfer coefficient can be calculated for the main assumption of continuous work of the engine. As appeared in the experiment, it was not fully

achieved. Then, the majority of our efforts has been directed to increase a level of heat exchange which is critical for successful operation of the engine. Such a requirement can be fulfilled if some additional devices are applied in the early version of the EHVE. These are a blower and distributors [40]. Another solution to this problem is given in Chap. 4. This is the first step to improve the EHVE.

The next step in developing the EHVE is described in Chaps. 5 and 7. The changes introduced in the engine design were as follows:

- inlet and outlet collectors were added to the numerical model of both heat exchangers and two blowers were introduced,
- a new kind of valve was designed,
- a new, more detailed calculation method was developed as the basis for computer simulations,
- numerical calculations according to the new method were performed for 2- and 4-stroke versions of the EHVE.

The heater was also changed, i.e., a typical design, easy for manufacturing, was applied. All versions of the engine worked in a closed thermodynamic cycle.

A 2-stroke version, which has two blowers, is presented in Chap. 5. It consists of a single heater and a single cooler. Again, this is a typical piston-crankshaft engine. Both the heater and the cooler have some additional volumes, considered here as collectors, which are taken into account. The collector design can be complicated as each of them does not have to influence the flow coming from both the engine and the blowers. This version uses a standard oil lubrication system. The working fluid is air and the cooling fluid is water. The engine was investigated numerically.

The algorithm based on standard numerical integration procedures was applied to a set of differential equations describing the behaviour of individual parts of the engine model. It was supplied with the conditions controlling flows between them. Most of the simulations started from a set of the assumed initial conditions representing initially loaded volumes and constant rotational speed and continued until a stable solution was achieved. More realistic versions of the software covered dynamical behaviour of the numerical model from the start from the zero rotation and an application of a starter. Those calculations continued after reaching the steady rotational speed and all thermodynamic variables stabilization. All equations were written for averaged conditions in particular model elements, treating the problem as time-dependent only.

The type of heat exchangers was simulated as counter-current devices, where the temperature drops remain almost constant along their lengths. The exchangers are treated as time-dependent only, assuming that all important changes are the same and considering each of them in a single plane only. It is situated at the outlet of the exchanger tubes, in both the heater and the cooler, respectively. This approximate approach allows for applying maximal and minimal temperatures of the exchanger walls in the discussed case. The heat volume delivered to and subtracted from the EHVE in the heater and the cooler are estimated accordingly.

Some attempts were made to conduct a more detailed analysis of the heat exchange process taking place inside the exchangers, dividing them into a number of sub-volumes, which was a time-space dependence modelling.

There were attempts aimed at stabilization of the flow inside the exchangers. This included separate settling chambers. A corresponding design of the EHVE is presented in Chap. 6. The way the separated settling chambers are built up is an engineering task, not considered in this book. The main results of the simulations conducted for this design are the values of power and efficiency which are not less than those obtained in the non-steady solution, see Chap. 5.

A 4-stroke version is described in Chap. 7. The experiment involving such a structure of the EHVE is foreseen. Two counter-current heat exchangers, a cooler and a heater, are applied in the engine. Blowers are used in order to increase the volume of heat exchange when the EHVE valves are closed. A disadvantage of this variant of the EHVE is a short period of full opening of the valves from the heater to the expander and from the compressor to the heater.

The valves should have possibilities to fulfil their tasks thanks to some new engineering solutions like rotary valves. The 4-stroke EHVE is an attractive proposition because it applies only one cylinder cover completely the full thermodynamic cycle, similar to internal combustion engines. This fact may be attractive in building multi-cylinder devices.

In order to provide the Reader with a view locating the idea of the EHVE among other modern externally heated engines, a comparison of its expected performance to similar, in terms of volume, Stirling engines, is presented in Chap. 8. As a measure of similarity, maximal pressures of the cycle are assumed and power and efficiency of both types of engines are presented. All data for Stirling installations have been taken from the experimental results.

The EHVE applications can vary broadly, i.e., they can be used at any places located close to sources of heat like dumps of garbage, cooling systems of nuclear reactors in submarines, on ships or yachts, even in the outer space when solar heat is employed. The externally heated engine is an invention to be employed when the existing sources of mineral fuels are exhausted. Prognostics when it happens are different but these fuels have to run out one day. Simultaneously, the amount of wastes is still growing and growing. Garbage will be burnt and, thus, some additional heat energy will be produced. The heat coming from bio-fuels received from plants can also be employed as a fuel. This energy, even not clean enough, can be used in the EHVE. Also, solar or nuclear heat can be employed.

Any party interested in the ideas presented here is invited to further cooperation in developing a working device, which can become a solution to the future problems of effective generation of mechanical energy.

References

1. Walker G (1980) Stirling engines. Clarendon Press, Oxford University, New York
2. Kolin I (1991) Stirling motor: history, theory, practice. Inter University Center, Dubrovnik
3. Watanabe T, Yamaguchi K, Momose Y (1985) 30 kW Stirling Engine. In: Proceedings of the 20th intersociety energy conversion engineering conference. Energy for the twenty-first century, vol 2. Miami Beach, FL, pp 326–331
4. Momose Y, Watanabe T (1986) Testing results of Stirling engine NS30A. In: 3rd International Stirling Engine Conference. Rome, Italy
5. Nilsson H (1988) Submarine power systems using the V4–275R Stirling engine, Archive Proc. IME, Part A: J. Power. Energy 202(41):257–267. doi:10.1243/PIME_PROC_1988_202_036_02
6. Carlsen H, Trærup J, Ammundsen N (1996) 40 kW Stirling engine for solid fuel. In: Proceedings of the 31st Intersociety Energy Conversion Engineering Conference, 1996. Washington, pp 1301–1306. doi:10.1109/IECEC.1996.553904
7. Raggi L, Katsuta M, Isshiki N, Isshiki S (1997) Theoretical and experimental study on regenerative rotary displacer stirling engine. In: Energy Conversion Engineering Conference, 1997. Proceeding of the 32nd IECEC-97, vol. 2, pp. 1017–1022, doi:10.1109/IECEC.1997.661908
8. Iwamoto S, Toda F, Hirata K, Taekuchi M, Yamamoto T (1997) Comparison of low- and high tempearture differential stirling engines. In: Proceedings of 8th International Stirling Engine Conference 1997: pp 29–38
9. Obernberger I, Carlssen H, Biedermann F (2003) State-of-the-art and future developments regarding small-scale biomass chip systems with a special focus on orc and Stirling engine technologies. In: International Nordic Bioenergy Conference, 2003
10. Hirata K, Kawada M (2005) Development of a multi-cylinder Stirling engine. In: Proceedings of 12th international Stirling engine conference, Sept. 2005, pp 315–324
11. Moss RW, Roskilly AP, Nanda SK (2005) Reciprocating Joule-cycle engine for domestic CHP systems. Appl Energy 80(2):169–185. doi:10.1016/j.apenergy.2004.03.007
12. Çinar C, Karabulut H (2005) Manufacturing and testing of a gamma type Stirling engine. Renew Energy 30(1):57–66. doi:10.1016/j.renene.2004.04.007
13. Batmaz I, Üstün S (2008) Design and manufacturing of a V-type Stirling engine with double heaters. Appl Energy 85(11):1041–1049. doi:10.1016/j.apenergy.2008.02.021
14. Scollo L, Valdez P, Barón J (2008) Design and construction of a Stirling engine prototype. Int J Hydrog Energy 33(13):3506–3510. doi:10.1016/j.ijhydene.2007.12.069
15. Karabulut H, Aksoy F, Oztürk E (2009) Thermodynamic analysis of a β-type Stirling engine with a displacer driving mechanism by means of a lever. Renew Energy 34(1):202–208. doi:10.1016/j.renene.2008.03.011
16. Karabulut H, Yücesu HS, Çinar C, Aksoy F (2009) An experimental study on the development of a β-type Stirling engine for low and moderate temperature heat sources. Appl Energy 86(1):68–73. doi:10.1016/j.apenergy.2008.04.003
17. Karabulut H, Çinar C, Oztürk E, Yücesu HS (2009) Torque and power characteristics of a helium charged Stirling engine with a lever controlled displacer driving mechanism. Renew Energy 35(1):138–143. doi:10.1016/j.renene.2009.04.023
18. Sripakagorn A, Srikam C (2011) Design and performance of a moderate temperature difference Stirling engine. Renew Energy 36(6):1728–1733. doi:10.1016/j.renene.2010.12.010
19. Abbas M, Boumeddane B, Said N, Chikouche A (2011) Dish Stirling technology: A 100 MW solar power plant using hydrogen for Algeria. Int J Hydrog Energy 36(7):4305–4314. doi:10.1016/j.ijhydene.2010.12.114
20. Gheith R, Aloui F, Ben Nasrallah S (2012) Optimization of Stirling engine performance based on an experimental design approach. Int J Energy Res 37(12):1519–1528. doi:10.1002/er.2964
21. Mehta AV, Gohil RK, Bavarva JP, Saradava BJ (2012) Waste heat recovery using Stirling engine. Int J Adv Eng Technol 3(1):305–310 http://www.technicaljournalsonline.com/ijeat/VOL20III/IJAET20VOL20III20ISSUE20I20JANUARY20MARCH202012/6820IJAET20Vol20III20Issue20I202012.pdf

22. Ramesh US, Kalyani T (2012) Improving the efficiency of marine power plant using Stirling engine in waste heat recovery systems. Int J Innov Res Dev 1(10):449–466 http://www.ijird.com/index.php/ijird/article/view/34969/28166
23. Harrod J, Mago PJ, Luck R (2012) Sizing analysis of a combined cooling, heating, and power system for a small office building using a wood waste biomass-fired Stirling engine. Int J Energy Res 36(1):64–74. doi:10.1002/er.1782
24. Song Z, Chen J, Yang L (2015) Heat transfer enhancement in tubular heater of Stirling engine for waste heat recovery from flue gas using steel wool. Appl Therm Eng 87:499–504. doi:10.1016/j.applthermaleng.2015.05.028
25. Aladayleh W, Alahmer A (2015) Recovery of exhaust waste heat for ICE using the beta type Stirling engine, J Energy (2015) ID 495418. doi:10.1155/2015/495418
26. Brzeski L, Kazimierski Z (2001) Experimental investigation of externally heated valve engine model, Proc Inst Mech Eng A J Power Energy 215(4):486–494. doi:10.1243/0957650011538749
27. Kongtragool B, Wongwises S (2003) A review of solar-powered Stirling engines and low temperature differential Stirling engines. Renew Sustain Energy Rev 7(2):131–154. doi:10.1016/S1364-0321(02)00053-9
28. Hirata K, Kagawa M (2005) Discussion of Marine Stirling Engine System. In: Proceeding of 7th International Symposium of Marine Engineering, Tokyo, 2005. https://www.nmri.go.jp/eng/khirata/list/stirling/isme2005.pdf
29. Cassady RJ, Frisbee RH, Gilland JH, Houts MG, LaPointe MR, Maresse-Reading CM, Oleson SR, Polk JE, Russell D, Sengupta A (2008) Recent advances in nuclear powered electric propulsion for space exploration. Energy Convers Manag 49(3):412–435. doi:10.1016/j.enconman.2007.10.015
30. Thombare DG, Verma SK (2008) Technological development in the Stirling cycle engines (Review). Renew Sustain Energy Rev 12(1):1–38. doi:10.1016/j.rser.2006.07.001
31. Tlili I, Musmar SA (2013) Thermodynamic evaluation of a second order simulation for Yoke Ross Stirling engine. Energy Convers Manag 68:149–160. doi:10.1016/j.enconman.2013.01.005
32. Iwamoto S, Hirata K, Toda F (2001) Performance of Stirling Engines. JSME Int J Ser B 44(1):140–147 https://www.nmri.go.jp/eng/khirata/list/ecoboy/jsmepaper_eng2001.pdf
33. Watanabe T et al. (1988) NS30A Stirling engine for heat pump use. In: The 4th International Conference on Stirling Engines, Tokyo, 1988
34. Lontsi F, Hamandjoda O, Fozao K, Stouffs P, Nganhou J (2013) Dynamic simulation of a small modified Joule cycle reciprocating Ericsson engine for microcogeneration systems. Energy 63:309–316. doi:10.1016/j.energy.2013.10.061
35. Xu Q, Cai M, Shi Y (2014) Dynamic heat transfer model for temperature drop analysis and heat exchange system design of the air-powered engine system. Energy 68:877–885. doi:10.1016/j.energy.2014.02.102
36. Brzeski L, Kazimierski Z (1995) New type of heat engine—externally heated air engine. In: SAE Technical Papers Series Paper 950092, International Congress and Exposition, Detroit, Michigan, Feb 27-March 2, 1995. doi:10.4271/950092
37. Brzeski L, Kazimierski Z (1995) Computer simulation of a new type heat engine operation. Comput Assist Methods Eng Sci 2(2):129–139
38. Brzeski L, Kazimierski Z (1996) A new concept of externally heated engine—comparisons with the Stirling engine. Proc Inst Mech Eng Part A, J Power Energy 210(51):363–371. doi:10.1243/PIME_PROC_1996_210_060_02
39. Kovač A (1980) Les moteurs volumétriques á cycle fermé: une vioe peu prospecteé dans le redéploiement énérgetique. Entropie 16(92):23–30
40. Kazimierski Z, Wojewoda J (2011) Externally heated valve air engine with two small heaters operating alternatively. In: Proceeding of SYMKOM 2011, Turbomachinery, vol 140. pp 105–114

Chapter 2
Early Design of the EHVE – Calculation Method and Thermodynamic Cycle

The EHVE operation has been explained in the Introduction, whereas the first publications devoted to this idea are [1, 2]. Besides, this design has been presented in [3, 4]. The experimental investigations published in [5] refer to a slightly altered early version of the EHVE, already mentioned in the Introduction, which will be presented in detail in Chap. 3.

2.1 Principle of the Early EHVE Operation

The early EHVE is shown in Fig. 2.1. It is composed of four essential parts: an expander, a compressor, a heater and a cooler. This is a 2-stroke engine. The volume over the piston is called an expander and that under it – a compressor.

A principle of the engine operation is shortly described below. If the piston starts to move downwards from its upper position, governed valve 1 opens and a high pressure working fluid flows from the heater to the expander, expanding during the further piston movement. At the same time, the fluid contained in the volume of the compressor (below the piston) is compressed. When the pressure in the compressor reaches the level of that in the discharged heater, self-acting valve 3 opens and the fluid exchange in the heater starts. Then, the governed valve closes and further compression of the working fluid in the heater is caused by the piston movement downwards until it reaches its lowest position. Here, valve 3 closes and the process of isochoric heating begins in the heater volume. The piston starts to move up, governed valve 2 opens and the fluid contained in the expander is pushed out to the cooler, simultaneously self-acting valve 4 opens and the cold fluid flows into the compressor from the cooler. Finally, the piston reaches its upper position, all valves are closed and the engine cycle is completed.

Z. Kazimierski and J. Wojewoda, *Externally Heated Valve Engine*,
Springer Tracts in Mechanical Engineering, DOI 10.1007/978-3-319-28355-5_2

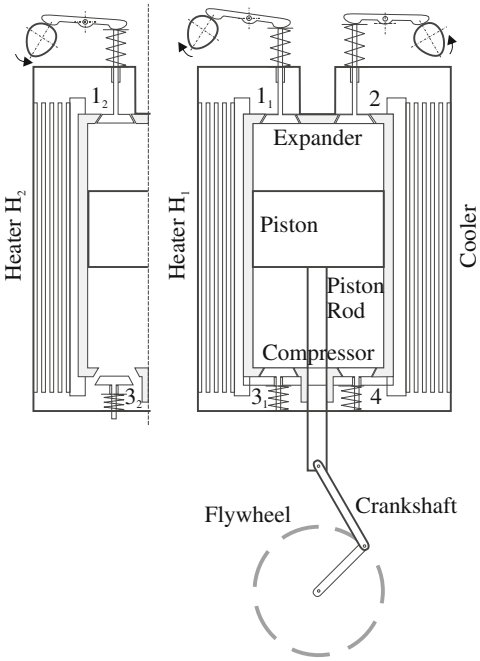

Fig. 2.1 Schematic diagram of the engine, *1*, *2* governed valves, *3*, *4* self-acting valves

The working air heating period can be prolonged if more than a single heater is used. Two such devices, working commutatively, are employed in the engine version under discussion. The heater H_1 is connected to the cylinders with a set of valves 1_1 and 3_1 and the heater H_2 with another set of valves 1_2 and 3_2. Besides, both cylinders use valves 2 and 4 connecting them to the cooler volume.

2.2 Basic Equations of the Theoretical Model

The flow of the working fluid in the closed cycle of the engine work is governed by the following set of equations – the energy and mass conservation equation and the equation of state. Here, this set is written for one of the heaters. The equations of energy and mass are formulated for the migrating volume V_U surrounded by the moving closed surface A_U. The local velocity of the surface $\mathbf{u}$ can vary from zero, the assumed control surface, to the velocity of fluid elements $\mathbf{v}$, assumed as the fluid surface. The relative velocity of the fluid flowing through the moving surface is denoted as $\mathbf{w} = \mathbf{v} - \mathbf{u}$.

The energy equation takes the form

$$\frac{\mathrm{d}}{\mathrm{d}t}\left(\iiint_{V_U} e_T \rho \,\mathrm{d}V_U\right) = -\iint_{A_U} i_T \rho \mathbf{wn}\,\mathrm{d}A_U - \iint_{A_U} \mathbf{nu} p \,\mathrm{d}A_U + \overbrace{\iint_{A_U} \dot{q}_A \,\mathrm{d}A_U}^{\dot{Q}_A} + \overbrace{\iiint_{V_U} \dot{q}_V \,\mathrm{d}V_U}^{\dot{Q}_V}, \tag{2.1}$$

where e_T – total internal energy, i_T – total enthalpy, $\mathbf{n}$ – unit normal vector, $\dot{q}_A$, $\dot{q}_V$ – surface and volume heat flux densities, respectively.

The equation of mass conservation has the form as follows

$$\frac{\mathrm{d}}{\mathrm{d}t}\left(\iiint_{V_U} \rho \,\mathrm{d}V_U\right) = -\iint_{A_U} \rho \mathbf{wn}\,\mathrm{d}A_U. \tag{2.2}$$

Finally, the equation of state is expressed as

$$p = \rho T (c_p - c_v). \tag{2.3}$$

It is assumed that the kinetic energy of the fluid inside the volumes of the engine elements is very low when compared to its internal energy, and Eqs. (2.1)–(2.3) will be solved taking mean values of the specific heats c_p and c_v in the range of temperatures and pressures of the engine cycle. The surface heat flux $\dot{Q}_A$ is determined with the local heat transfer coefficient α_A. The details of the α_A determination are given in the further part of this section devoted to the heater operation modelling.

Additionally, it is assumed that the fluid parameters are only time-dependent. As regards the cylinder, it is obvious but in the case of the heater and the cooler, it will be explained below. The heater and the cooler are assumed as counter-current heat exchangers, where temperature drops almost continuously along their lengths. We assume that all important changes in the heater and the cooler are the same along them. The collectors of heat exchangers are not taken into account as they are included in their volumes.

An exception to this assumption will be introduced separately for the heater further on. The mass and energy streams specified on the RHS of Eqs. (2.1) and (2.2) can be rewritten in the form

$$c_v \frac{\mathrm{d}\,(T \rho V_U)}{\mathrm{d}t} = -\sum_{j=1}^{J} c_p T_j \underbrace{(\rho \mathbf{vn} A_U)_j}_{\dot{m}_j} - p\frac{\mathrm{d}V_U}{\mathrm{d}t} + \sum_{l=1}^{L} \underbrace{(\dot{q}_A A_U)_l}_{\dot{Q}_A} + \dot{Q}_V, \tag{2.4}$$

$$\frac{\mathrm{d}\,(\rho V_U)}{\mathrm{d}t} = -\sum_{j=1}^{J} \underbrace{(\rho \mathbf{vn} A_U)_j}_{\dot{m}_j}, \tag{2.5}$$

where $\dot{m}_j$ are mass flow rates passing through valves ($j = 1, 2$ for the expander, $j = 3, 4$ for the compressor, and $j = 1, 3$ for the heater, correspondingly) and only one small heater is considered now.

The mass flow rates $\dot{m}_j$, $j = 1, 2, 3, 4$, are calculated according to the known gas dynamics formulae supplemented by the coefficient which defines the effective valve cross-section flow areas determined empirically for a given valve geometry and flow conditions [1–3]. The formulae for $\dot{m}_j$ are stated for quasi-stationary treatment of the air flow through valves. The set for $\dot{m}_j$ has to be solved always with the current values of pressures and temperatures in selected elements of the engine. This set of equations is employed in simulations of the working fluid flow through the engine elements. The numerical models of the expander, the compressor, the heater and the cooler are presented in the subsections below.

2.3 Modelling Operation of the Engine Parts

2.3.1 Expander

The unknown variables for the expander are as follows: the pressure p_E, the temperature T_E and the density ρ_E. The time-dependent volume of the expander comes from the simple geometry

$$V_E(t) = A_{CE}\left(h_{E0} + \frac{s}{2}(1 - \cos\,\omega t)\right) \tag{2.6}$$

where d_C is cylinder diameter, h_{E0} – clearance over the position at its upper point, s – piston stroke and the cross-section area is defined by $A_{CE} = \frac{\pi d_C^2}{4}$. The angular velocity of the crankshaft is ω.

The current value of the crankshaft angle is denoted by $\alpha = \omega t$ and the cross-section area of governed valves is described by the formula

$$A_j(\alpha) = \frac{A_{j\,max}}{2}\left(1 - \cos\pi\frac{\alpha - \alpha_{j,k}}{\Delta\alpha_{j,k}}\right). \tag{2.7}$$

The subscript k ($k = o, c$) determines the moment of the jth valve opening ($k = o$) and closing ($k = c$). $A_{j\,max}$ is the maximal value of the jth valve cross-section area and $\Delta\alpha$ is the angle determining the time of A_j variation from 0 to $A_{j\,max}$.

It is assumed for the expander that the heat produced inside the cylinder by friction forces is transferred out through the cooled walls of this cylinder, which can be described as

$$\dot{Q}_A + \dot{Q}_V = 0. \tag{2.8}$$

This is an approximation because $\dot{Q}_V$ contains not only friction effects but also a small amount of the heat transferred with hot fluid during the expansion phase.

The set of Eqs. (2.3)–(2.5) applied to the expander can be presented in the form

$$p_E = \rho_E T_E (c_p - c_v), \tag{2.9}$$

$$\frac{\mathrm{d}T_E}{\mathrm{d}\alpha} = \frac{1}{\omega \rho_E V_E}\left(\dot{m}_1(\kappa T_H - T_E) - \dot{m}_2(\kappa - 1)T_E - \frac{\omega p_E}{c_v}\frac{\mathrm{d}V_E}{\mathrm{d}\alpha}\right), \tag{2.10}$$

$$\frac{\mathrm{d}\rho_E}{\mathrm{d}\alpha} = \frac{1}{\omega V_E}\left(\dot{m}_1 - \dot{m}_2 - \rho_E \omega \frac{\mathrm{d}V_E}{\mathrm{d}\alpha}\right). \tag{2.11}$$

The algebraic formulae for modelling the flows $\dot{m}_1$ and $\dot{m}_2$ (and consequently $\dot{m}_3$ and $\dot{m}_4$ discussed in the next subsection) are built with Bernoulli and continuity equations for the working fluid. This attempt includes losses determined below by the coefficients ζ_j, $j = 1, \ldots, 4$. The equation for these rates is as follows

$$\dot{m}_j = \frac{\zeta_j A_j p_b}{\sqrt{R T_b}}\left(\frac{p_a}{p_b}\right)^{\frac{1}{\kappa}} \sqrt{\frac{2\kappa}{\kappa - 1}\left[1 - \left(\frac{p_a}{p_b}\right)^{\frac{\kappa-1}{\kappa}}\right]} \quad \text{for } j = 1, 2, 3, 4. \tag{2.12}$$

The above formula takes into account the ratio of pressures on both sides of any valve, p_a and p_b. If

$$\frac{p_a}{p_b} \le \left(\frac{2}{\kappa + 1}\right)^{\frac{\kappa}{\kappa-1}}, \tag{2.13}$$

then Eq. (2.12) takes a different form

$$\dot{m}_j = \frac{\zeta_j A_j p_b \sqrt{\kappa}}{\sqrt{R T_b}}\left(\frac{2}{\kappa + 1}\right)^{\frac{\kappa+1}{2(\kappa-1)}}. \tag{2.14}$$

In such an attempt, the flows through the valves are treated as the quasi-stationary ones. The $\dot{m}_j$ values depend on the surrounding pressures, temperatures and valve cross-sections $A_j(\alpha)$. The equation of conservation described here does not take into account the so called inverse flow between the engine parts. Such a flow is impossible in the case of self-acting valves. After a careful analysis, it is also possible to set opening and closing times of the governed valves in the way which allows for avoiding any return flow through them. The values of the coefficients of losses ζ_j were assumed to be equal to 0.85, cf. [6], as typical in similar designs. It should be mentioned that flows through valves cause also different dynamic effects, which apart from the mentioned losses, are not included in modelling. If the high speed behaviour of wave generation is to be included, any changes have to include very high velocity ranges estimated as 400–800 m/s along the length of heat exchangers. Their length is assumed to be equal to 2 m at maximum, a travelling wave can cover it many times

within a single cycle of work. Therefore, our quasi-static attempt to modelling shows an averaged behaviour and such a detailed description would change also some minor characteristics and not the general view of the cycle. In slow speed engines like the EHVE, dynamic effects are usually inconsiderable, the expected Mach number is low if compared to the value when dynamic effects prevail over the static ones.

We need to calculate the pressures p_a and p_b and the temperatures T_a, T_b on both sides of all valves as

$$\begin{aligned}
&\text{for valve 1 :}\\
&\text{if } p_H > p_E \ : \ p_b = p_H, \quad T_b = T_H, \quad p_a = p_C, && \text{(2.15a)}\\
&\text{if } p_E > p_H \ : \ p_b = p_E, \quad T_b = T_E, \quad p_a = p_H, && \text{(2.15b)}\\
&\text{for valve 2 :}\\
&\text{if } p_E > p_{Cl} \ : \ p_b = p_E, \quad T_b = T_E, \quad p_a = p_{Cl}, && \text{(2.15c)}\\
&\text{if } p_{Cl} > p_E \ : \ p_b = p_{Cl}, \quad T_b = T_{Cl}, \quad p_a = p_E, && \text{(2.15d)}
\end{aligned}$$

In the above equations values of temperatures and pressures in heat exchangers are considered as those related to cooperating elements. This averaged attempt does not include any non-stationary behaviour in the close vicinity of the valves. When such effects are included, it is followed by qualitative only and not quantitative changes.

2.3.2 Compressor

The unknown variables for the compressor are as follows: the pressure p_C, the temperature T_C and the density ρ_C. The time-dependent compressor volume is, similarly to the expander, denoted as

$$V_C(t) = A_{CC}\left(h_{C0} + \frac{s}{2}(1 + \cos \omega t)\right), \tag{2.16}$$

where $A_{CC} = \frac{\pi}{4}\left(d_C^2 - d_{PR}^2\right)$, d_{PR} – piston rod diameter (Fig. 2.1), h_{C0} – clearance under the piston at its lowest position.

The mass flow rates $\dot{m}_3$ and $\dot{m}_4$ through self-acting valves 3 and 4 are calculated similarly as for the governed valves [1]. However, their cross-section areas are calculated simultaneously during the engine operation process, because A_3 and A_4 clearly depend on pressures in the compressor p_C, the heater P_H and the cooler p_{Cl}. In the case of these valves, the pressures p_a and p_b and the temperatures T_a, T_b on both sides of all valves are as follows

Table 2.1 Physical data of the self-acting valves

Valve No.	Mass m_i (kg)	Spring stiffness k_i (N/m)	Damping coefficient c_i (Ns/m)	Max. lift h_i (m)	Diameter d_i (m)
3	0.0755	5000	15.75	0.0074	0.030
4	0.0755	5000	15.75	0.0074	0.030

$$\text{for valve 3 :}$$

$$\text{if } p_C > p_H : \; p_b = p_C, \quad T_b = T_C, \quad p_a = p_H, \tag{2.17a}$$

$$\text{if } p_H > p_C : \text{no flow}, \tag{2.17b}$$

$$\text{for valve 4 :}$$

$$\text{if } p_C > p_{Cl} \; : \text{ no flow}, \tag{2.17c}$$

$$\text{if } p_{Cl} > p_C \; : \; p_b = p_{Cl}. \quad T_b = T_{Cl}, \quad p_a = p_C, \tag{2.17d}$$

The self-acting valve movement is determined with an additional set of differential equations, taking into account the inertia of its movable parts. Each mass is supported by a spring and viscous damping is also introduced into its model. For the self-acting valves, we assume the data shown in Table 2.1.

The angle of valve 3 opening $\alpha_{3,0}$ is determined from the condition

$$p_C \geq p_H$$

and similarly, $\alpha_{4,0}$ from

$$p_C \geq p_{Cl}.$$

Also for the compressor, it is assumed that

$$\dot{Q}_A + \dot{Q}_V = 0.$$

As a result, we get the following set of equations describing the working fluid inside the compressor volume

$$\frac{\mathrm{d}T_C}{\mathrm{d}\alpha} = \frac{1}{\omega \rho_C V_C}\left(\dot{m}_4(\kappa T_{Cl} - T_C) - \dot{m}_3(\kappa - 1)T_C - \frac{\omega p_C}{c_v}\frac{\mathrm{d}V_C}{\mathrm{d}\alpha}\right), \tag{2.18}$$

$$\frac{\mathrm{d}\rho_C}{\mathrm{d}\alpha} = \frac{1}{\omega V_C}\left(\dot{m}_4 - \dot{m}_3 - \rho_C \omega \frac{\mathrm{d}V_C}{\mathrm{d}\alpha}\right), \tag{2.19}$$

$$p_C = \rho_C T_C (c_p - c_v). \tag{2.20}$$

The algebraic formulae for the flows $\dot{m}_3$ and $\dot{m}_4$ are given when the pressures p_C, p_H, p_{Cl}, temperatures and the actual cross-section values $A_j(\alpha)$ are calculated together.

2.3.3 Cooler

The cooler volume is much higher than the volumes of other engine parts. Taking into account the isobaric model of the working fluid, the cooling process under the constant pressure p_{Cl} is assumed. The fluid mass contained in the cooler is almost constant. The pressure p_{Cl} is the lowest, basic pressure of the engine cycle. There exists a link between p_{Cl} and the total fluid mass enclosed in all engine volumes $V_E + V_C + V_H + V_{Cl}$ for a given rotational frequency. The level of the basic pressure p_{Cl} is controlled by introducing the proper total mass of the working fluid into the engine volumes before it starts. The cooler works as a stationary heat exchanger, which causes the working fluid temperature drop from $T_{E\,min}$ to T_{Cl}, which is the temperature of the fluid at the compressor inlet, the pressure p_{Cl} is assumed constant in this version of the EHVE.

2.3.4 Heater

The unknown variables for the heater are: the pressure p_H, the temperature T_H and the density ρ_H. They depend on time and space. The heater volume V_H is assumed constant. The surfaces surrounding V_H are not mobile. The heat generation connected with the friction forces acting inside the heater $\dot{Q}_{VH}$ is neglected as it is very inconsiderable when compared to the heat flux $\dot{Q}_{AH}$ delivered to the heating fluid. In the range of the crankshaft angle rotation $\alpha \geq \alpha_{3,o}$, after opening of valve 3, the working fluid exchange occurs. The hot fluid flowing into the expander is pushed out by a comparatively cool fluid coming from the compressor.

The next issue concerns the heaters H_1 and H_2, generally referred to as heaters. In this stage of the development of the EHVE, we considered two different models of the heater system. The first model treats thermodynamic parameters of the heater as time-dependent only. This assumption allows the treatment which will be explained later. The other one divides the heater volume into n sub-volumes which transfer the working fluid from one to another and different averaged conditions are met in each of them. Thus, the number of differential equations describing the state of any heater increases by $2n$ but the solution is expected to be more accurate. The second model takes into account a dependence of its parameters on time and space, which is the tube length.

The first heater operational model will be considered now. It is treated as a counter-current heat exchanger where changes of its parameters are almost constant along its length. This allows one to calculate its changes in a single plane, as being time-dependent only. This plane is chosen at the outlet of the heater.

For the first model in the range $\alpha_{1,o} \leq \alpha \leq \alpha_{3,c}$, when valves 1 and 3 are open, the heat flux $\dot{Q}_{AH}$ delivered through the heater surface area

$$A_H = n_H \pi d_H l_H,$$

(n_H is here a number of tubes of the diameter d_H and the length l_H) is described by the equation

$$\dot{Q}_{AH} = \alpha_A A_H (T_{w_H} - T_H), \tag{2.21}$$

where T_{wH} is the heater wall temperature. The heat transfer coefficient α_A is determined as a function of the Nusselt number Nu, i.e.,

$$\alpha_A = \frac{\mathrm{Nu}\lambda_H}{d_H},$$

The current value of the Nusselt number is varying as $\mathrm{Nu} = f(\mathrm{Re}, \mathrm{Pr})$. Values of λ, Re and Pr are the heat conductivity, the Reynolds and Prandtl numbers, respectively, all for the air flowing inside the heater tubes. The values of the specific heat c_p, the viscosity μ and the above quoted λ used in the calculations of Re and Pr numbers are taken as averaged values of these parameters in the range of temperatures and pressures occurring for $\alpha_{1,o} \leq \alpha_{3,c}$. The velocity of the working fluid inside the tubes necessary for determination of the Reynolds number has also been taken as the mass averaged value for $\alpha_{1,o} \leq \alpha \leq \alpha_{3,c}$. Any unsteadiness of the flow inside the tubes which can cause an increase in α_A is not included in this procedure.

The basic equations of state, energy and mass for the first model of the heater operation derived from Eqs. (2.3)–(2.5) take the following form for the range of the rotation angles $\alpha_{1,o} \leq \alpha \leq \alpha_{3,c}$

$$\frac{\mathrm{d}T_H}{\mathrm{d}\alpha} = \frac{1}{\omega \rho_H V_H} \left(\dot{m}_3 (\kappa T_C - T_H) - \dot{m}_1 (\kappa - 1) T_H + \frac{\dot{Q}_{AH}}{c_v} \right), \tag{2.22}$$

$$\frac{\mathrm{d}\rho_H}{\mathrm{d}\alpha} = \frac{1}{\omega V_H} (\dot{m}_3 - \dot{m}_1), \tag{2.23}$$

$$p_H = \rho_H T_H (c_p - c_v). \tag{2.24}$$

For $\alpha = \alpha_{3,c}$, the H_1 heater volume is closed. The density of the fluid inside the heater H_1 is constant and the heat transfer is assumed as isochoric. This period of heating lasts for the first heater till the end of the running cycle and during the whole next cycle, it means until $\alpha = 4\pi$. At the value $\alpha = 2\pi$, the heating period of the second heater H_2 is finished and it is switched into the engine operation. The next period begins for $\alpha = 2\pi$, valves 1_2 and 3_2 work in the range $360° \leq \alpha \leq 540°$. Then, for the heater H_2, isochoric heating lasts until 1080°. It is assumed that during the isochoric process of heating, a kind of whirl movement of the air inside the heater tubes takes place. The experimental investigations of the prototype, which

were performed a few years later, show, however, the fact that the amount of heat delivered to the engine in real conditions was insufficient. The value of the heat transfer coefficient $\alpha_{A,iso}$, which was expected to be 1200 W/m^{2}K, was much lower. For a solution of this problem, see Chap. 4.

When the isochoric process begins at α_{3c}, the equation of continuity yields $\rho_{H,iso} = \text{constant}$. This value can be calculated from the equation of state for α_{3c}, e.g.,

$$\rho_{H,iso} = \frac{p_H(\alpha_{3c})}{T_H(\alpha_{3c})R},$$

then,

$$M_{H,iso} = \rho_{H,iso} V_H, \tag{2.25}$$

where the mass locked in the heater is $M_{H,iso}$. In [1, 2], Eq. (2.21) was used, hence the value of $\alpha_{A,iso}$ is applied in this equation.

We do not know what type of flow would appear during the isochoric process, thus we use a general formula

$$\dot{Q}_{iso} = M_{H,iso} c_v \left(T_H - T_H(\alpha_{3,c})\right) \frac{\omega}{\alpha}. \tag{2.26}$$

The EHVE has to work continuously and therefore

$$T_H(4\pi) = T_H(0).$$

We can calculate the value of α_A from the equality of Eqs. (2.21) and (2.26)

$$\alpha_A = \frac{M_{H,iso} c_v \left(T_H - T_H(\alpha_{3,c})\right) \frac{\omega}{\alpha}}{A_H(T_{wH} - T_H)}. \tag{2.27}$$

For $\alpha_{3,c} \leq \alpha \leq 4\pi$ at the engine rotational speed of 1500 rpm, the value of α_A should be about 1200 W/m^{2}K if the condition of the continuous work of the engine is to be assured. This was not confirmed in the experiment performed.

The pressure is calculated also from the isochoric formula

$$p_H(\alpha) = p_H(\alpha_{3,c}) \frac{T_H(\alpha)}{T_H(\alpha_{3,c})}. \tag{2.28}$$

The second model of the heater constitutes a certain modification of the first one. It has been assumed that the pressure is the same in the whole volume of the heater and the solution for $p_H(\alpha)$ is taken from the first model and α_A assures continuous work of the engine. The amount of heat delivered to the working fluid is the same in both models. The characteristic feature of the second model is such that the whole space of the heater $V_H(\alpha)$ is divided into n elementary control volumes and the temperature differences not only in time but also along the heater tube length are determined. The elementary control volumes and the elementary heating surfaces are

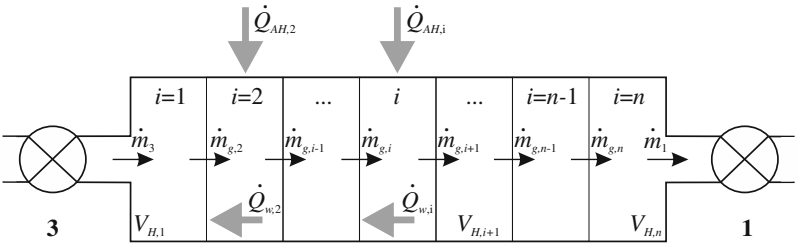

Fig. 2.2 Schematic diagram of the heater divided into n elementary control volumes

$$V_{H,i} = \frac{V_H}{n}, \qquad A_{H,i} = \frac{A_H}{n}. \tag{2.29}$$

A scheme of the heater division into the elementary volumes and the nomenclature used are explained in detail in Fig. 2.2.

Solutions to the equations of temperatures $T_{H,i}(\alpha)$, $i = 1, 2, \ldots, n$ are received on the basis of the following set of energy conservation equations

$$\begin{aligned}
\frac{\mathrm{d}T_{H,1}}{\mathrm{d}\alpha} &= \frac{1}{\omega\rho_{H,1}V_{H,1}}\left(\dot{m}_3(\kappa T_C - T_{H,1}) - \dot{m}_{g,2}(\kappa-1)T_{H,1} + \frac{\dot{Q}_{w,1}}{c_v} + \frac{\dot{Q}_{AH,1}}{c_v}\frac{\rho_{H,1}}{\rho_H}\right),\\
&\text{for the first cell}: \ i = 1\\
\frac{\mathrm{d}T_{H,i}}{\mathrm{d}\alpha} &= \frac{1}{\omega\rho_{H,i}V_{H,i}}\left(\dot{m}_{g,i}(\kappa T_{H,i-1} - T_{H,i}) - \dot{m}_{g,i+1}(\kappa-1)T_{H,i} + \frac{\dot{Q}_{w,i}}{c_v} + \frac{\dot{Q}_{AH,i}}{c_v}\frac{\rho_{H,i}}{\rho_H}\right),\\
&\text{for the } i\text{−th cell}: \ i = 2, 3, \ldots, n-1,\\
\frac{\mathrm{d}T_{H,n}}{\mathrm{d}\alpha} &= \frac{1}{\omega\rho_{H,n}V_{H,n}}\left(\dot{m}_{g,n}(\kappa T_{H,i-1} - T_{H,n}) - \dot{m}_1(\kappa-1)T_{H,n} + \frac{\dot{Q}_{w,n}}{c_v} + \frac{\dot{Q}_{AH,n}}{c_v}\frac{\rho_{H,n}}{\rho_H}\right),\\
&\text{for the } n\text{−th cell}: \ i = n.
\end{aligned} \tag{2.30}$$

The density of the working fluid in each cell is calculated from

$$\rho_{H,i} = \frac{p_H(\alpha)}{T_{H,i}(c_p - c_v)}. \tag{2.31}$$

The density ρ_H used in Eqs. (2.30) is the same as the one defined in the first model. Additionally, it can be determined by the formula

$$\rho_H = \sum_{i=1}^{n} \frac{\rho_{H,i}V_{H,i}}{V_H}. \tag{2.32}$$

The internal mass flow rates between the cells are calculated from the equation of mass conservation for each of the volumes

$$\dot{m}_{g,i} = \dot{m}_{g,i-1} - \omega V_{H,i-1} \frac{\mathrm{d}\rho_{H,i-1}}{\mathrm{d}\alpha}, \quad \text{for } i = 1, 2, \ldots, n, \tag{2.33}$$

where $\dot{m}_{g,i-1} = \dot{m}_3$ for $i = 1$ at the heater inlet.

The heat fluxes $\dot{Q}_{AH,i}$ for a single cell are calculated from the formula analogous to Eq. (2.21), i.e.,

$$\dot{Q}_{AH,i} = \alpha_A A_{H,i} (T_{wH} - T_{H,i}), \tag{2.34}$$

where α_A is calculated according to the procedure applied in the first model.

For the isochoric process in the locked volume, i.e., in the range $\alpha_{3,c} \leq \alpha \leq 4\pi$, additional heat fluxes $\dot{Q}_{w,i}$ between cells caused by the above-mentioned whirl motion are introduced. These heat streams are proportional to the assumed local mass flow rates $\dot{m}_T(\alpha)$ of the fluid circulating between cells, hence we have the following set of equations

$$\begin{aligned} \dot{Q}_{w,1} &= \dot{m}_T(\alpha) c_p (T_{H,2} - T_{H,1}), && \text{for: } i = 1, \\ \dot{Q}_{w,i} &= \dot{m}_T(\alpha) c_p (T_{H,i-1} - 2T_{H,i} + T_{H,i+1}), && \text{for: } i = 2, 3, \ldots, i-1, \\ \dot{Q}_{w,n} &= \dot{m}_T(\alpha) c_p (T_{H,n-1} - T_{H,n}), && \text{for: } i = n. \end{aligned} \tag{2.35}$$

The mixing air streams $\dot{m}_T(\alpha)$ are the same for all cells and diminish in time according to the formula

$$\dot{m}_T(\alpha) = \dot{m}_T(0) \mathrm{e}^{-\frac{\Delta T}{\omega}(\alpha - \alpha_{3,c})}. \tag{2.36}$$

The exponent value determines the intensity of $\dot{m}_T(\alpha)$, diminishing in time.

The heater is a counter-current heat exchanger in the models. Unfortunately, the heat exchange in the range of isochoric heating described in Chap. 3 entails a rather painful conclusion that the heat exchange in this range was insufficient. For this reason, the model assumed in Chap. 3 should be changed to yield the flows in heater tubes of the Reynolds number higher by 10^4 at least. The first attempt to achieve this is made in Chap. 4.

2.4 Engine Power and Efficiency

The mechanical work produced or consumed in the range of $\alpha_A \leq \alpha \leq \alpha_B$ by the expander is expressed by the formula

$$L_{E\,A-B} = \int_{\alpha_A}^{\alpha_B} p_E(\alpha) \frac{\mathrm{d}V_E}{\mathrm{d}t} \frac{\mathrm{d}\alpha}{\omega}, \tag{2.37}$$

the current value of varying $\frac{\mathrm{d}V_E}{\mathrm{d}t}$ comes from the derivation of Eq. (2.6).

The compressor work in the range of $\alpha_A \leq \alpha \leq \alpha_B$ is determined with a similar formula

$$L_{C\,A-B} = \int_{\alpha_A}^{\alpha_B} p_C(\alpha) \frac{\mathrm{d}V_C}{\mathrm{d}t} \frac{\mathrm{d}\alpha}{\omega}, \tag{2.38}$$

and the current value of $\frac{\mathrm{d}V_C}{\mathrm{d}t}$ is calculated from the derivative of Eq. (2.16).

The sum of these two parts represents the work for the whole cycle $0 \leq \alpha \leq 2\pi$

$$L_{E+C} = L_{E0-2\pi} + L_{C\,0-2\pi}. \tag{2.39}$$

Now, we can define the power created in the engine as

$$P = \frac{\omega}{2\pi} L_{E+C}. \tag{2.40}$$

The amount of heat introduced by the heater in the range of $\alpha_{1,o} \leq \alpha \leq \alpha_{3,c}$ is calculated by the following integral

$$Q_{H\,I} = A_H \int_{\alpha_{1,o}}^{\alpha_{3,c}} \alpha_A \left(T_{wH} - T_H\right) \frac{\mathrm{d}\alpha}{\omega}. \tag{2.41}$$

For the range of $\alpha_{3,c} \leq \alpha \leq 4\pi$, when isochoric heating takes place in the closed volume of H_1, the amount of the delivered heat is

$$Q_{H\,II} = c_v M_H \left(\alpha_{3,c\,iso}\right) \left(T_H(4\pi) - T_H\left(\alpha_{3,2}\right)\right), \tag{2.42}$$

where $M_H(\alpha_{3,c})$ is the constant amount of air mass closed in the heater during the isochoric heating period. The next cycle of the EHVE begins when valves 1_2 and 3_2 are open at $2\pi \leq \alpha \leq 3\pi$. Then, heating of the H_2 heater starts at 3π and continues until 6π. The temperature $T_H(4\pi)$ should be close to $T_H(0)$ if the heat delivered to the EHVE is sufficient, as has been assumed here. The total amount of heat delivered during the cycle to the working fluid is a sum of

$$Q_H = Q_{H\,I} + Q_{H\,II}. \tag{2.43}$$

Finally, the engine cycle efficiency is calculated as a ratio of amounts of the generated work to the delivered heat

$$\eta_C = \frac{L_{E+C}}{Q_H}. \tag{2.44}$$

The engine cycle efficiency calculated according to Eq. (2.44) does not take into account yet mechanical losses caused mainly by friction between piston rings and cylinders. These losses can consume up to 10 % of the generated engine power. Therefore, the work and power calculated according to Eqs. (2.39) and (2.40), respectively, can be determined as indicative only.

2.5 Thermodynamic Cycle of the Early EHVE

This cycle is elaborated numerically in [3]. The thermodynamic cycle of a new type of the heat engine has been presented in the traditional coordinate systems: $p - \frac{1}{\rho}$ (pressure – specific volumes), Fig. 2.3, and $T - s$ (temperature – specific entropy), Fig. 2.4. The cycle is determined on the basis of the solution to the energy and mass conservation equations and the equation of state.

These diagrams are only illustrative and they give a general view to the engine heat cycle character. The mechanical work gained and the heat delivered during the cycle is calculated on the basis of the numerical solution to the presented set of model equations.

For this version of the EHVE, the timing of the valves is chosen in such a way that it is foreseen that valves 1 and 3 slightly overlap, [1, 3]. In Fig. 2.3, a simple $p - \frac{1}{\rho}$ diagram of the engine thermodynamic cycle for a single heater obtained from the values read from the results of numerical simulations is presented. The essential assumption for this diagram is

$$T_H(4\pi) = T_H(0).$$

The $T - s$ and $p - \frac{1}{\rho}$ diagrams for the engine heat cycle are depicted as a kind of an envelope formed by means of loops illustrating the operation of the engine parts, i.e., the compressor, the heater, the expander and the cooler. The loops present the thermodynamic state of the air remaining inside the volumes of the above-mentioned engine parts, although the mass of the air in these volumes changes within very wide limits (except for the cooler).

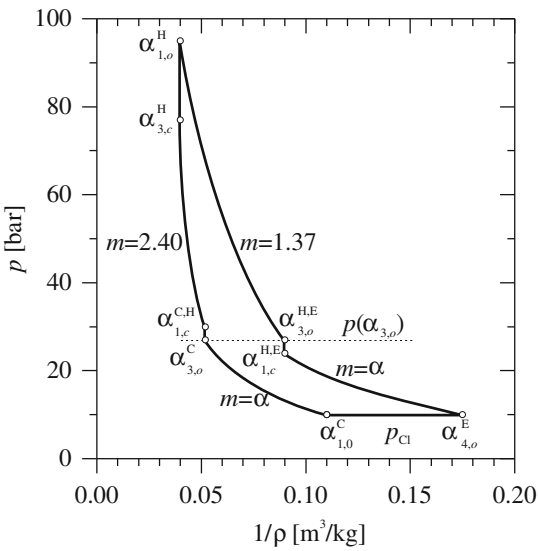

Fig. 2.3 $p - \frac{1}{\rho}$ diagrams of the engine thermodynamic cycle

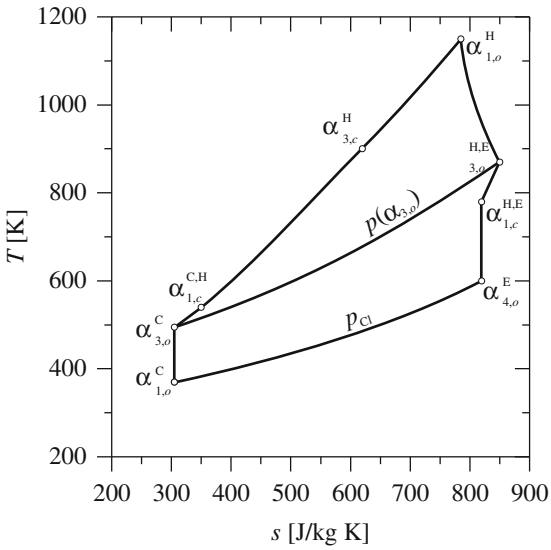

Fig. 2.4 $T - s$ diagram of the engine thermodynamic cycle

The $T - s$ diagram from Fig. 2.4 for the engine thermodynamic cycle is plotted in the way presented below. The diagram starts from the point $\alpha^C_{1,o}$ of the compressor – see the left bottom point on the diagram. Then, isentropic compression to the point $\alpha^C_{3,o}$ takes place. For $\alpha > \alpha^C_{3,o}$, the air flows through valve 3 from the compressor to the heater and is compressed and heated there. Therefore, the substitutive processes for the compressor-heater assembly should connect the point $\alpha^C_{3,o}$ of the compressor with the point $\alpha^H_{3,c}$ of the heater, cf. Fig. 2.3. The first part of this substitutive process lies between the points $\alpha^C_{3,o}$ and $\alpha^{C,H}_{1,c}$. It is assumed that this part of the process is nearly isochoric because volumes of the compressor, the heater and the expander are connected with one another. The second part of the substitutive process from $\alpha^{C,H}_{1,c}$ to $\alpha^H_{3,c}$ has a form of the polytrope with the compression index $m \approx 2.40$, again we recall Fig. 2.3. Then, isochoric heating is observed from the point $\alpha^H_{3,c}$ to the point $\alpha^H_{1,o}$ of the heater. The substitutive process for the heater-expander assembly runs from the point $\alpha^H_{1,o}$ of the heater to a certain point situated between the points $\alpha^H_{3,o}$ of the heater and $\alpha^E_{3,o}$ of the expander on the isobar $p(\alpha_{3,o})$, see Fig. 2.4. This point is denoted by $\alpha^{H,E}_{3,o}$. The process from $\alpha^H_{1,o}$ to $\alpha^{H,E}_{3,o}$ can be modelled by a polytrope with the expansion index $m \approx 1.37$. Then, a nearly isochoric process between the substitutive point $\alpha^{H,E}_{3,o}$ and the substitutive point $\alpha^{H,E}_{1,c}$ is assumed. The reason for this assumption is the same as for the compressor-heater assembly. The positions of $\alpha^{H,E}_{3,o}$ and $\alpha^{H,E}_{1,c}$ are determined taking into account the air mass in the heater and expander volumes for $\alpha = \alpha_{3,o}$ and $\alpha_{1,c}$, respectively. The point $\alpha^{H,E}_{1,c}$ lies on the isentrope, illustrating thus an expansion in the closed cylinder of the expander. The lowest point of this expansion is determined by the point $\alpha^E_{4,o}$, which is situated on the isobar p_{Cl}. The isobar p_{Cl} connects the point $\alpha^E_{4,o}$ and the point $\alpha^C_{1,o}$, closing

the engine cycle. If isochoric heating were insufficient, the EHVE would have to be further developed.

For better understanding of the attempt undertaken in our considerations for modelling of the engine work, we have assumed the working fluid to have properties of ideal gas. This is of course a simplification but the results obtained without using it show only some quantitative and not qualitative differences.

Let us consider the process taking place inside the compressor volume when it is closed and all changes are forced by the movement of the piston, $\dot{m}_j = 0$. The equation of energy conservation (2.18) in this case can be written as

$$\mathrm{d}T_C = -\frac{1}{\rho_C V_C}\frac{p_C}{c_V}\mathrm{d}V_C, \tag{2.45}$$

whereas the equation of mass conservation (2.19) can take the form

$$\frac{\mathrm{d}\rho_C}{\rho_C} = -\frac{\mathrm{d}V_C}{V_C}. \tag{2.46}$$

From Eqs. (2.45) and (2.46) we get the relation

$$c_V \frac{\mathrm{d}T_C}{T_C} = R\frac{\mathrm{d}\rho_C}{\rho_C}, \tag{2.47}$$

which presents no increase in entropy. Then, after some transformations, with $R = c_p - c_V$, we get

$$\frac{\mathrm{d}T_C}{T_C} = (\kappa - 1)\frac{\mathrm{d}\rho_C}{\rho_C}. \tag{2.48}$$

The above equation can be finally transformed to

$$\frac{\mathrm{d}p_C}{p_C} = \kappa\frac{\mathrm{d}\rho_C}{\rho_C}, \tag{2.49}$$

which describes a differential form of an isentropic process inside the closed compressor volume. A similar discussion can be conducted for the expander. During the further development of the model, a corresponding attempt is undertaken in Sect. 5.3. for the improved version of the EHVE.

The $T - s$ and $p - \frac{1}{\rho}$ diagrams for a new type of the externally heated engine show that the cycle is composed of 8 processes – 2 isentropes, 3 isochores, 1 isobare and 2 polytropes. The presented diagrams have only an illustrative character and are discussed on the basis of the numerical solution to the set of the governing equations presented. Both diagrams are given for comparisons with the corresponding thermodynamic drawings illustrating the cycles of other known heat engines.

2.6 Results of the Simulations of the Early EHVE

The second part of the heat $Q_{H,II}$ is calculated with Eq. (2.42). An example of the engine subject to the presented computer simulations has the cylinder volume of 1 L with the data shown in Table 2.2, whereas the piston rod volume is ignored. For the heat exchangers, the data presented in Table 2.3 have been assumed, both the heaters H_1 and H_2 are here taken into account.

For all of the governed valves, the maximal flow area values are $A_{j\,max} = 7 \times 10^{-4}\,\mathrm{m}^2$. The data for the self-acting valves have already been given in Sect. 2.3.2. Additionally, there was an assumption of the required overlapping value of valves 1 and 3, $\delta_{ME} = \alpha_{1,2} - \alpha_{3,0} = 12°$. The engine rotational speed was set to $n = 1500\,\mathrm{rpm}$.

A wide discussion on the engine power and the efficiency η_C determined according to formulae (2.40) and (2.44) as functions of the angular velocity ω, the heater volume V_H and its wall temperature T_{wH} for the cooler pressure $p_{Cl} = 10\,\mathrm{bar}$ has been presented in [1]. The preliminary optimization of the engine cycle for that value of cooler pressure shows that the power of 30 kW per 1 L of cylinder volume at 1500 rpm and the efficiency level η of about 38 % can be obtained, if the amount of heat delivered is satisfactory. For continuous operation, the following relationship should be held

$$T_H(4\pi) = T_H(0),$$

for the first heater, and

$$T_H(6\pi) = T_H(2\pi)$$

for the second one. All the results presented below are based on this assumption. Figures 2.5 and 2.6 present periodic solutions to the problem within one engine cycle for $p_{Cl} = 10$ and 30 bar, respectively. The first model of the heater operation has

Table 2.2 Dimensions of the engine cylinders

Cylinder	Diameter d (m)	Stroke s (m)	Dead height h_0 (m)
Expander	0.13	0.0753	0.0050
Compressor	0.13	0.0753	0.0120

Table 2.3 Dimensions of the heat exchangers

Exchanger	Diameter d (m)	Length l (m)	Number of pipes n (−)	Exchange area A_H (m^2)	Volume V (m^3)
Heater H	0.008	0.4	20	0.2	0.33×10^{-3}
Cooler Cl					5.00×10^{-3}

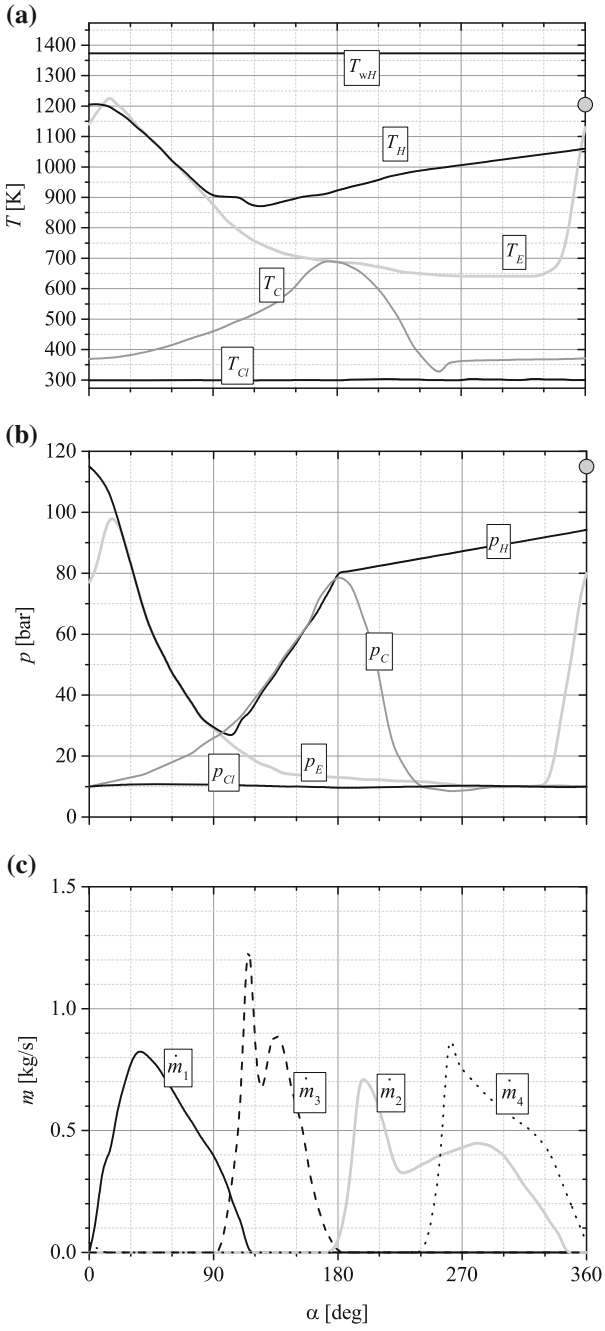

Fig. 2.5 Diagrams of **a** temperatures, **b** pressures and **c** valve mass flow rates as functions of the crankshaft angle α for the cooler pressure $p_{Cl} = 10\,\text{bar}$ and heating at $T_{wH} = 1373\,\text{K}$. Other important parameters were $T_{Cl} = 363\,\text{K}$, $V_H = 0.33 \times 10^{-3}\,\text{m}^3$, $n = 1500\,\text{rpm}$, $\delta_{ME} = 12°$ according to the first heater model. The circles in parts **a** and **b** show the final parameters of the heater H_2 at 360°

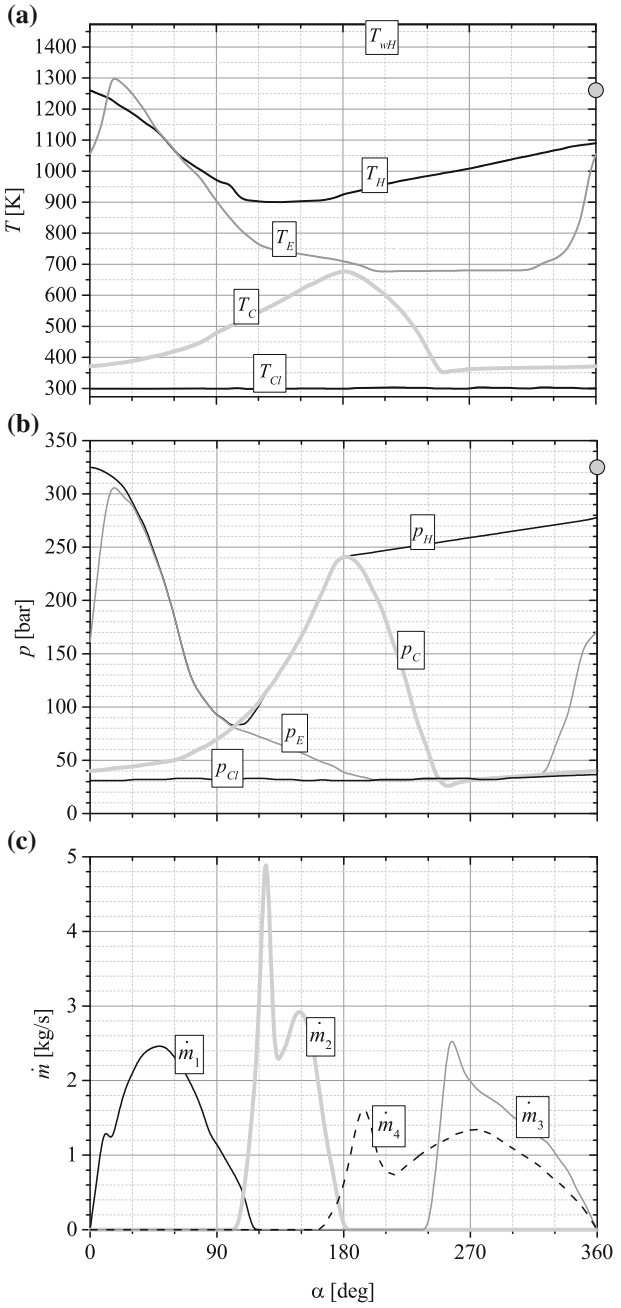

Fig. 2.6 Diagrams of **a** temperatures, **b** pressures and **c** valve mass flow rates as functions of the crankshaft angle α for the cooler pressure $p_{Cl} = 30$ bar and heater wall temperature $T_{wH} = 1473$ K. Other important parameters were $T_{Cl} = 363$ K, $V_H = 0.33 \times 10^{-3}$ m^3, $n = 1500$ rpm, $\delta_{ME} = 12°$ according to the first model. The circles in parts **a** and **b** show the final parameters of the heater H_2 at 360°

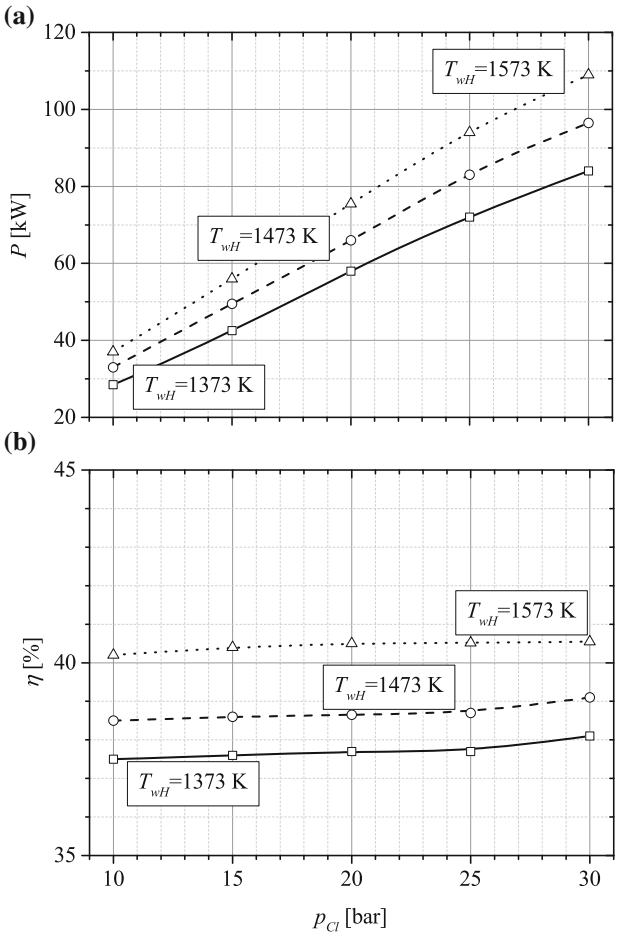

Fig. 2.7 Diagrams of the engine power P, (**a**), and and the efficiency, η_C (**b**) as functions of the cooler pressure p_{Cl} for the different heating wall temperatures $T_{wH} = 1373$, 1473 and 1573 K

been employed in this calculation. In both figures, the action of the second heater is marked with circles at the end of the cycle as the heaters switch off in this point.

The next task of this section is to determine the engine power and efficiency according to Eqs. (2.40) and (2.44) for a higher value of the basic pressure of the cycle, i.e., the one in the cooler. We assume this increase from 10 up to 30 bar, and for the results see Fig. 2.7a, b. There is a well pronounced, almost linear increase in power values for both the cooler pressure and the heater wall temperatures, respectively. The obtained efficiency values remain almost constant for the considered range of the cooler pressure p_{Cl} and yield rather flat horizontal lines. However, a significant increase from about 37 % to almost 41 % occurs when the heater wall temperature increases from 1373 to 1573 K. The discussed output parameters of the engine model

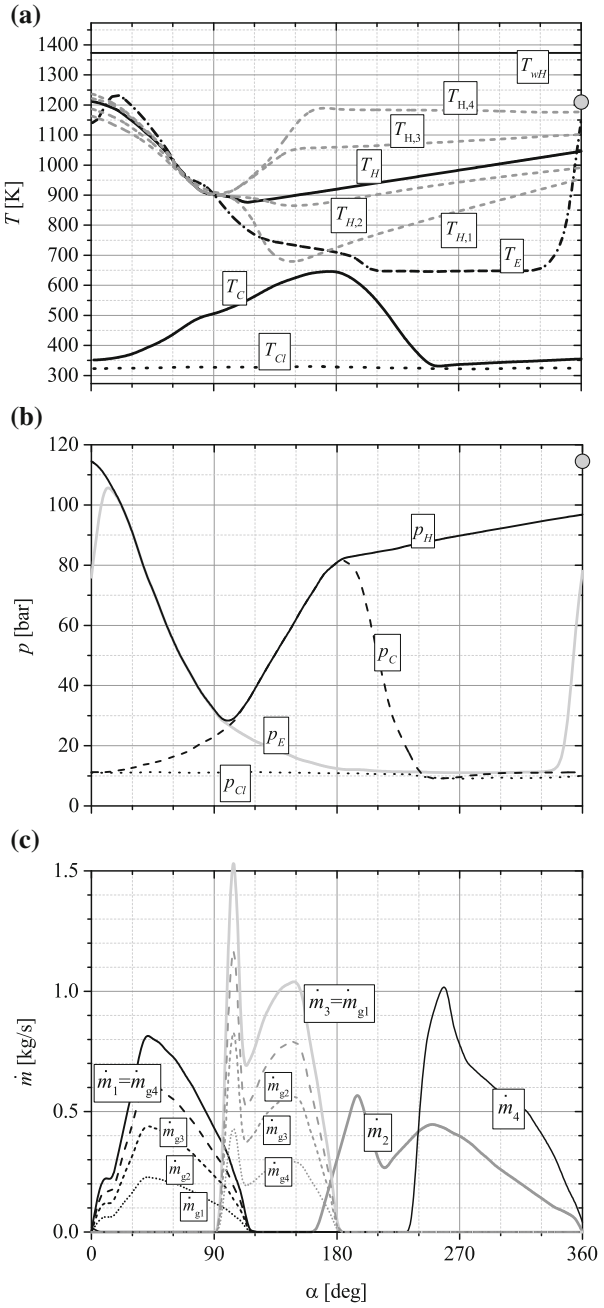

Fig. 2.8 Diagrams of **a** temperatures, **b** pressures and **c** valve mass flow rates as functions of the crankshaft angle α: $p_{Cl} = 10\,\text{bar}$, $T_{Cl} = 363\,\text{K}$, $T_{wH} = 1373\,\text{K}$, $V_H = 0.33 \times 10^{-3}\ \text{m}^3$, $n = 1500\,\text{rpm}$, $\delta_{ME} = 12°$. The temperatures T_H and the mass flow rates $\dot{m}_{g,i}$ are shown for $n = 4$ according to the second heater model. The circles in parts **a** and **b** show the final parameters of the heater H_2 at 360°

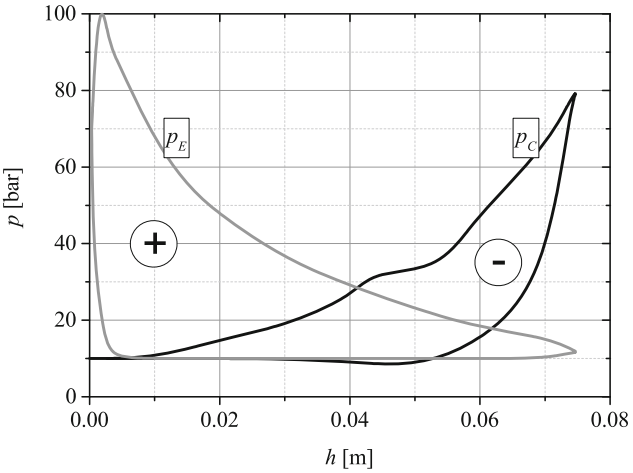

Fig. 2.9 Diagrams of the expander and compressor pressures as functions of the piston positions h according to the first model of the heaters, where $0 \leq h \leq s$, (p_C and p_E are taken from Fig. 2.5)

are calculated without taking into account any mechanical losses which exist in the real device, so these parameters are rather indicative, and not effective values.

Nevertheless, the power of about 100 kW per 1 L of the engine cylinder volume, which is theoretically achieved for $p_{Cl} = 30$ bar and $T_{wH} = 1473$ and 1573 K, (Fig. 2.7), shows that the presented engine performance can be potentially close to those achieved by best recently made internal combustion piston engines. The results definitely depend on an amount of the heat delivered to the EHVE. Once more, it is underlined that these are only theoretical results, $\alpha_A \geq 1200$, taking into account a very inconsiderable isochoric heating process, proven experimentally later and mentioned earlier in this chapter and formerly in [5].

The second model of the heater, which is an improved version of the first one, allows for estimation of spatial differences in the heater temperature during the engine cycle. A very simple example of such calculations has been performed according to the description presented in the previous section. The heater volume has been divided into only four parts, $n = 4$, for better clarity of the presentation of the idea. The results of the temperature distribution are shown in Fig. 2.8a. The pressures in respective elements are depicted in the part (b) and the mass flow rates are given in the part (c). When we compare this figure to Fig. 2.5, the character of all pressures is preserved, while both the temperatures and the mass flow rates present much more detailed characters, respectively. On average, the cell heater model simplifies the behaviour of that which is not divided into parts.

An important illustration of pressures inside the compressor and the expander as functions of the piston position h is depicted in Fig. 2.9. These relations can be used for calculations of the EHVE power as indicated by the + and − signs within both the expander and compressor volumes, respectively.

Two small heaters H_1 and H_2 are employed in this version of the EHVE. For a long time, as discussed above, their volumes are closed and only an isochoric heating process takes place inside their volumes.

Unfortunately, the experimental investigations described next in Chap. 3 show that isochoric heating is too poor for the EHVE to operate efficiently. Then, all of the above presented results exhibit mostly a theoretical character only as they were obtained with the numerical simulations based on the assumption that the heat delivered to the engine model was sufficient. With respect to this fact, the idea of the EHVE presented until now needs further improvements by replacing the isochoric heating process with a more effective one.

The first attempt is described in Chap. 4. Other, entirely different approaches are to be found in Chaps. 5–7.

References

1. Brzeski L, Kazimierski Z (1995) New Type of Heat Engine – Externally Heated Air Engine. In: SAE Technical Papers Series Paper 950092. International Congress and Exposition. Detroit, Michigan. doi:10.4271/950092 27 Feb–2 March 1995
2. Brzeski L, Kazimierski Z (1995) Computer simulation of a new type heat engine operation. Comput. Assist Methods Eng Sci 2(2):129–139
3. Kazimierski Z, Brzeski L, Wojewoda J (1995) Thermodynamical cycle of a new type of the externally heated engine. Arch Thermodyn 16(3–4):197–215
4. Kazimierski Z, Brzeski L (2000) Construction and investigation of a new type heat engine. Report on Project 113/T10/97/13 for the State Committee for Scientific Research. (In Polish)
5. Brzeski L, Kazimierski Z (2001) Experimental investigation of externally heated valve engine model. Proc Inst Mech Eng A J Power Energy 215(4):48694. doi:10.1243/0957650011538749
6. Dejc ME, Zaranin AE (1984) Gasodynamics. Energoizdat Press, Leningrad. (In Russian)

Chapter 3
Experimental Investigations of the EHVE

As already mentioned in the Introduction, the experiment was carried out on a modified variant of the early version of the EHVE. Instead of a single, compact cylinder as the one depicted in Fig. 2.1, two parallel cylinders were applied.

Those investigations were mainly focused on:

- confirmation of the operating abilities of the prototype;
- examination of the agreement between the measured and theoretically calculated variations of pressures inside volumes of the expander and the compressor;
- verification if the heat supply to the engine was sufficient.

3.1 Prototype of the EHVE

The experimental investigations with a prototype of the EHVE were carried out in the years in 1998–1999 and their results were published in [1]. They have remained unique till now.

The principle of operation of this version of the EHVE assumes that volumes of the heat supplying the exchanger and both working cylinders are similar. Owing to this, satisfactory engine power can be achieved, see [2–4]. Kovacs [5] in his proposed engine assumed that the working cylinder was located between two large-volume heat exchangers, a heater and a cooler. It means that, contrary to the engine discussed here, only a single large volume of the heater was used. Any experimental results for the engine described in [5] have not been known until now.

The idea of the EHVE requires a relatively short opening time of valve 1 in order to attain a high compression ratio inside the working cylinder. The timing gear dynamics may cause problems in such a case of valve operation, so a specific design is needed. In the prototype, the volume of the applied cylinders $V_C = 432.8\,\mathrm{cm}^3$ is determined by availability of ready made pistons of the diameter 83 mm. The stroke

Z. Kazimierski and J. Wojewoda, *Externally Heated Valve Engine*,
Springer Tracts in Mechanical Engineering, DOI 10.1007/978-3-319-28355-5_3

of the engine is designed to be 80 mm. All the remaining dimensions, including the heaters, have to assure their final volume proportional to that of the cylinder.

Such a limited volume of the heat exchanger and a directly related moderate value of the surface of heat exchange requires an increase in heat transfer, especially during the period when the heater space remains cut off from the engine cylinders, i.e., valves 1 and 3 are closed. For experimental purposes, two types of heaters were prepared, namely:

- an annular heater with inlet channels possessing spiral ducts in order to generate a whirl motion inside,
- a multi-hole heater with a custom-formed heat exchange surface.

Both heaters are schematically shown in Fig. 3.1a, b. As heat sources, electrical radiators were used in that stage of experiments due to their availability.

An effective technical solution of the annular heater generating a whirl motion is complicated and would involve much more financial means than it was available within the framework of that stage of the prototype investigations. The measured effect of a spiral air motion inside the annular heater was rather moderate and both types of applied heaters demonstrated a very similar and not high level of effectiveness. The heat exchangers were fed with a working fluid, the atmospheric air, delivered from the space located over the compressor piston through hot, curvilinear pipes. As a result, any fouling of the heater surfaces by the lubricant used in the engine did not take place. A standard oil pump was used as in typical internal combustion engines.

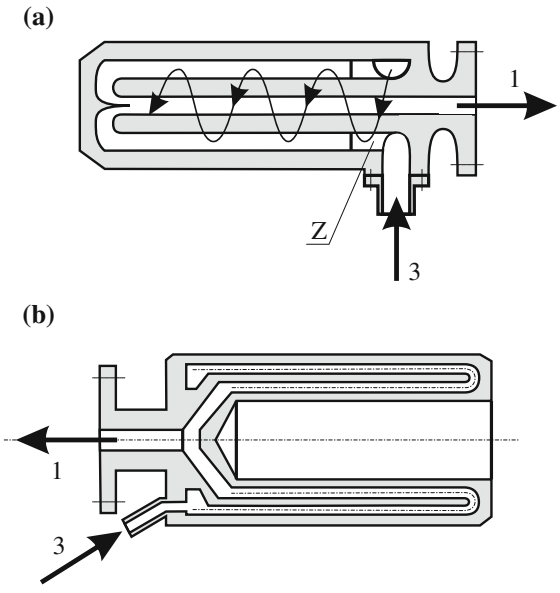

Fig. 3.1 Scheme of the heaters: **a** annular heater with a whirl air motion caused by elements *Z*; **b** multi-hole heater

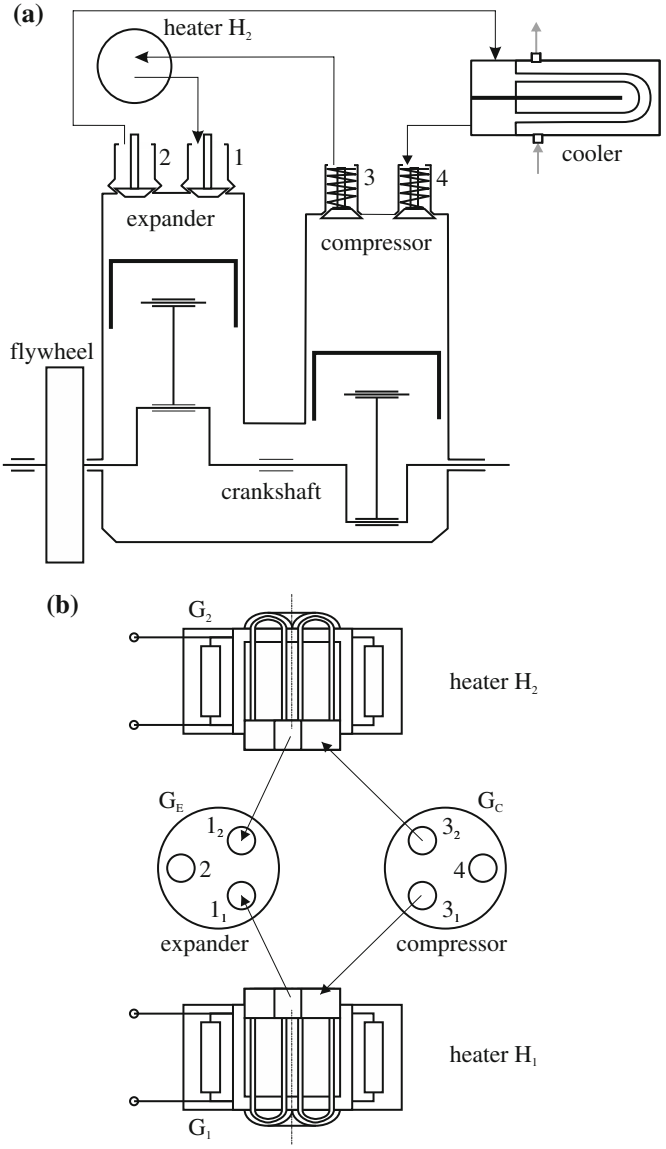

Fig. 3.2 **a** Scheme of the engine model related to the vertical cross-section; **b** scheme of the expander and compressor heads, G_E and G_C, with the location of valves 1_1, 1_2 and 3_1, 3_2 and *2* and *4*, the heaters H_1, H_2, the radiators G_1, G_2 and connections of the heaters with valves 1_1, 1_2 and 3_1, 3_2. The angles of the opening of valves 1_1, *2*, 3_1 and *4* are 0°, 170°, 100° and 225°, respectively. The angles of the closing of valves 1_1, *2*, 3_1 and *4* are 108°, 346°, 180° and 360°, correspondingly

As mentioned above, in that stage of the prototype testing, only the electrical radiators G_1, G_2, see Fig. 3.2b were used as heat sources in the heat exchange process. Both of them were commercial devices and were characterized by the nominal electric power of 5955 W each. Their dimensions fit the heater H_1, H_2 dimensions and were as follows: the inner/outer diameters equal to 150/350 mm, respectively, and the length of 220 mm. Their power is related to the above geometrical values. The working temperature of the heating radiators G_1, G_2 was controlled automatically by means of a microprocessor control system.

A general view of the engine prototype with radiators removed and without any measuring apparatus is presented in Fig. 3.3. The space underneath the pistons was not pressurized at the engine test start. The sealing system is identical to that used in any conventional internal combustion engine. Figure 3.4 shows an engine equipped with the electrical radiators G_1 and G_2, a flywheel, a starter and a supplementary compressor Cr with an air tank. For testing purposes, a sliding vane oil pump was used as the engine brake, i.e., external load simulation.

An upper view into the engine head side with a valve cam governing system exposed is presented in Fig. 3.5. It was custom made but the design is similar to solutions met in most of internal combustion engines. In Fig. 3.6, other views of the top of the EHVE are shown, in part (a), an engine head can be seen from the rear side. In part (b), a system controlling the governed valve by means of the teeth belt is presented.

The other EHVE heat exchanger, i.e., the cooler applied during the experiments, has the form of a U-tube and a large volume when compared to the heaters. It used

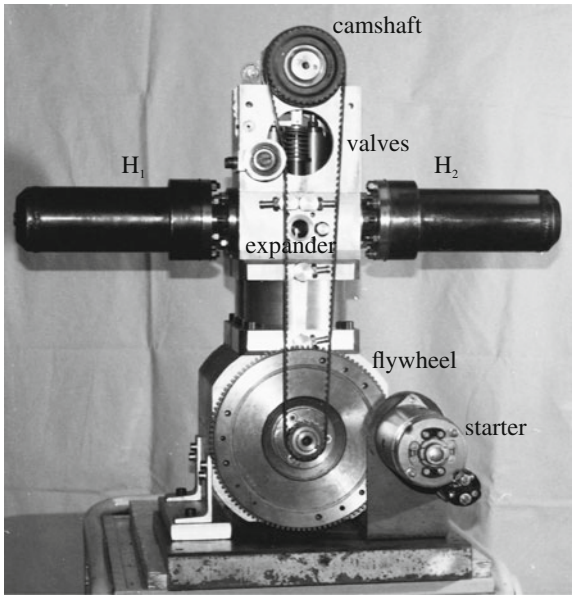

Fig. 3.3 General view of the engine prototype without electrical radiators and apparatus, H_1, H_2 – heaters

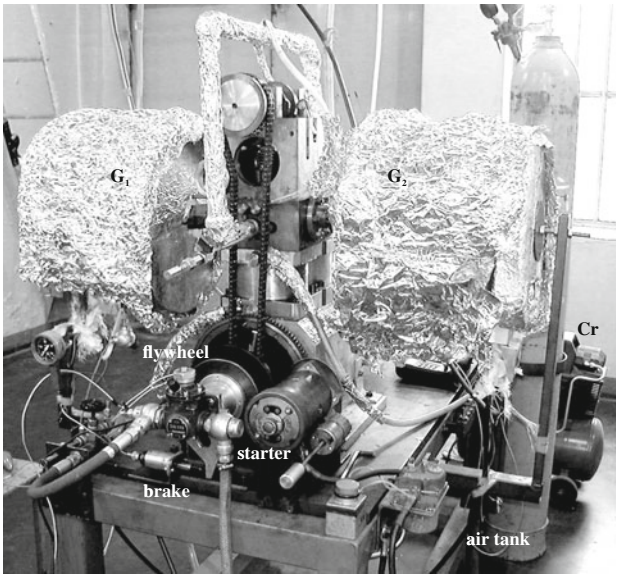

Fig. 3.4 Complete test stand of the model engine. Engine block in the middle with heaters (electric radiators) at its sides. A supplementary air compressor with an air tank *Cr* used to start the engine is situated at the back. An engine starter and a brake system are installed at the front

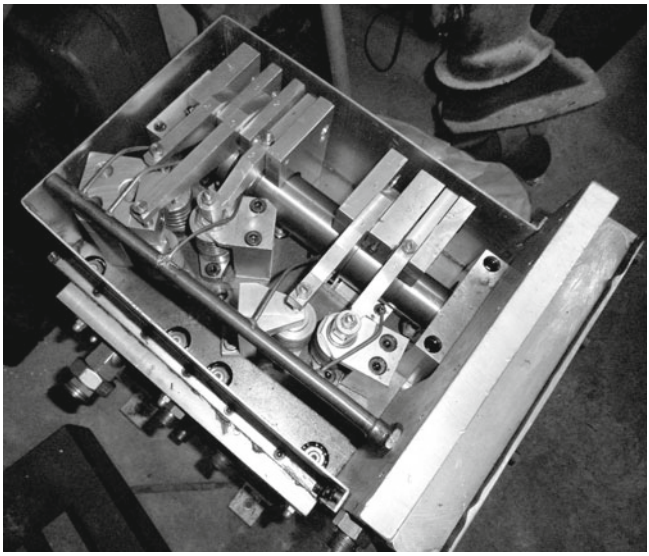

Fig. 3.5 EHVE valve actuation system view

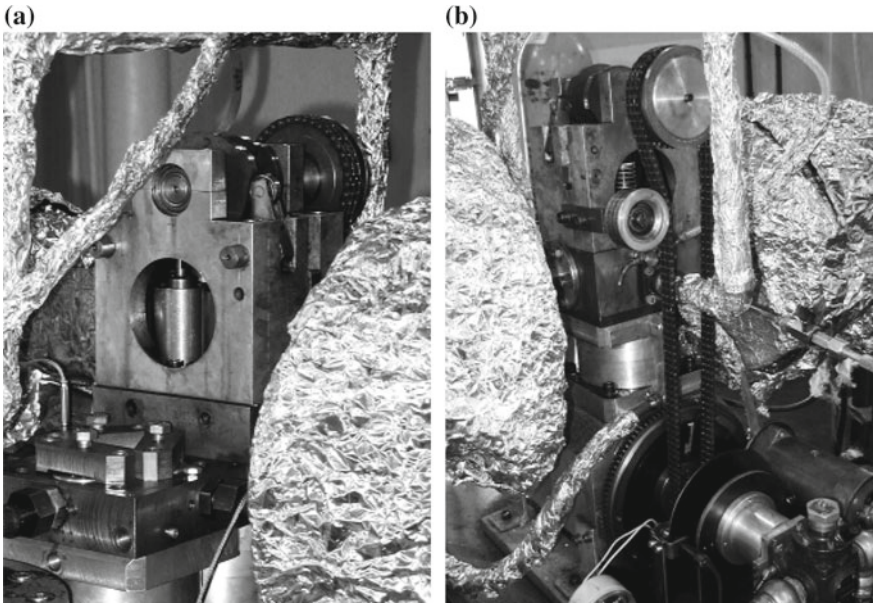

Fig. 3.6 **a** Rear view of the engine head; **b** front view, a system of control of the governed valves is shown. In both photographs, the heaters are covered with insulation foil

tap water as the cooling fluid. A typical value of water temperature at the inlet to the cooler was 288 K, whereas the temperature of the working fluid (air) entering the compressor volume was on average 340 K. For a detailed description of the engine prototype, see [6].

As seen from the photographs, the materials used to build the prototype are the same as in conventional internal combustion engines. The only exception are heater pipes that were made of high quality, heat-resistant commercial steel. Appropriate stress calculations were performed for all mechanical engine parts, with particular care for the heater pipes.

3.2 Experimental Measurement System

A general view of the almost complete experimental test stand, only without the measurement apparatus, is presented in Fig. 3.4. The most important components of the sensors and the way of performing the measurements are described further on.

The time-averaged temperatures of the working fluid at the outlets of both heaters were measured with thermocouples in front of their individual valves 1_1 and 1_2, as T_{H1} and T_{H2}, respectively. In the cooler, the temperature of the air downstream of the compressor inlet $T_{c,0}$ and the cooler tube wall temperature T_{wCl} were also measured

with thermocouples. The pressure inside the cooler space p_{Cl}, which appeared to be almost constant during a cycle of the engine operation, was determined with a typical gauge manometer.

The heat sources in the form of electrical radiators were relatively not expensive and well controlled when applied to the prototype. After initial tests, it appeared that the heat stream delivered by the heater radiators was not high enough to drive effectively the EHVE loaded with the external torque coming from the brake. Therefore, in that stage of the experiment, it was able only to overcome the frictional drags inside the EHVE plus a residual torque generated by the brake during its idle run.

Thus, the experimental investigations of the prototype were concentrated on the measurements of the working cycle variables in order to confirm if the numerical modelling process delivered correct results. These included collecting the pressures changes inside the expander and compressor cylinders as functions of time, $p_E(t)$ and $p_C(t)$. The pressures were always measured when H_1 and H_2 were fully heated by the radiators G_1 and G_2, see Fig. 3.2b. The pressure distributions were made after a few cycles of the EHVE operation. Typically, two independent time series of $p_E(t)$ and $p_C(t)$ measurements were collected by the computer data acquisition system. In order to achieve a confirmation of the measured values, the first set of data came from piezoresistive pressure transducers, whereas the piezoelectric ones were applied in the second series. All the pressure values were transformed into the electrical signals, which were, in turn, sent to a digital storage oscilloscope connected to a computer through an IEEE-488 universal measuring interface. A custom made computer program was used to control the measurement procedure.

The rotational speed of the engine crankshaft was measured by checking the upper position of the expander piston, which was usually the starting point of the pressure graphs, for all measurement series. Due to external load and internal friction, the largest deviation of the crankshaft speed during one operation cycle from its mean value was 10 % on average.

A more detailed description of the experimental test stand, the measuring system with an algorithm of the working medium flow are to be found in [6]. Summarizing, a standard apparatus was used, similar to that used recently in all investigations on conventional internal combustion engines.

3.3 Comparison of the Experimental and Simulation Results

The experimental results containing the time series for pressures $p_E(t)$ and $p_C(t)$, collected with two types of the pressure transducers, appeared to be very similar, confirming thus the confidence in the correctness of the measurements. All collections always started at the beginning of the engine cycle when both its heaters were fully warmed and took typically a few cycles of stable work. Then, representative examples were chosen for analysis and presentation.

The heater H_l was more efficient than the second one and usually the temperature T_{H1} taken in front of valve 1_1 was about 40 °C higher than T_{H2}. Measurements were performed for the same temperature of the heating elements of both the radiators G_1 and G_2. This way, for every second cycle of the EHVE operation with the heater H_2, the diagrams of pressures p_E and p_C exhibit lower maximal values than for the cycles of operation with heater H_1. For comparison, the diagrams for the expander and compressor pressures obtained experimentally and theoretically will be shown separately for cycles of engine operation with the heaters H_1 and H_2. Another reason for this separation comes from the observation that valves 1_1 and 1_2 have slightly different working characteristics.

The theoretical simulation of the engine model operation applies the algorithm described earlier in Chap. 2 and the custom-developed program which could include the mechanical dynamics of the crankshaft system in the simulations. This way, the angular velocity of the engine became another varying function of time [7]. At this stage, it is assumed that the cooler is a heat exchanger modelled in a way analogous to the heater calculations described in detail later in Chap. 5.

For the heater, it is theoretically assumed that during the phase of isochoric heating, the theoretical value of the heat transfer coefficient is

$$\alpha_{A,iso} = \alpha_{A,critical},$$

where the value of $\alpha_{A,critical}$ is calculated for the investigated engine from Eq. (2.27) derived in Chap. 2.

As results from the test measurements, the isochoric heating was poor and $\alpha_{A,iso}$ was low during the experiment for a long time. The measurement of T_{H1} and T_{H2} in the range of isochoric heating, explained in Sect. 3.2 and made with thermocouples, continuously decreased, but it should be considered as it reflects the temperature just upstream of valves 1_1 or 1_2. Similar phenomena have to occur for the temperature of the working fluid inside heater tubes. A new value of the temperature T_H also decreased in the next cycle. The p_H pressure value is connected to temperature and decreased as well. So, after a few cycles of the engine operation, the power distribution in both the expander and the compressor decreased to a level lower than the resistance and the EHVE stopped. It means that the heat delivered to the engine during the isochoric process was too low.

An important control parameter of the simulations is the converging value of the total mass of the working fluid enclosed inside the whole volume of the cylinders, heaters and cooler. It takes into account the above-mentioned method of pressure measurement, which lasts for a short time after the EHVE starts its operation. The experiments were performed for heater temperatures from 550 to 800 °C. The rotational speed of the engine n varied from 384 to 720 rpm.

In Figs. 3.7, 3.8 and 3.9, chosen experimental results are presented and compared with respective simulations. These figures present typical examples of both attempts and most of them are reported in [6]. Figures 3.7 and 3.8 show comparisons for the engine cycle operation with the heater H_1, whereas Fig. 3.9 refers to the heater H_2.

One can observe some differences between the experimental and theoretical values for $p_E(t/T)$ in Figs. 3.7 and 3.8 in the first quarter of those diagrams. They are caused by strong spatial flow disturbances, which used to appear during the opening of valve 1_1. The pressure transducer is located relatively close to valve 1_1, thus local pressure disturbances are recorded by it although the spatially averaged, time-dependent pressure $p_E(t)$ inside the expander cylinder may not exhibit such intense changes. Valve 1_2 is situated farther from the pressure transducer than valve 1_1, so the p_C disturbances presented in Fig. 3.9, when valve 1_2 opens, are rather inconsiderable when compared to those shown in Figs. 3.7 and 3.8. On the other hand, it also appears that the experimental curve of p_E shown in Fig. 3.9, presenting the engine operation with the heater H_2 and valve 1_2, is located below the theoretical prediction.

Contrary to the above, it does not appear in the comparison shown in Figs. 3.7 and 3.8 for the EHVE operation with the heater H_1 and valve 1_1. It follows from air leakage taking place along the sealed rod of valve 1_2, which does not come out for valve 1_1. Leakages of the working fluid are the main reason for the differences between the theoretical and experimental charts of the pressure p_C inside the compressor cylinder. They look very similar when Figs. 3.7 and 3.9 are compared.

The leaks recorded for valves 3_1 and 3_2 are the reason that the experimental trace p_C, for relative cycle times located in the last quarter of the horizontal time axis, is located above the theoretical prediction (cf. Figs. 3.7, 3.8 and 3.9). As a result, at the beginning of the working cycle, the air compression starts from a pressure value higher than the theoretical one. The maximal values of the experimental pressure in the compressor for the compression ratio attained in the EHVE should be above the

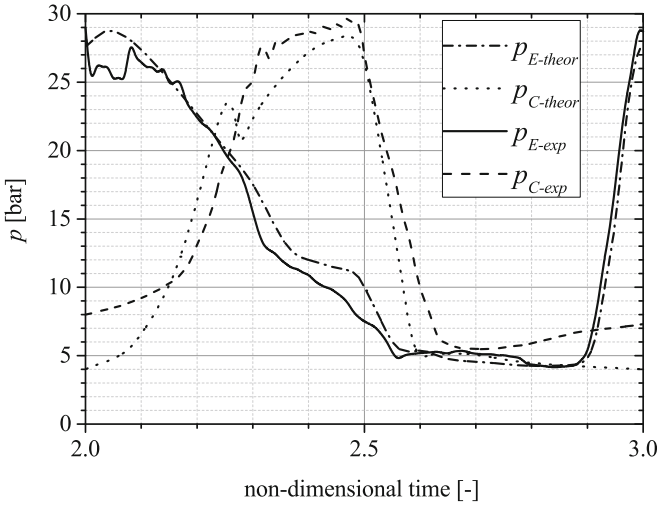

Fig. 3.7 Diagram of the experimental and computational pressures as functions of non-dimensional time in the expander p_E and the compressor p_C for $T_{H1} = 738\,^{\circ}\mathrm{C}$ at the engine rotational speed of 697 rpm

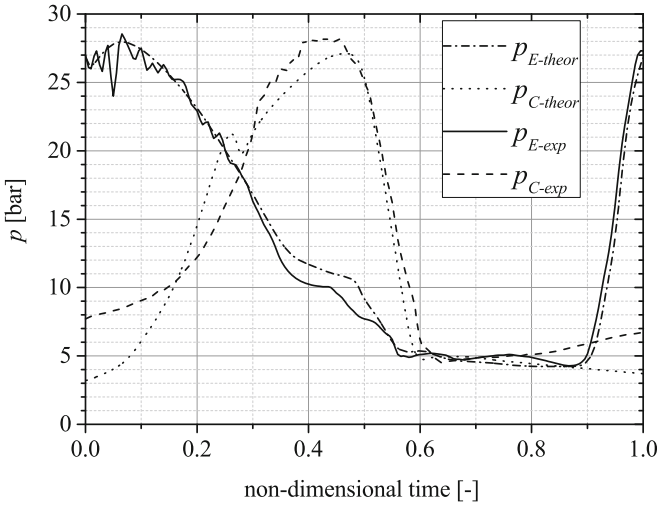

Fig. 3.8 Diagram of the experimental and computational pressures as functions of non-dimensional time in the expander p_E and the compressor p_C for $T_{H1} = 644\,°\text{C}$ at 555 rpm

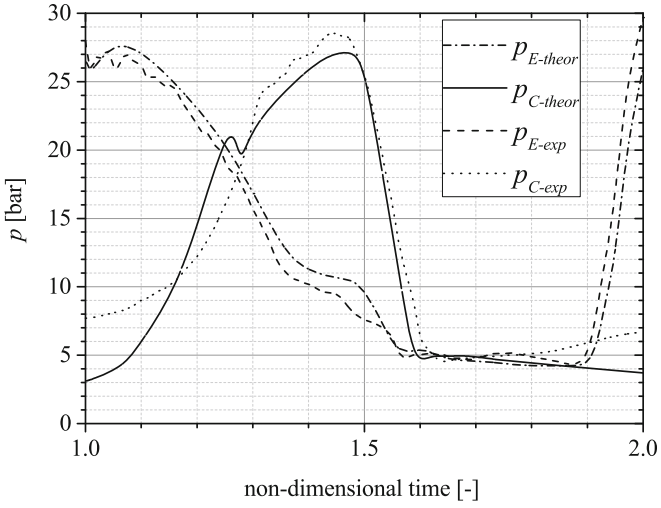

Fig. 3.9 Diagram of the experimental and computational pressures as functions of non-dimensional time in the expander p_E and the compressor p_C for $t_{H2} = 698\,°\text{C}$ at 691 rpm

maximal measured values. This is also caused by working fluid leakages through the compressor piston rings.

No leakages of the working fluid are included in the theoretical model employed in the discussed comparisons because they are usually a function of inaccuracies of manufacturing and assembly processes of the engine parts and, hence, are difficult to be simulated with an appropriate level of accuracy. The leakages recorded during testing of the EHVE are on the same level as for other conventional internal combustion engines, except for the additional problem at the sealed rods of valves 1. These seals have to be redesigned and manufactured with additional attention. It turned out that the seal for valve 1_1 worked perfectly, whereas the one for valve 1_2 did not operate faultlessly. However, it should be taken into account that the engine prototype was manufactured in a workshop of moderate technological capabilities.

Most of the differences between the simulation values and the experimental measurements for the pressure distributions analysed inside the EHVE cylinders result from the leakages and were taken into account in the theoretical model. Even so, from the analysis of the discrepancies presented in Figs. 3.7, 3.8 and 3.9, it can be concluded that all experimental records taken from the prototype testing are reflected in the theoretical simulation results.

The heat stream obtained from electric radiators was too low to produce a significant external torque in the EHVE. The internal power generated by the engine was consumed by its frictional resistance and the residual torque of the brake working in its idle run. Nevertheless, the prototype proved its capability and if better sources of heat had been used, it could have delivered a useful amount of mechanical work.

As described above, the initial conditions for the calculations of $p_{E\,theor}$ and $p_{C\,theor}$ in the numerical integration of a system of ordinary differential equations are determined using values chosen from the experimental data. The internal power of the engine theoretical model calculated on the basis of the diagrams $p_{E\,theor}$ and $p_{C\,theor}$, see Figs. 3.7, 3.8 and 3.9, is marked in Fig. 3.10 by rectangles for the EHVE operation with the heater H_1 and triangles for operation with the heater H_2, correspondingly. The curves in Fig. 3.10 are the results of an interpolation of the discrete values marked by the above mentioned symbols. The upper, solid curve in Fig. 3.10 refers to the engine operation with the more efficient heater H_1, whereas the lower, broken curve corresponds to the operation with the heater H_2. The real internal power of the engine is located in the band between these curves.

As has been expected, the shape of the internal power diagram plotted in Fig. 3.10 is typical of the so-called resistance characteristics, which is usually a function of the engine rotational speed. This expectation is supported by the fact that the entire internal energy produced by the engine was consumed by the resistance generated by friction forces and external load. All differences between the measured and predicted values of pressures are due to errors in the estimations explained above.

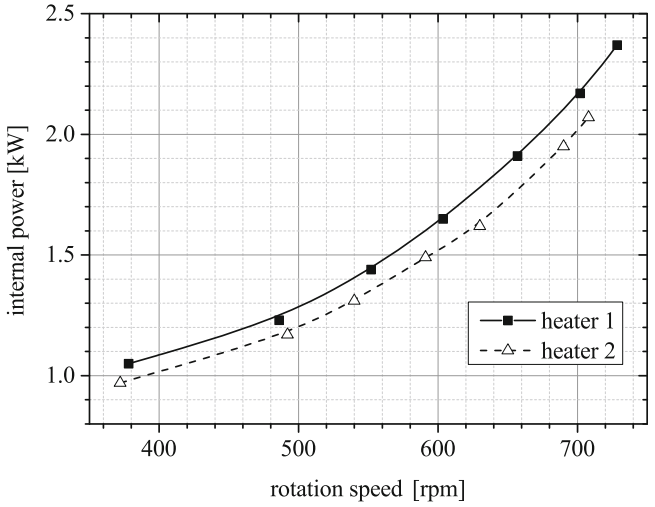

Fig. 3.10 Internal power of the investigated model of the EHVE for both heaters

3.4 Remarks on the Experiment

The performed tests have proven the following:

1. The engine prototype has an operational ability.
2. The comparisons of the experimental and theoretical pressures in the expander and the compressor show satisfactory agreement both in the recorded and simulated shapes and their values, respectively.
3. The heat delivered to the EHVE is too low when compared to the theoretical simulations.

As mentioned earlier, the pressures were always measured at the beginning of the EHVE operation when both the heaters H_1 and H_2 were fully warmed for a short time. The achieved heat transfer rate described by the coefficient α_A in this model was equal to approximately $190 \frac{\mathrm{W}}{\mathrm{m^2 K}}$.

It appears that during the experiments conducted for a long time, the isochoric heating yields a low amount of heat delivered to the EHVE. The experience gained during the experiments shows that a sufficient heat transfer can be obtained for the air flowing through the EHVE heaters if a forced circulation of this medium is applied. Such a solution will be employed in the next stage of the investigations.

The forced air circulation allows for an application of a single heater of arbitrarily large volume and a large surface of heat exchange. It should be then followed by a significant increase in the engine rotational speed. The demand for a high compression ratio of the engine to be about 10, when a heater of large volume is applied, is then related to some modifications in the governed valve system. As observed, the

self-acting valves caused many problems during the experiments, which suggests they cannot be used for a high rotational speed of the EHVE. In the developed version of the engine, they will be eliminated and their task will be accomplished by a set of governed valves.

To attain a high value of the heat transfer coefficient α_A in the heater, turbulent flow has to be applied. Hence, some additional devices will be introduced. The first attempt to improve the EHVE is described in Chap. 4. The next steps of the development are presented in Chaps. 5, 6 and 7.

References

1. Brzeski L, Kazimierski Z (2001) Experimental investigation of externally heated valve engine model. Proc Inst Mech Eng A, J Power Energy 215(4):48694. doi:10.1243/0957650011538749
2. Brzeski L, Kazimierski Z (1995) New type of heat engine—externally heated air engine. In: SAE Technical Papers Series Paper 950092, International Congress and Exposition, Detroit, Michigan, 27 February–2 March 1995. doi:10.4271/950092
3. Kazimierski Z, Brzeski L, Wojewoda J (1995) Thermodynamical cycle of a new type of the externally heated engine. Arch Thermodyn 16(3–4):197–215
4. Brzeski L, Kazimierski Z (1995) Computer simulation of a new type heat engine operation. Comput Assist Methods Eng Sci 2(2):129–139
5. Kovač A (1980) Les moteurs volumétriques á cycle fermé: une vioe peu prospecteé dans le redéploiement énérgetique. Entropie 16(92):23–30
6. Kazimierski Z, Brzeski L (2000) Construction and investigation of a new type heat engine. Report on project 113/T10/97/13 for the state committee for scientific research, April 2000 (in Polish)
7. Brzeski L, Kazimierski Z (2001) Computer simulation of the closed cycle flow in the new type 4-stroke externally heated air engine. In: Proceedings of the 5th Int. Symp. on Exp. and Aerodyn. of Int. Flows, Gdansk; Sept. 4–7, 2001, p. 573

Chapter 4
Early EHVE with Two Small Heaters and Additional Devices to Improve Heat Exchange

4.1 Engine Assembly – Additional Devices

The heat delivered to the EHVE should be sufficiently intensive when valves 1 and 3 are closed. The isochoric process, which takes place then in the early EHVE, yields rather poor heat exchange, which was confirmed during the experimental investigations [1]. The heaters H_1 and H_2, where the isochoric heating occurs at 1.5 of the engine cycle, could not deliver enough heat to maintain long operation of the prototype. It seemed to be possible in the early version of the engine, but some additional devices should be added in order to increase the effectiveness of heat exchange.

The early EHVE presented in Fig. 4.1 comprises a double-side action piston, a slider-crank mechanism and self-acting valves 3 and 4. An attempt to achieve such a solution was undertaken in [2]. A blower and two distributors were introduced, however, now an entirely different arrangement is proposed, cf. Figs. 4.1 and 4.2. Additional devices are: two blowers B_1 and B_2 and rotary valves RV. The two blowers work continuously.

Let us consider valves 1_1 and 3_1 working with the heater H_1. Another set is assembled at H_2, which is similar as they work in the engine alternatively. If EHVE valves 1_1 and 3_1 are open, the working fluid flows through the heater H_1 and passes along the blower loop. The rotary valves RV remain closed for the flow to the heater H_1. The blower B_1 has to overcome the resistance in the installation elements located out of the H_1 loop.

When EHVE valves 1_1 and 3_1 are both closed, the rotary valves change their positions and the working fluid flows through the heater H_1. The working fluid flows during 1.5 cycle of the engine operation, cf. Fig. 4.3. The heater H_1, taking the heat from another source, acts in the range $180° \leq \alpha \leq 720°$ and accumulates the heat inside its volume. Then, valves 1_2 and 3_2 open at $\alpha = 360°$ until $\alpha = 540°$ as shown in Fig. 4.3. The heater H_2 is excluded during this time from the engine activity. Valves 1_2 and 3_2 close at $\alpha = 540°$ and H_2 is introduced into the action in the range $\alpha = 540° \leq \alpha \leq 1080°$, accumulating the heat inside.

Z. Kazimierski and J. Wojewoda, *Externally Heated Valve Engine*,
Springer Tracts in Mechanical Engineering, DOI 10.1007/978-3-319-28355-5_4

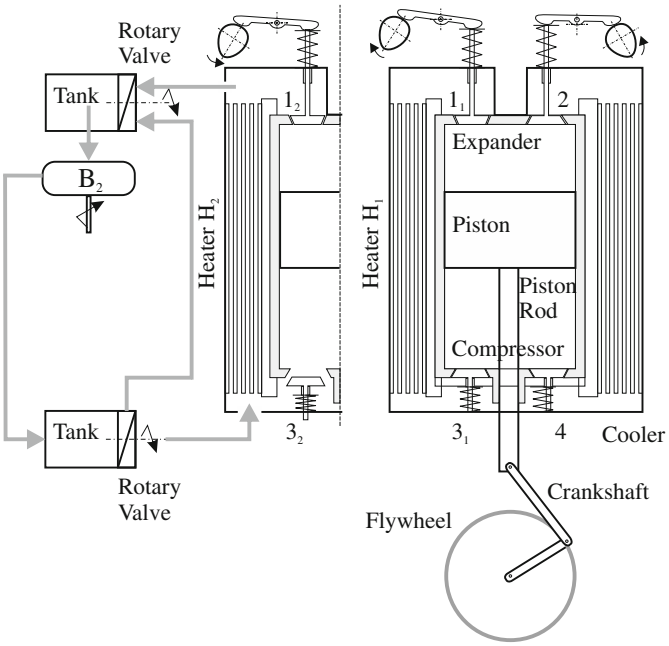

Fig. 4.1 General scheme of the early EHVE. *1*, *2*, *3*, *4* – governed valves, B_2 – blower in the H_2 loop

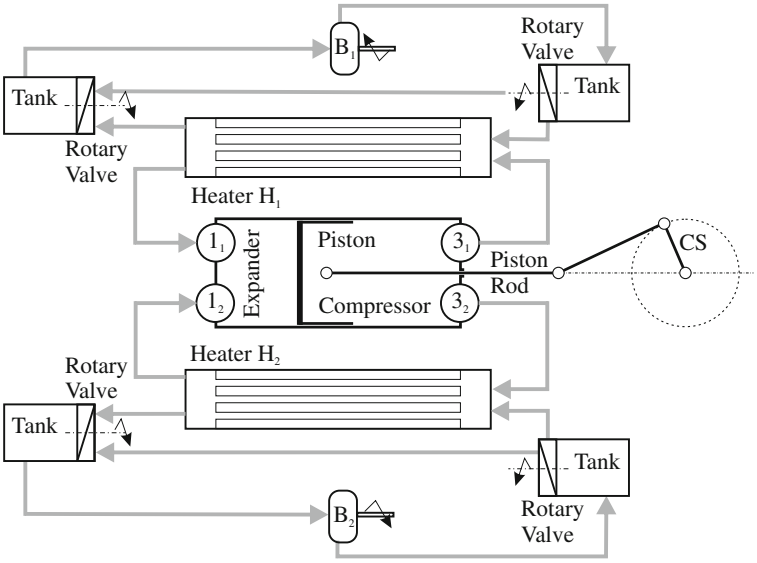

Fig. 4.2 Scheme of the EHVE with two small heaters, *1*, *3* – valves, B_1, B_2 – blowers

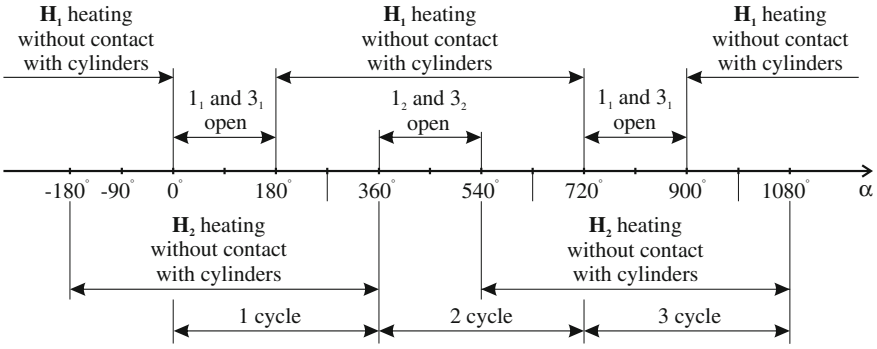

Fig. 4.3 Diagram of the engine timing when the two small heaters H_1 and H_2 are applied in the heating process

Engine valves 1 and 3 are open again and their working cycle repeats. The experiments presented in Chap. 3 show that the temperature at the end of activities of the heaters decreased. It is the proof that the heat delivered during the isochoric process inside them was too low. Hence, an idea to add some devices in order to improve a level of heat exchange. If the blower loops B_i are to be considered, they have to assure such a level of the mass flow rates $\dot{m}_{Bi}$ that the values of the Reynolds numbers obtained as a result of their action will be $\mathrm{Re}_{Bi} > 10^4$. The flow in the heaters is then turbulent and, due to an increase in $\dot{m}_{Bi}$, the heat exchange level attains the required level. The control parameters will be the blower mass flow rates.

4.2 Calculations of the Engine

We assume that the engine cylinder operates approximately in such a way that the heat exchange inside it does not exist. For the cylinder, the most important are time-dependent relations and it has been taken into account, whereas a dependence of spatial variables has been neglected, so the model is described and simulated in the time domain only.

Heat exchangers, which play an important role in the engine, are in a different situation. The problem of a large cooler has been solved in [3]. The small heaters H_1 and H_2 are now the subject of consideration. In fact, the temperature of air grows from the heater inlet to outlet. Both heaters are counter-current flow-type heat exchangers, where the temperature drop remains almost constant along the length of their tubes. The heaters are treated as time-dependent only, assuming that all important changes are the same along their length and considering each of them in a single plane only. This plane is situated at the outlet of exchanger tubes. Such an approximate approach used here allows for applying the maximal temperature of heater internal walls. It also allows a moderate number of equations to be used in the case of a time-dependent

model. These are nonlinear, ordinary differential equations based on mass and energy conservation, supplemented by some nonlinear algebraic formulae.

The flow in the small heaters H_1 and H_2 is turbulent and the heat exchange coefficient α_A can be calculated in the following steps

$$\mathrm{Re}_H = \frac{4\dot{m}_H}{\pi d_h \mu_H n_H}, \tag{4.1a}$$

$$\mathrm{Nu}_H = 0.022\,\mathrm{Re}^{0.8}\,\mathrm{Pr}^{0.6}, \tag{4.1b}$$

$$\alpha_A = \frac{\mathrm{Nu}\lambda_H}{d_H}, \tag{4.1c}$$

where λ_H is the conductivity of air at the given temperature and μ_H is the air dynamic viscosity.

For the heater H_1 within the range $\alpha_{10} \le \alpha \le \alpha_{32}$, valves 1_1 and 3_1 are open. When both of them are closed at $\alpha = \alpha_{32}$ (usually about 180°), the period of heating in H_1 caused by the blower B_1, which begins its operation, starts and lasts until $\alpha = 4\pi$. This blower yields its mass flow rate $\dot{m}_{B1}$ and the air velocity appears in H_1. A similar situation takes place in the heater H_2, which ends its activity at $\alpha = 360°$, see Fig. 4.3. It means that the inflow to the heaters H_1 and H_2 comes from B_1 and B_2, respectively. If we ignore any small leakages, it can be assumed that $\dot{m}_{Bi}$ is the same on both sides of the heater tubes. As results from the continuity equation, $\rho_H =$ constans. The value of ρ_H can be calculated from the equation of state, e.g.,

$$\rho_H = \frac{p(\alpha_{32})}{RT(\alpha_{32})}.$$

The mass of the air inside any heater H_i is

$$M_{Hc} = \rho_{Hc} V_H. \tag{4.2}$$

The EHVE has to work continuously and, thus, we have the relation

$$T_H(4\pi) = T_H(0)$$

for H_1 and

$$T_H(6\pi) = T_H(2\pi)$$

for H_2, respectively.

The temperature $T_H(\alpha_{32})$ can change, because if B_i begins its activity at the blower path loop, the hot air comes and mixes with the air already being inside the heater H_i. The resulting temperature has to be assumed because we do not know the design of the H_i and the mixing conditions. But it is sure that

$$T_H^{mix} > T_H(\alpha_{32}).$$

We give up this assumption on T_H^{mix} for the data given in these considerations and take finally

$$T_H(\alpha_{32}) = T_H^{mix}.$$

A linear increase in $T_H(\alpha_{32})$ to the value $T_H(4\pi)$ is assumed. The reason for the growth is heating in the volume of H_1 or H_2. The pressure $p_H(\alpha)$ is determined from the known rule Eq. (2.28). The calculation method is described in detail in Chap. 2. Using the above method, we can calculate $p_E(\alpha)$ and $p_C(\alpha)$ and determine work of the EHVE according to Eqs. (2.37) and (2.38). It is the work generated by the engine, without that consumed by additional devices.

The work of all auxiliary devices will be calculated later. When both heaters work while valves 1_1 and 3_1 are open, the heat delivered is

$$Q_{H,I} = A_H \int_{\alpha_{10}}^{\alpha_{3c}} \alpha_{AH}(T_{wH} - T_H)\frac{\mathrm{d}\alpha}{\omega}. \tag{4.3}$$

When valves 1 and 3 are closed, the heat delivered in H_1 is

$$Q_{H,II} = M_{Hc}c_v\left(T_H(0) - T(\alpha_{32})\right). \tag{4.4}$$

The same takes place for the heater H_2.

The total amount of the delivered heat is

$$Q_H = Q_{H,I} + Q_{H,II}. \tag{4.5}$$

The above value of Q_H is used in the calculations of the EHVE efficiency. The temperatures $T_H(0)$ and $T_H(\alpha_{32})$ are taken from Eq. (2.21).

Now, let us consider the blower mass flow rate $\dot{m}_{Bi}$. The pressure drop in the blower B_1 Δp_B, hence Π_B is calculated as

$$\Pi_B = \frac{p(\alpha) + \Delta p_B}{p(\alpha)}.$$

According to Eq. (5.48), an increase in the enthalpy h_b in the blowers can be determined if their efficiency is 0.7, whereas their power (for a single blower) is

$$P_B = \frac{\dot{m}_B h_b}{\eta_B}. \tag{4.6}$$

The work according to Eq. (5.47) of a single blower is

$$L_B = P_B\frac{2\pi}{\omega}. \tag{4.7}$$

The work of the EHVE is

$$L = L_E + L_C - 2L_B - L_{RV}, \tag{4.8}$$

where L_{RV} is the work consumed by the rotary valves.

The efficiency of the EHVE is

$$\eta = \frac{L}{Q_H}. \tag{4.9}$$

No pre-heater at this stage was applied, even though the temperature of the working fluid downstream of the expander was high enough to use it.

4.3 Results of the Numerical Simulations

The computations were carried out for the following data assumed for the model: crankshaft angular velocity $\omega = 157$ rad/s, equivalent to 1500 rpm, and important values of the temperatures of the exchanger walls set to $T_{wH} = 1273$ K and $T_{Cl} = 300$ K. The other data are presented in Tables 4.1, 4.2, 4.3 and 4.4.There was a piston rod located in the compressor volume, whose diameter $D_{PR} = 0.05$ m affected its value.

The pressure inside the cooler volume was assumed as $p_{Cl} = 10^6$ MPa. Any increase in it causes improvement of the engine performance but rather a low value is analysed here.

The values of the above angles, which determine the behaviour of the valve governing system data, are chosen after the preliminary optimization calculations.

At the beginning of the calculations, we assume the volumes of the engine compressed to chosen initial values. We determine values of the generated power $p_E(\alpha)$ and $p_C(\alpha)$ with formulae (2.37) and (2.38) (coming from the procedure described in Chap. 2), which gives $P = 25.85$ kW at the pressure level of $p_{Cl} = 10^6$ MPa in the cooler. An amount of the heat delivered to the EHVE is determined from Eqs. (4.3), (4.4) and (4.5). As a result, the obtained efficiency value is approx. 33 %. The obtained temperatures, pressures and flows through the engine valves are presented in Fig. 4.4.

Table 4.1 Dimensions of the cylinders of the EHVE

Cylinder	Diameter d (m)	Stroke s (m)	Dead height h_0 (m)
Expander	0.13	0.0753	0.0007
Compressor	0.13	0.0753	0.0018

Table 4.2 Dimensions of the EHVE heat exchangers

Exchanger	Diameter	Length	Number of pipes	Exchange area	Volume
	d (m)	l (m)	n (−)	A_H (m^2)	V (m^3)
Heater H	0.008	0.4	20	0.2	0.00040
Cooler Cl					0.00500

Table 4.3 Control parameters of the governed valves

Valve No.	Opening α_{io}	Closing α_{ic}	Transient $\Delta\alpha_i$	Max. flow area (m^2)
1	0°	130°	40°	0.0007
2	180°	356°	40°	0.0007

Table 4.4 Physical data of the self-acting valves

Valve No.	Mass m_i (kg)	Spring stiffness k_i (N/m)	Damping coefficient c_i (Ns/m)	Max. lift h_i (m)	Diameter d_i (m)
3	0.0755	5000	15.75	0.0074	0.030
4	0.0755	5000	15.75	0.0074	0.030

If the work of the blowers and the rotary valves is subtracted from the previously calculated work, i.e., Eq. (4.8), we can estimate real efficiency of the EHVE. Power of the blowers will not be determined from Eq. (4.6). Thus, they have to be overbalanced and we assume their work, or the power consumed by B_i and RV, to be larger than in the calculations. We assume the power of the blowers and the rotary valves to be equal approximately to 3 kW. The power of the EHVE is then 22.85 kW. Finally, the efficiency of the engine is $\eta = 29\,\%$. The diagram $p - V$ presenting operation of this engine is given in Fig. 4.5.

A solution in the custom written program built with a GCC compiler/linker is obtained with standard C++ language library procedures and solvers presented in [4]. The Runge-Kutta 4th-order method is applied in the integration process. All simulations were started from identical, fixed initial conditions, continued until the solution reached integrated values differing in relative measures no more than 0.01 % from those obtained at the end of the previous cycle. The numerical errors were within the limits of accuracy of double precision numbers. An adaptive step-size integration method with a forced decrease in the step near switching values like valve opening/closing was applied. The size of the integration step and limits of acceptance of the consecutive solutions were chosen as a result of the careful analysis of a wide range of their values. It should be mentioned that the system presents a quick

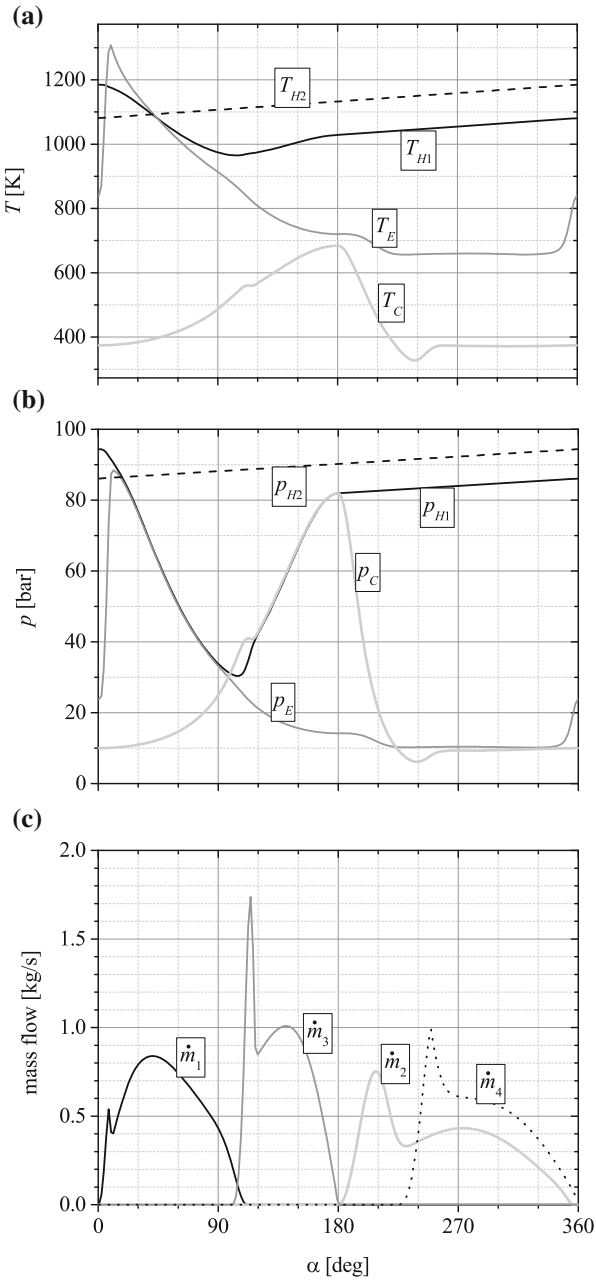

Fig. 4.4 Diagrams of (**a**) temperatures, (**b**) pressures and (**c**) valve mass flow rates as functions of the crankshaft angle α; $p_{Cl} = 10\,\text{bar}$, $T_{Cl} = 300\,\text{K}$, $T_{wH} = 1273\,\text{K}$, $V_H = 0.4 \times 10^{-3}\,\text{m}^3$, 1500 rpm. Appropriate elements are marked with their symbolic descriptions

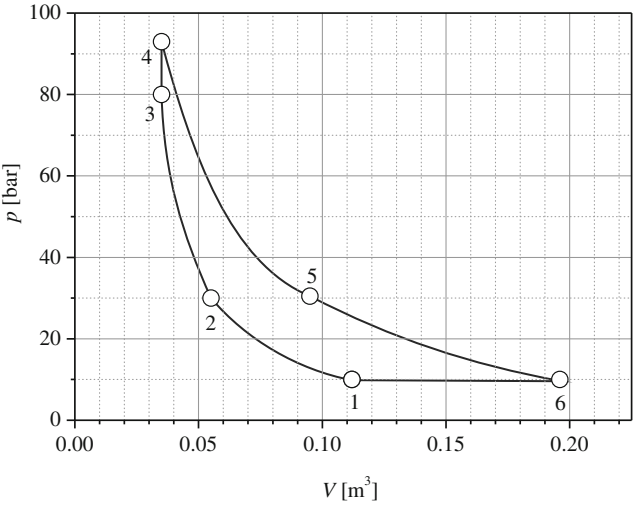

Fig. 4.5 Diagram of the $p - V$ relation for the early EHVE. *1–2* isentropic compression in C, *2–3* compression in C and heating, *3–4* heating in heaters, *4–5* decompression in E and heaters, *5–6* isentropic decompression in E, *6–1* isobaric flow through the large cooler Cl at the lowest pressure of 10 bar

convergence of the solution and rather low sensitivity to step changes. Typically, a stable solution was reached after 100–150 cycles of the simulated full crankshaft revolutions.

4.4 Remarks on this Version of the EHVE

A two-stroke externally heated valve engine, entirely different from the Stirling type engine, with two small heaters operating alternatively and a large cooler, was investigated numerically. The heat exchangers are of a counter-current type. Two small heaters of the volumes lower than that of the expander, $V_H / V_E \leq 0.5$, exemplify the idea presented in [5]. The experimental results published in [1] and described here in Chap. 3 showed, however, that heat transfer was poor during the period when the engine valves were closed and an isochoric process in the heater took place. Thus, the heating process had to be longer and should last for 1.5 cycle of the engine operation.

In order to provide proper heat exchange, the two blowers and the rotary valves connecting them to the engine were applied in the numerical model. The additional devices are presented in Figs. 4.1 and 4.2, correspondingly.

The results of the computer simulations in the form of pressures, temperatures and mass flows through the engine valves are shown in Fig. 4.4. Additional devices are applied in order to provide the heat for proper operation of the early EHVE. The

diagram $p - V$ for the operation of the EHVE with additional devices is shown in Fig. 4.5.

The power and efficiency of the engine rotating at 1500 rpm is $P = 22.85$ kW and 33 %, respectively. The efficiency could become higher if a pre-heater, like in many Stirling engines, is applied.

References

1. Brzeski L, Kazimierski Z (2001) Experimental investigation of externally heated valve engine model. Proc Inst Mech Eng A J Power Energy 215(4):486–494. doi:10.1243/0957650011538749
2. Kazimierski Z, Wojewoda J (2011) Externally heated valve air engine with two small heaters operating alternatively. In: Proceedings of SYMKOM 2011, Turbomachinery, vol. 140, pp. 105–114
3. Wojewoda J, Kazimierski Z (2010) Numerical model and investigation of the externally heated valve Joule engine. Energy 35(5):2099–2108. doi:10.1016/j.energy.2010.01.028
4. Press WH (2007) Numerical recipes: the art of scientific computing. Cambridge University Press, Cambridge
5. Brzeski L, Kazimierski Z (1995) New type of heat engine—externally heated air engine. In: SAE Technical Papers Series Paper 950092, International Congress and Exposition, Detroit, Michigan. Accessed 27 Feb–2 Mar 1995. doi:10.4271/950092

Chapter 5
Newly Developed 2-Stroke EHVE

Although this chapter is also devoted to a 2-stroke type of the EHVE, the major difference between it and the previous version refers to a size of heat exchangers which introduce an essential change in heat delivery. They were small when compared to the volume of the working cylinder, $V_H/V_E < 1$, and here their size is more substantial, i.e., $V_H/V = 3 - 5$. Additionally, new devices are added, i.e., two centrifugal blowers B_1 and B_2. They were not present in the description presented in Chap. 2 or in [1–3]). Also, a complete physical model of the engine is included. The added blowers have to consume some inconsiderable amount of generated power and modelling of their operation is accounted for. The power needed to drive typical centrifugal blowers increases monotonously with their dimensions but its "low" level is assumed not to exceed 10 % of that generated by the engine. What is important, we expect the flow in the exchangers to be turbulent. An example of our optimization process related to the blowers is presented in Fig. 5.10.

The idea of introducing the EHVE is directly related to a very important advantage of the engine. In fact, it can use the most available and cheap working fluid – atmospheric air. This is followed by another favour – any source of externally delivered heat, either from solar heat or generated during a nuclear reaction or coming from combustion of any natural or artificial fuel, can be used. The model treats the delivered energy in terms of numbers and although is directly related to typical levels of parameters applied presently in heat engines, it can be adopted to any other available data. The only condition is constant delivery of a particular amount of energy to the working fluid at the rate which assures the efficient work. As most mineral fuels will run out one day, the idea seems to be worth further development.

The EHVE is designed to produce a moderate amount of mechanical energy based on an external source of heat. It operates in a closed heat cycle and consists of a few essential parts, namely: an expander, a compressor, a heater, a cooler, and two blowers recirculating the internal flows of the working fluid. The essence of the development in this version consists in application of these two blowers connected to the engine heater and cooler and working in loops of high and low pressures. When the engine valves are closed, then the operation of the blowers becomes significant in order to enforce the fluid circulation in each of the heat exchangers. The expander

Z. Kazimierski and J. Wojewoda, *Externally Heated Valve Engine*,
Springer Tracts in Mechanical Engineering, DOI 10.1007/978-3-319-28355-5_5

and compressor of the engine are of similar design as those described in Chap. 2 or in [4], although the investigations are aimed to increase the performance of the engine on the basis of the experience gathered during the experiments performed with the prototype of the EHVE. We should remind that our idea was developed independently of that referred in [5], where the work of heat exchangers was not presented at all although their behaviour is extremely important from the viewpoint of the engine operation.

The heater comes into contact through valves 1 and 3 when they are open with the expander and the compressor only for $\frac{1}{2}$ of the engine work cycle. For the rest of time when valves 1 and 3 are closed, see Figs. 5.3 and 5.4, additional loops for the heat exchangers are introduced to avoid the situation described in Chap. 3 which showed that the isochoric heating process was very poor. All these alternations are to be described in detail below.

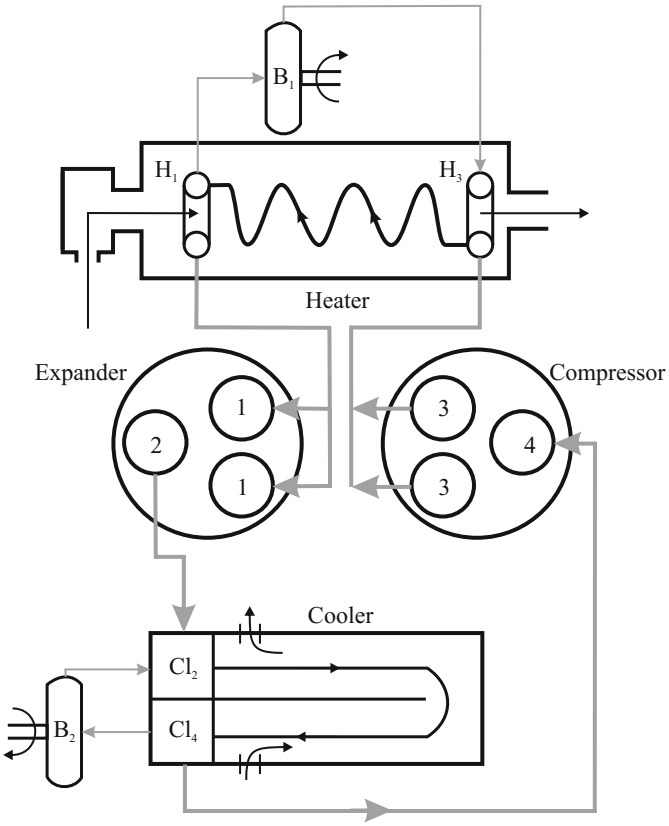

Fig. 5.1 Scheme of the transversal cross-section of the engine, the heater collectors marked as H_1 (outlet) and H_3 (inlet) and the cooler, Cl_2 (inlet) and Cl_4 (outlet), B_1 and B_2 blowers, *1–4* cam governed valves

5.1 Principles of Operation of the Improved EHVE

This version of the EHVE is still a 2-stroke-type engine, in its basic version equipped with two cylinders. Multi-cylinder arrangement is available, like for most internal combustion engines, although this would be a multiplication of 2 in each case and is not a subject of discussion presented here. Each cylinder is designed to act in a different way, either as an expander or a compressor. They act in anti-phase, i.e., the phase angle between compressor and expander pistons equals 180°. Aside of them, there are two moderate-volume heat exchangers, a heater and a cooler. To raise the rate of heat exchange, the internal blowers B_1 and B_2 work in the internal loops of the working fluid forcing turbulent flow inside each of the exchangers. The engine works in a closed heat cycle with atmospheric air being again its working fluid. Schematic views of the modified EHVE are presented in Figs. 5.1 (transversal cross-section) and 5.2 (longitudinal view).

Additionally, to fully understand the idea of modification, the flows of the working medium, with the blowers included in their arrangement, are shown in Fig. 5.3 for the heater loop and in Fig. 5.4 for the cooler one. There are some aspects of the EHVE design which are taken from well-known solutions used in internal combustion engines. These include:

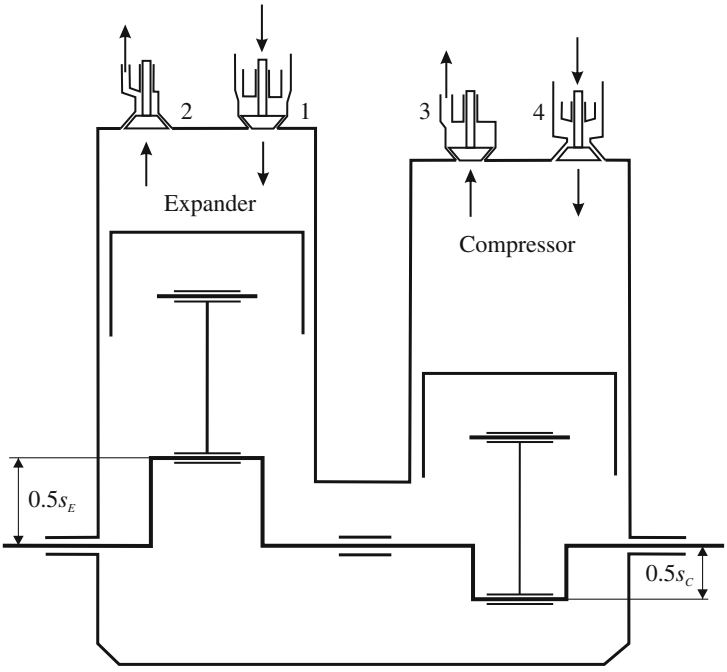

Fig. 5.2 Scheme of the longitudinal cross-section of the engine

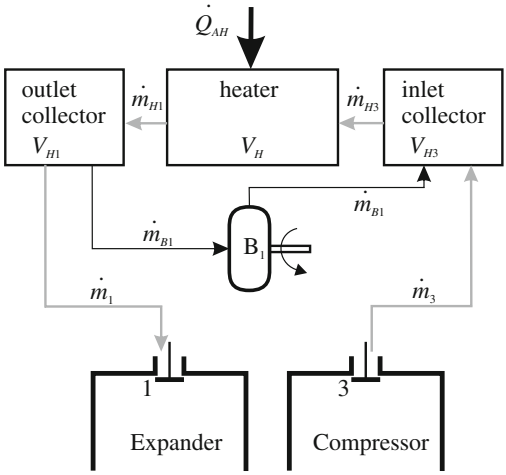

Fig. 5.3 Scheme of the fluid flow in the heater loop

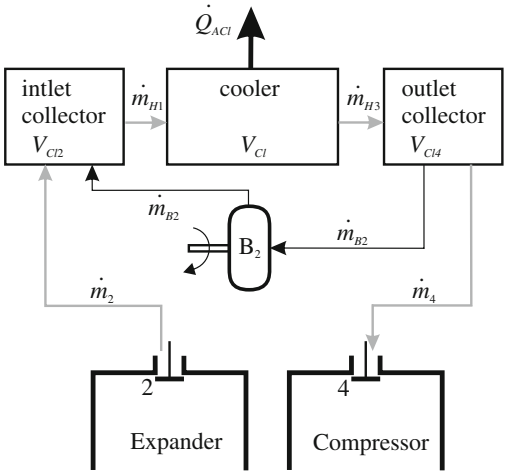

Fig. 5.4 Scheme of the fluid flow in the cooler loop

- two of the engine valves are driven with a standard camshaft mechanism, and the others probably should have a form of the rotary type,
- a conventional crankshaft to transform the energy is applied,
- sealing systems can be similar or even identical to diesel engines,
- an oil lubrication system is the same as typical solutions in the above-mentioned popular applications.

The above favours can make manufacturing of the EHVE easy when using proven solutions and the recognized technology. Contrary to problems of sealing or lubrication widely met in Stirling-like devices, the bridge to apply external heating to standard piston heat engines can be made easier.

5.1.1 EHVE Operating Regime

When the piston of the expander starts to move downwards from its upper position, valve 1 opens and the working fluid flows from the heater to the expander under high pressure and temperature. This is shown schematically in Figs. 5.1 and 5.2. Valve 1, which, as a matter of fact, consists of two identical valves to fill better the expander, is applied like in modern internal combustion engines. Both valves 1 close at the angle α_{1c} and, further on, the piston movement makes the hot air expand in the locked volume of the expander until the piston comes to its lowest position. Simultaneously, the air locked in the compressor volume with all the valves closed is subject to compression in order to flow then into the heater.

Valve 3 opens at approximately 100° and the compressed working fluid goes into the heater under high pressure. Two valves 3, similarly to the design of valves 1, are used to deliver efficiently the compressed fluid to the heater. When the piston inside the compressor attains its upper position, the compressed fluid stops to be supplied to the heater, and valves 3 close. Then, the pistons in both cylinders start to move again. The expander piston moves upwards and valve 2 opens, so the overworked fluid is taken by the cooler. Simultaneously, the piston in the compressor moves downwards, valve 4 opens and the cold fluid from the cooler comes into its volume. Eventually, the expander piston arrives at its primary position, valves 2 and 4 close and the two-stroke engine heat cycle is completed then.

Technically, if valves 1 and 3 are driven with a standard camshaft, they open in opposite directions to valves 2 and 4, which complies with the operation regime

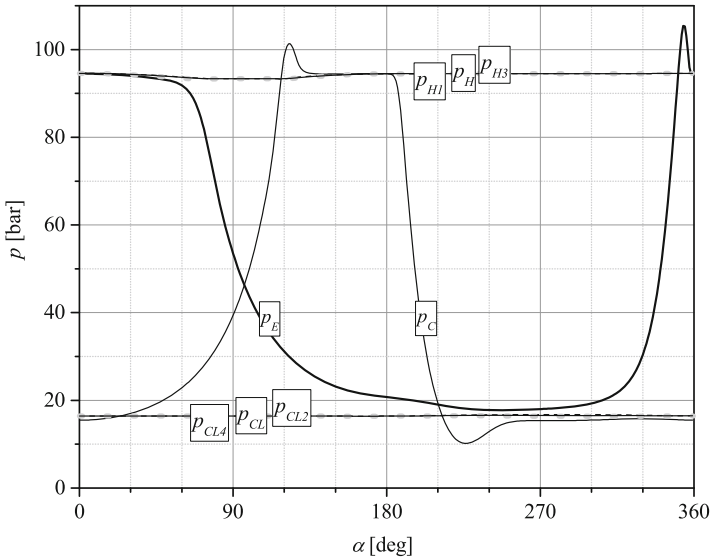

Fig. 5.5 Pressures in essential parts of the engine at 3000 rpm as a function of the crankshaft angle

of standard valves applied in internal combustion engines. As a modification, rotary valves 1 and 3 may be introduced in order to assure the desired characteristics of their opening. The collectors of heat exchangers (Figs. 5.3 and 5.4) have to be included in the design of the EHVE. The simulation results presented in Fig. 5.5 show that the pressure in the heater and its collectors remains almost constant. It is a visible reason for the applied changes in the heat delivery system.

5.2 Theoretical Model

In general, it is assumed that the engine cylinder, which is cooled as in internal combustion engines, operates in such a way that there is no heat exchange inside it. The time-dependent relations that are included in the model are most significant. On the other hand, a dependence of spatial variables is ignored, thus the model is described as time-dependent only. The important assumptions of design of heat exchangers are presented below. Both of them are supplemented with two collectors at their ends, cf. Figs. 5.3 and 5.4. The inlet and outlet collectors are excluded from the model of exchangers and no heat exchange inside the collectors is assumed to exist. They also act as settling chambers, which are important as far as the behaviour of blowers is concerned. According to the preliminary calculations, the working fluid parameters in the collectors, such as pressures and temperatures, remain almost

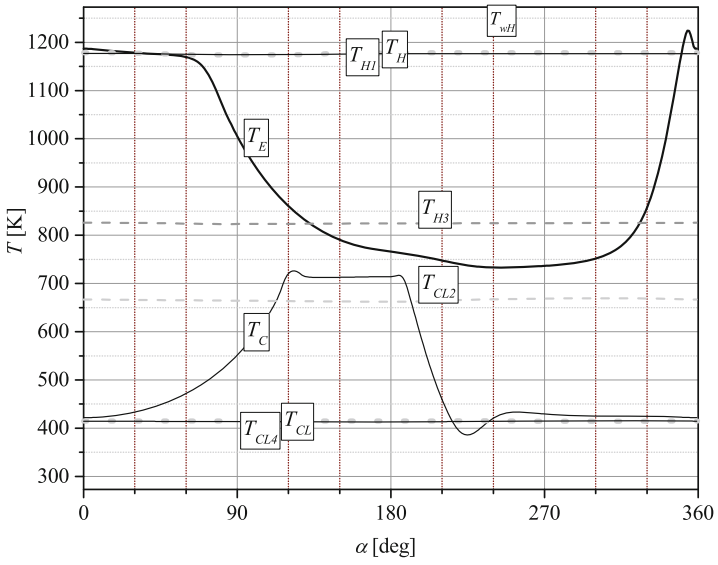

Fig. 5.6 Temperatures in basic engine elements at 3000 rpm as functions of the crankshaft angle, heat exchangers wall temperatures were assumed as $T_{Hw} = 1273\,\mathrm{K}$, $T_{wCl} = 300\,\mathrm{K}$

constant, see Figs. 5.5 and 5.6. It happens when the rotational speed of the engine crankshaft is constant, at a volume of the collectors being higher than that of the cylinder. The above conditions allow us to consider operation of the blowers as almost stationary, see Sect. 5.5 for more details. The blowers, assumed to be driven by the engine itself, have to consume some inconsiderable power generated in the EHVE. The spatial changes can exert a significant effect on both heat exchangers. They were already calculated as space and time variables in [6], because the temperature of the working fluid inside the heater in fact increases from the inlet to outlet collectors. However, this issue can be tackled in a simpler way described below.

The proper parts of the heater and the cooler are considered as counter-current heat exchangers with a temperature drop almost constant along their length. They are modelled as time-dependent only, on the assumption that all important changes are the same along their overall length. This allows one to analyse each of them in a single plane only, located at the outlet from the exchanger tubes. As a consequence of this approximate modelling, we can apply an assumption of maximal and minimal temperatures of the exchanger walls. The amounts of heat volumes delivered to the heater and subtracted in the cooler are estimated accordingly to this hypothesis. As regards the exchangers, this approach is applicable in calculating the profits resulting from using the blowers. Its accuracy is continuously checked during the computer simulations which are presented in Sect. 5.5. Obviously, this is an approximation in treatment of the parameters, however, it allows a moderate number of equations to be used in the time-dependent model. This includes a set of non-linear ordinary, differential equations of mass and energy conservation, supplemented with some non-linear algebraic formulae and switching conditions describing internal flows in the model of the engine. Also a geometry of cylinders and valves, character of mass flow rates through them is included in the description.

5.2.1 Geometry of the Cylinder Volumes and the Valves

The volume of the expander results from a simple geometry

$$V_E = A_E \left(h_{0E} + \frac{s_E}{2} (1 - \cos \omega t) \right), \tag{5.1}$$

where its cross-section area is

$$A_E = \pi d_E^2 / 4$$

and the varying volume is obtained after the derivation of Eq. (5.1)

$$\frac{\mathrm{d}V_E}{\mathrm{d}t} = A_E \frac{s_E \omega}{2} \sin \omega t. \tag{5.2}$$

Similarly, the volume of the compressor is calculated in the form of

$$V_C = A_C \left(h_{0C} + \frac{s_C}{2} (1 + \cos \omega t) \right), \tag{5.3}$$

where its area is

$$A_C = \pi d_C^2 / 4,$$

and its derivative represents the rate of volume changes as

$$\frac{\mathrm{d}V_C}{\mathrm{d}t} = -A_C \frac{s_C \omega}{2} \sin \omega. \tag{5.4}$$

The varying cross-section areas of the valves – A_j for $j = 1, 2, 3, 4$ are calculated in subsequent angle ranges from the following expressions

$$\text{for } \alpha_{j,0} \le \alpha \le \alpha_{j,0} + \Delta\alpha_j : \quad A_j(\alpha) = \frac{1}{2} A_{j,max} \left(1 - \cos \pi \frac{\alpha - \alpha_{j,0}}{\Delta\alpha_j} \right); \tag{5.5a}$$

$$\text{for } \alpha_{j,0} + \Delta\alpha_j \le \alpha \le \alpha_{j,c} - \Delta\,\alpha_j, : \quad A_j(\alpha) = A_{j,max}; \tag{5.5b}$$

$$\text{for } \alpha_{j,c} - \Delta\alpha_j \le \alpha \le \alpha_{j,c} : \quad A_j(\alpha) = \frac{1}{2} A_{j,max} \left(1 - \cos \pi \frac{\alpha - \alpha_{j,c}}{\Delta\alpha_j} \right); \tag{5.5c}$$

where the maximal values are represented by

$$A_{j,max} = \pi d_j h_j \sin 45°, \tag{5.6}$$

and any other values are simply zeros, indicating the valve is closed. In all the above listed formulae, $\alpha = \omega t$ is a current value of the engine crankshaft rotation angle. All the values related to the governed valves $\alpha_{j,0}, \alpha_{j,c}, \Delta\alpha_j, d_j, h_j$ are assumed constant and based on typical valve designs. The last term in Eq. (5.6) is the value typically applied in designs of the valve shape.

5.2.2 Mass Flow Rates through the Valves

In the modelling, we use Bernoulli and continuity equations for gas, which include losses determined by the coefficients ζ_j. Such forms are used also in Sects. 2.3.1 and 2.3.2 for calculation of mass flow rates. The equation for these rates for $j = 1, 2, 3, 4$ is as follows

$$\dot{m}_j = \frac{\zeta_j A_j p_b}{\sqrt{R T_b}} \left(\frac{p_a}{p_b} \right)^{\frac{1}{\kappa}} \sqrt{\frac{2\kappa}{\kappa - 1} \left[1 - \left(\frac{p_a}{p_b} \right)^{\frac{\kappa - 1}{\kappa}} \right]}. \tag{5.7}$$

The above formula depends on the ratio of pressures on both sides of any valve, p_a and p_b. If

$$\frac{p_a}{p_b} \leq \left(\frac{2}{\kappa+1}\right)^{\frac{\kappa}{\kappa-1}}, \tag{5.8}$$

then Eq. (5.7) takes a different form

$$\dot{m}_j = \frac{\zeta_j A_j p_b \sqrt{\kappa}}{\sqrt{RT_b}} \left(\frac{2}{\kappa+1}\right)^{\frac{\kappa+1}{2(\kappa-1)}}. \tag{5.9}$$

As can be seen, any rate $\dot{m}_j$ depends on current values of variable pressures, temperatures and cross-sections. Flows through the valves are treated in a quasi-stationary way. The program simulating the operation of the valves in this version of the EHVE uses the above formulae (5.7)–(5.9) as they all are governed valves, contrary to the variant described in Chap. 2, where some self-action valves were employed and hence additional differential equations describing their operation were needed.

The values of the coefficients of losses ζ_j equal to 0.85 found in the literature, e.g., [7], are typical in similar structures. The pressures p_a and p_b and the temperatures T_a, T_b in Eqs. (5.7)–(5.9) are calculated for particular valves in the following way

$$\text{for } j = 1$$

$$\text{if } p_{H1} > p_E \;:\; p_b = p_{H1}, \quad T_b = T_{H1}, \quad p_a = p_C, \tag{5.10a}$$

$$\text{if } p_E > p_{H1} \;:\; p_b = p_E, \quad T_b = T_E, \quad p_a = p_{H1}, \tag{5.10b}$$

$$\text{for } j = 2$$

$$\text{if } p_E > p_{Cl2} \;:\; p_b = p_E, \quad T_b = T_E, \quad p_a = p_{Cl2}, \tag{5.10c}$$

$$\text{if } p_{Cl2} > p_E \;:\; p_b = p_{Cl2}, \quad T_b = T_{Cl2}, \quad p_a = p_E, \tag{5.10d}$$

$$\text{for } j = 3$$

$$\text{if } p_C > p_{H3} \;:\; p_b = p_C, \quad T_b = T_C, \quad p_a = p_{H3}, \tag{5.10e}$$

$$\text{if } p_{H3} > p_C \;:\; p_b = p_{H3}, \quad T_b = T_{Cl2}, \quad p_a = p_C, \tag{5.10f}$$

$$\text{for } j = 4$$

$$\text{if } p_C > p_{Cl4} \;:\; p_b = p_C, \quad T_b = T_C, \quad p_a 6 = p_{Cl4}, \tag{5.10g}$$

$$\text{if } p_{Cl4} > p_C \;:\; p_b = p_{Cl4}. \quad T_b = T_{Cl4}, \quad p_a = p_C. \tag{5.10h}$$

Taking into account the assumption of quasi-stationary flows through the valves, the corresponding mass flow rates are presented in Fig. 5.7. This approximation is burdened with some errors in the calculations of $\dot{m}_j$ due to the fact that the non-stationary behaviour in the close vicinity of the valves is excluded.

The internal mass flow rates $\dot{m}_{H1}$ and $\dot{m}_{H3}$ between parts of the heater will be discussed in the next subsection.

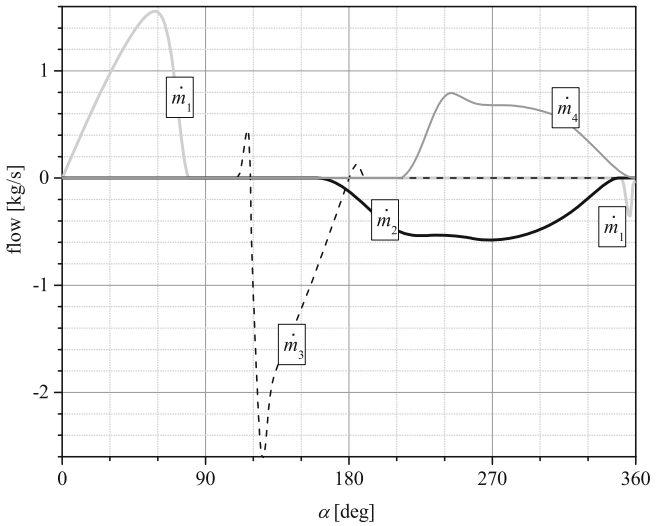

Fig. 5.7 Mass flow rates of the engine valves for 3000 rpm as a function of the crankshaft angle

5.2.3 Essential Equations for the New 2-Stroke EHVE

Let us start our considerations of the behaviour of the working fluid inside the EHVE from the expander. The equation of mass conservation is expressed by

$$\frac{\mathrm{d}\rho_E}{\mathrm{d}t} = \frac{1}{V_E}\left(\pm\dot{m}_1 \pm \dot{m}_2 - \rho_E \frac{\mathrm{d}V_E}{\mathrm{d}t}\right). \tag{5.11}$$

The equation of conservation described here takes into account the so-called inverse flows between the engine parts.

Varying signs of the mass flow rates $\dot{m}_1$ and $\dot{m}_2$ expressing the directions of the related flows through valves 1 and 2 are determined as follows

$$\dot{m}_1 \begin{cases} \text{if} & p_{H1} > p_E, \text{ sign "+"} \\ \text{if} & p_E > p_{H1}, \text{ sign "−"}, \end{cases} \tag{5.12a}$$

$$\dot{m}_2 \begin{cases} \text{if} & p_E > p_{Cl2}, \text{ sign "−"} \\ \text{if} & p_{Cl2} > p_E, \text{ sign "+"}. \end{cases} \tag{5.12b}$$

The equation of energy conservation applied to the expander is

$$\frac{\mathrm{d}T_E}{\mathrm{d}t} = \frac{1}{\rho_E V_E}\left[-T_E(\pm\dot{m}_1 \pm \dot{m}_2) + \kappa\left(\begin{Bmatrix} +\dot{m}_1 T_{H1} \\ -\dot{m}_1 T_E \end{Bmatrix} + \begin{Bmatrix} +\dot{m}_2 T_{Cl2} \\ -\dot{m}_2 T_E \end{Bmatrix} - \frac{p_E}{c_v}\frac{\mathrm{d}V_E}{\mathrm{d}t}\right)\right]. \tag{5.13}$$

The signs of the mass flow rate terms $\dot{m}_1$ and $\dot{m}_2$ in the above equations can be determined from Eq. (5.12). The alternative values of the temperature in the parenthesis are also chosen accordingly to the relations expressing the mass flow rates indicating the volumes currently connected through the flow. Such a notation is repeated later for other parts of the engine.

Finally, the last important value characterizing behaviour of the working fluid, i.e., the pressure p_E inside the expander, is calculated from the equation of state for ideal gas

$$p_E = \rho_E T_E R. \tag{5.14}$$

We need some explanation of the above. If the experimental equation of state for real gas (e.g., the one introduced by Peng and Robinson) is taken into account, the error for the extreme parameters of air, at 100 bar and 1000 °C, is smaller than 2 %. So, we will apply Eq. (5.14) here, and also for other parts of the engine.

For the compressor, we have very similar dependencies. We start from its equation of mass conservation which is expressed as

$$\frac{\mathrm{d}\rho_C}{\mathrm{d}t} = \frac{1}{V_C}\left(\pm\dot{m}_3 \pm \dot{m}_4 - \rho_C \frac{\mathrm{d}V_C}{\mathrm{d}t}\right). \tag{5.15}$$

The direction of a flow is determined by a choice of the signs of their mass flow rates as a set of conditional formulae

$$\dot{m}_3 \begin{cases} \text{if} & p_C > p_{H3}, \text{ sign "}-\text{"} \\ \text{if} & p_{H3} > p_C, \text{ sign "}+\text{"}, \end{cases} \tag{5.16a}$$

$$\dot{m}_4 \begin{cases} \text{if} & p_C > p_{Cl4}, \text{ sign "}-\text{"} \\ \text{if} & p_{Cl4} > p_C, \text{ sign "}+\text{"}. \end{cases} \tag{5.16b}$$

Next, the equation of energy conservation for the compressor is expressed as

$$\frac{\mathrm{d}T_C}{\mathrm{d}t} = \frac{1}{\rho_C V_C}\left(-T_C(\pm\dot{m}_3 \pm \dot{m}_4) + \kappa\left(\begin{Bmatrix} +\dot{m}_3 T_{H3} \\ -\dot{m}_3 T_C \end{Bmatrix} + \begin{Bmatrix} +\dot{m}_4 T_{Cl4} \\ -\dot{m}_4 T_C \end{Bmatrix} - \frac{p_C}{c_v}\frac{\mathrm{d}V_C}{\mathrm{d}t}\right)\right). \tag{5.17}$$

where the signs for the mass flow rates and alternative temperatures are determined from Eq. (5.16). As mentioned earlier, in Eqs. (5.13) and (5.17), we assume that no heat exchange takes place in the cylinders of the EHVE. In the last step for the compressor, we calculate the pressure inside its volume from the equation of state

$$p_C = \rho_C T_C R. \tag{5.18}$$

The heater model differs from the previous attempts and is divided into three parts of constant volumes, namely

1. inlet collector – V_{H3},
2. proper heater of a counter-current type – V_H,
3. outlet collector – V_{H1}.

These volumes suppose to play different roles for the model of the exchanger as explained earlier in this chapter.

Geometrical properties of the proper heater, its volume and heat exchange surface, are expressed by simple geometrical formulae

$$V_H = \frac{\pi d_H^2}{4} l_H n_H, \tag{5.19a}$$

$$A_H = \pi d_H l_H n_H. \tag{5.19b}$$

The working fluid flows from the volume of the compressor to the inlet collector of the heater V_{H3} through valve 3 (Fig. 5.3). Then, it reaches the proper heater volume V_H, transfers to the outlet collector V_{H1}, and finally leaves to the expander volume through valve 1. The blower B_1 forces the transport of the fluid internally from the outlet collector of the heater to its inlet. We assume that the temperature value calculated for the outlet collector is also transferred to the inlet one and the pressure drop between them is maintained by the blower B_1. The heater collectors are treated as settling chambers stabilizing the internal flows through their volumes. The mass flow rates $\dot{m}_{H1}$ and $\dot{m}_{H3}$ are usually different and they are calculated with Eq. (5.7) for the following relations of pressures and temperatures

$$\text{for } j = \mathrm{H_3}$$

$$\text{if } p_{H3} > p_H \ : \ p_b = p_{H3}, \quad T_b = T_{H3}, \quad p_a = p_H, \tag{5.20a}$$

$$\text{if } p_H > p_{H3} \ : \ p_b = p_H, \quad T_b = T_H, \quad p_a = p_{H3}, \tag{5.20b}$$

$$\text{for } j = \mathrm{H_1}$$

$$\text{if } p_H > p_{H1} \ : \ p_b = p_H, \quad T_b = T_H, \quad p_a = p_{H1}, \tag{5.20c}$$

$$\text{if } p_{H1} > p_H \ : \ p_b = p_{H1}, \quad T_b = T_{H1}, \quad p_a = p_H. \tag{5.20d}$$

We need to calculate the values of the cross-sections for the internal flows to be applied then in Eq. (5.7), which are

$$A_{H1} = A_{H3} = \frac{\pi d_H^2}{4} n_H. \tag{5.21}$$

The losses in flows through the valves are assumed as $\zeta_{H1} = \zeta_{H3} = 0.85$. The signs of the mass flow rates representing the directions of the internal flow $\dot{m}_{H1}$ and $\dot{m}_{H3}$ will be defined below.

The blower working in the hot air circulation loop forces the flow and assures that the Reynolds number calculated for the exchanger tubes is not smaller than 10^4, when valves 1 and 3 remain closed and $\dot{m}_1 = \dot{m}_3 = 0$, see Fig. 5.3, due to fact the internal flow through the heater exists. In such a situation, the Reynolds number

caused by the flow from the first blower can be calculated using the formula

$$\mathrm{Re}_H = \frac{4\dot{m}_{B1}}{\pi d_H \mu_H n_H}, \tag{5.22}$$

where the blower mass flow rate $\dot{m}_{B1}$ is calculated according to the above-mentioned condition $\mathrm{Re}_H = 10^4$. The Nusselt number for the proper heater tubes is determined by

$$\mathrm{Nu}_H = 0.022\,\mathrm{Re}_H^{0.8}\mathrm{Pr}_H^{0.6}. \tag{5.23}$$

Here, Re_H is calculated as a value that varies and uses current values of the internal flow rate $\dot{m}_H$ flowing through the heater. The value $\dot{m}_{B1}$ is a fraction of $\dot{m}_H$, but it occurs when valves 1 and 3 are closed and the blower B_1 works in the internal loop, Fig. 5.3. The coefficient of heat transfer for the working fluid is calculated as

$$\alpha_{AH} = \frac{\mathrm{Nu}_H \lambda_H}{d_H}. \tag{5.24}$$

The heat stream supplied in the volume of the heater is a time-dependent function and is determined in the following way

$$\dot{Q}_{AH} = \alpha_{AH} A_H (T_{wH} - T_H). \tag{5.25}$$

where T_{wH} is the maximal temperature of the heater wall. For a given rotational speed of the engine, its assumed values are included in Table 5.1. T_H in the above formula is also a time-dependent temperature of the air inside heater tubes, at their outlet position, as described earlier in the theoretical model.

In the next step, the pressures in both collectors are discussed. At the inlet to the boosted heater collector H_3, the pressure increases by Δp_{H3}, see Eq. (5.29). The proper heater contains long tubes, which, as a consequence, is followed by the pressure friction losses Δp_{Hf}, calculated for the overall tube length. Thus, the pressure in the outlet heater collector H_1 decreases by Δp_{Hf} and is expressed in Eq. (5.37).

Now, the fundamental equations related to the heater will be considered. The calculations of the inlet collector V_{H3} result from the basic formulae for this part of the heater. The equation of mass conservation takes the form as follows

$$\frac{\mathrm{d}\rho_{H3}}{\mathrm{d}t} = \frac{1}{V_{H3}} \left(\pm\dot{m}_3 \pm \dot{m}_{H3} + \dot{m}_{B1}\right). \tag{5.26}$$

Table 5.1 Rotations and thermodynamic parameters of the EHVE

n_{EHVE}	(rpm)	3000	2500	2000	1500	1000
$T_{wH\,max}$	(K)	1273	1173	1073	973	873
ρ_{H1}	(kg/m^3)	27.9	28.0	28.2	28.3	28.5
ρ_{Cl4}	(kg/m^3)	14.0	14.1	14.3	14.5	14.9

The signs of the mass flow rates in this part of the heater are chosen from the conditions

$$\dot{m}_3 \begin{cases} \text{if} & p_C > p_{H3}, \text{ sign "+"} \\ \text{if} & p_{H3} > p_C, \text{ sign "−"}, \end{cases} \tag{5.27a}$$

$$\dot{m}_{H3} \begin{cases} \text{if} & p_{H3} > p_H, \text{ sign "−"} \\ \text{if} & p_H > p_{H3}, \text{ sign "+"}. \end{cases} \tag{5.27b}$$

The equation of energy conservation in the collector H_3 is described by

$$\frac{\mathrm{d}T_{H3}}{\mathrm{d}t} = \frac{1}{\rho_{H3} V_{H3}} \Bigg[- T_{H3}(\pm\dot{m}_3 \pm \dot{m}_{H3} + \dot{m}_{B1}) + \kappa \left(\left\{ \begin{matrix} +\dot{m}_3 T_C \\ -\dot{m}_3 T_{H3} \end{matrix} \right\} + \left\{ \begin{matrix} +\dot{m}_{H3} T_H \\ -\dot{m}_{H3} T_{H3} \end{matrix} \right\} + \dot{m}_{B1} T_{H1} \right) \Bigg]. \tag{5.28}$$

As the blowers operate unidirectionally in order to force the desired internal flow, the positive mass flow rate of the blower B_1 is taken into account. The last equation for this collector expresses the pressure p_{H3} inside its volume and includes the blower mass flow rate

$$p_{H3} = \rho_{H3} T_{H3} R + \Delta p_{H3}. \tag{5.29}$$

Let us consider the basic equations for the behaviour of the working fluid in the proper part of the heater V_H. We start again from the equation of mass conservation which takes the form of

$$\frac{\mathrm{d}\rho_H}{\mathrm{d}t} = \frac{1}{V_H} \left(\pm\dot{m}_{H1} \pm \dot{m}_{H3} \right), \tag{5.30}$$

where the alternatives for directions of the internal flows between heater elements are described by the following conditions

$$\dot{m}_{H1} \begin{cases} \text{if} & p_{H1} > p_H, \text{ sign "+"} \\ \text{if} & p_H > p_{H1}, \text{ sign "−"}, \end{cases} \tag{5.31a}$$

$$\dot{m}_{H3} \begin{cases} \text{if} & p_H > p_{H3}, \text{ sign "−"} \\ \text{if} & p_{H3} > p_H, \text{ sign "+"}. \end{cases} \tag{5.31b}$$

The equation of energy conservation in the volume V_H is expressed by the derivative of temperature T_H

$$\frac{\mathrm{d}T_H}{\mathrm{d}t} = \frac{1}{\rho_H V_H} \Bigg[- T_H(\pm\dot{m}_{H1} \pm \dot{m}_{H3}) + \kappa \left(\left\{ \begin{matrix} +\dot{m}_{H1} T_{H1} \\ -\dot{m}_{H1} T_H \end{matrix} \right\} + \left\{ \begin{matrix} +\dot{m}_{H3} T_{H3} \\ -\dot{m}_{H3} T_H \end{matrix} \right\} \right) + \frac{\dot{Q}_{AH}}{c_v} \Bigg]. \tag{5.32}$$

The signs of the internal mass flow rates $\dot{m}_{H1}$ and $\dot{m}_{H3}$ are chosen according to Eq. (5.31), but the current value of the heat stream $\dot{Q}_{AH}$ reflects the behaviour of the complete heater. The equation of state for this part of the heater gives the value of the pressure at the end of its tubes

$$p_H = \rho_H T_H R. \tag{5.33}$$

Finally, let us discuss the outlet heater collector of the volume V_{H1}. The equation of mass conservation takes here the form of

$$\frac{\mathrm{d}\rho_{H1}}{\mathrm{d}t} = \frac{1}{V_H}\left(\pm\dot{m}_{H1} \pm \dot{m}_1 - \dot{m}_{B1}\right), \tag{5.34}$$

where the alternatives for directions of the current flows including the collector, expander and local blower are

$$\dot{m}_{H1}\begin{cases}\text{if} & p_H > p_{H1}, \text{ sign "+"} \\ \text{if} & p_{H1} > p_H, \text{ sign "}-\text{"}\end{cases} \tag{5.35a}$$

$$\dot{m}_1\begin{cases}\text{if} & p_{H1} > p_E, \text{ sign "}-\text{"} \\ \text{if} & p_E > p_{H1}, \text{ sign "+"}\end{cases} \tag{5.35b}$$

The equation of energy conservation for this collector is represented by

$$\frac{\mathrm{d}T_{H1}}{\mathrm{d}t} = \frac{1}{\rho_{H1}V_{H1}}\Bigg[-T_{H1}(\pm\dot{m}_{H1} \pm \dot{m}_1 - \dot{m}_{B1}) + \kappa\left(\left\{\begin{matrix}+\dot{m}_{H1}T_H \\ -\dot{m}_{H1}T_{H1}\end{matrix}\right\} + \left\{\begin{matrix}+\dot{m}_1 T_E \\ -\dot{m}_1 T_{H1}\end{matrix}\right\}\right) - \dot{m}_{B1}T_{H1}\Bigg]. \tag{5.36}$$

The directions of the mass flow rates $\dot{m}_{H1}$ and $\dot{m}_1$ together with alternative values of temperatures in the connected volumes are given in Eq. (5.35).

The value of the pressure inside this collector volume V_{H1} results from the equation of state

$$p_{H1} = \rho_{H1}T_{H1}R - \Delta p_{Hf}. \tag{5.37}$$

Eventually, a cooler of the constant volume is considered. It is also divided into three parts, as has been done for the heater, namely

1. inlet collector – V_{Cl2},
2. proper cooler of a counter-current type – V_{Cl},
3. outlet collector – V_{Cl4}.

The values of the volume of the cooler and the cooling surface are expressed by geometrical relations

$$V_{Cl} = \frac{\pi d_{Cl}^2}{4} l_{Cl} n_{Cl}, \tag{5.38a}$$

$$A_{Cl} = \pi d_{Cl} l_{Cl} n_{Cl}. \tag{5.38b}$$

The working fluid is flowing from the expander to the inlet collector of the cooler V_{Cl2} through valve 2, see Fig. 5.4. Then, it is transferred from the inlet collector through the proper cooler V_{Cl} to the outlet collector V_{Cl4}, finally reaching the volume of the compressor through valve 4.

The blower B_2 makes the working medium transfer from the outlet collector to the inlet one inside the cooler. The temperature in the outlet collector is assumed to transfer directly to the inlet and a pressure drop between them is covered by the B_2 blower operation. Moreover, as for the heater, the cooler collectors are treated as settling chambers stabilizing the flow. The blower, which operates in the cooling loop, causes that the value of the Reynolds number is not lower than 10^4 during the phases when valves 2 and 4 are closed and the cooler volume is cut off from any cylinder. It is calculated as a function of the blower B_2 as

$$\mathrm{Re}_{Cl} = \frac{4\dot{m}_{B2}}{\pi d_{Cl} \mu_{Cl} n_{Cl}}, \tag{5.39}$$

where the value of the flow rate $\dot{m}_{B2}$ is determined according to the above equation for values of $\mathrm{Re_{Cl}} = 10^4$.

The current value for the Nusselt number for the proper cooler part tubes is obtained from

$$\mathrm{Nu}_{Cl} = 0.022\,\mathrm{Re}_{Cl}^{0.8}\,\mathrm{Pr}_{Cl}^{0.6}. \tag{5.40}$$

where the value of $\mathrm{Re_{Cl}}$ varies and uses currently determined values of the flow rate $\dot{m}_{Cl}$ flowing through the cooler. The value $\dot{m}_{B2}$ being a fractional part of $\dot{m}_{Cl}$ occurs when valves 2 and 4 are closed and the blower B_2 works in the internal cooler loop. The heat transfer coefficient in this volume of the engine is

$$\alpha_{ACl} = \frac{\mathrm{Nu}_{Cl} \lambda_{Cl}}{d_{Cl}}. \tag{5.41}$$

The amount of the heat stream in the complete cooler section yields the following function calculated at each time step

$$\dot{Q}_{ACl} = \alpha_{ACl} A_{Cl} (T_{wCl} - T_{Cl}). \tag{5.42}$$

where, in agreement with the described theoretical model, the temperature T_{wCl} takes the minimal value of the cooler wall, and T_{Cl} is the temperature of the air inside the cooler tubes, at their outlet. The temperature of the working fluid along the cooler diminishes, being, in fact, between the values obtained in the collectors Cl_2 and Cl_4, but the heat stream expressed by Eq. (5.42) is calculated for the overall length of its tubes. From the theoretical model, the temperature is determined at the outlet from

the cooler tubes, the final plane of the proper part of the cooler, and depends on time only.

Dependencies for the pressures in the collectors of the cooler are determined similarly to those of the heater. The inlet boosted collector is now the one marked by Cl_2 and the outlet collector is Cl_4, respectively. The action of the blower causes a pressure increase in Cl_2 by Δp_{Cl2}, and a decrease in Cl_4 by Δp_{Clf} in order to force properly the internal flow.

The mass flow rates in and out of the cooler are, like in the heater, not equal to each other and their calculations are conducted on the basis of Eq. (5.7), with the alternative conditions

$$\text{for } j = Cl_2$$

$$\text{if } p_{Cl2} > p_{Cl} \; : \; p_b = p_{Cl2}\,, \quad T_b = T_{Cl2}\,, \quad p_a = p_{cl}\,, \tag{5.43a}$$

$$\text{if } p_{Cl} > p_{Cl2} \; : \; p_b = p_{Cl}\,, \quad T_b = T_{Cl4}\,, \quad p_a = p_{Cl2}\,, \tag{5.43b}$$

$$\text{for } j = Cl_4 \tag{5.43c}$$

$$\text{if } p_{Cl} > p_{Cl4} \; : \; p_b = p_{Cl}\,, \quad T_b = T_{Cl}\,, \quad p_a = p_{Cl4}\,, \tag{5.43d}$$

$$\text{if } p_{Cl4} > p_{Cl} \; : \; p_b = p_{Cl4}\,, \quad T_b = T_{Cl4}\,, \quad p_a = p_{Cl}\,. \tag{5.43e}$$

The values of the cross-sections and the loss coefficients in the cooler flows, assumed as for the heater, required to solve Eq. (5.7), are as follows

$$A_{Cl2} = A_{Cl4} = \frac{\pi d_{Cl}^2 n_{Cl}}{4}, \tag{5.44a}$$

$$\zeta_{Cl2} = \zeta_{Cl4} = 0.85\,. \tag{5.44b}$$

The approach applied to the cooler is the same as the one used for the heater. All necessary parameters applied in the simulations are determined from reasonable values reflecting real working conditions.

5.2.4 Power and Efficiency

The formulae for determination of the work of the expander and the compressor are calculated for the varying angle $0° \le \alpha \le 360°$, related to a full cycle of work in a similar way as for the 2-stroke engine

$$L_E = \int_{\alpha=0°}^{\alpha=360°} p_E(\alpha) \frac{\mathrm{d}V_E}{\mathrm{d}\alpha} \mathrm{d}\alpha\,, \tag{5.45a}$$

$$L_C = \int_{\alpha=0°}^{\alpha=360°} p_C(\alpha) \frac{\mathrm{d}V_C}{\mathrm{d}\alpha} \mathrm{d}\alpha\,, \tag{5.45b}$$

The above-mentioned pressures are determined in such a way that mass flow losses in the valves are accounted for in order to make simulations realistic. Thus, the effective work of the engine is a sum of the following components including losses caused by the blowers and friction

$$L = L_E + L_C - L_{B1} - L_{B2} - L_f\,, \tag{5.46}$$

where the values of work consumed by the blowers are

$$L_{Bi} = \frac{2\pi \dot{m}_{Bi} h_{SBi}}{\omega_{Bi}\eta_{Bi}} \quad \text{for } i = 1, 2. \tag{5.47}$$

The symbols used will be explained later in Sect. 5.3, whereas an enthalpy isentropic increase of the blowers is expressed as

$$h_{SBi} = \frac{\kappa}{\kappa - 1} 2RT_{Bi}\left(\Pi_{Bi}^{\frac{\kappa}{\kappa-1}} - 1\right). \tag{5.48}$$

The total power output generated in the externally heated 2-stroke engine is then

$$P = \frac{\omega}{2\pi} L. \tag{5.49}$$

The heat transferred by the working fluid inside the heater, following the theoretical model, is calculated as the integral

$$Q_H = \int_{\alpha=0^\circ}^{\alpha=360^\circ} \dot{Q}_{AH} \frac{\mathrm{d}\alpha}{\omega}, \tag{5.50}$$

where the heat stream value results from Eq. (5.25). Finally, the theoretical and practical efficiencies of the engine are in cases without and with use of a pre-heater

$$\eta = \frac{L}{Q_H}, \tag{5.51a}$$

$$\eta_{PH} = \frac{L}{Q_{H-PH}}. \tag{5.51b}$$

The value of the efficiency can be discussed in more detail. The amount of the delivered heat Q_H has been considered up to now without application of any additional heat exchanger in the model. However, the temperature of the working fluid leaving the volume of the heater (Figs. 5.1 and 5.6) is very high, so adding an additional heat exchanger can take the form of a pre-heater and should be applied as described in [8]. The operation of a pre-heater increases the temperature in front of the inlet to the heater and provides considerable savings of the energy of the heating fluid by decreasing this way the denominator in Eq. (5.51a) from Q_H to Q_{H-PH}. Hence, the overall efficiency of the EHVE should increase considerably.

5.3 Results of the Simulations

The simulation process uses a custom written program built with the standard C++ language which applies chosen library procedures and solvers described in [9]. The integration procedure involves a typical Runge-Kutta 4th order method in the numerical task which, due to the applied attempt of time dependent algorithm, was reduced to a solution of a system of nonlinear, ordinary differential equations. The set includes the following formulae (5.11), (5.13), (5.15), (5.17), (5.26), (5.28), (5.30), (5.32), (5.34), (5.36) with appropriate switching conditions controlling the internal flows between engine parts, supplemented by a system of non-linear, algebraic equations describing behaviour of particular parts of the model.

All simulation runs started from identical initial conditions which represent the particular amount of the working fluid and its thermodynamic properties enclosed in all engine volumes. For particular purposes, some parameters which influence the obtained results were investigated. The integration process continued until the solution reached integrated values, different in relative measures by no more than 0.01 % from those obtained in the previous cycle. This way, a stationary, periodic solution to this problem for engine operation at a given, constant rotational speed of the engine was reached. The numerical errors were due to the procedures applied and their accuracy was within the limits of double precision numbers. An adaptive step-size integration method with an additional, forced decrease in the step near switching values in order to find the proper moment and identify switching conditions for events like valve opening/closing was applied. The size of the integration step and limits of approval of the consecutive results were selected on the basis of a thorough analysis of a wide range of their values. It should be mentioned that due to the nature of equations applied, the system presents quick convergence of the solutions and low sensitivity to integration step changes.

The satisfying agreement of the integrated values with the experimental results published earlier in Chap. 3 for the early variant of the engine allows us to apply the procedures for the modified version. In most cases, a stable solution was attained after 100–200 cycles of simulated full crankshaft revolutions. The performance numbers for the engine, as power which is described according to Eqs. (5.46) and (5.49), and efficiency – according to Eqs. (5.51a), were calculated at the end of each working cycle. To make the results realistic, many physical losses were taken into account. The heat transfer through the engine model cylinders was not considered, although we assume they are to be water-cooled as in standard internal combustion engines. The losses caused by the heat transfer obviously depend on a kind of insulation applied in the design, so they cannot be accurately included. Therefore, we estimate the total errors of the calculation in terms of the effective power and efficiency to fall within 5 % of the results presented in Fig. 5.11. In order to show a full picture of the behaviour of the elements of the engine, in Figs. 5.5, 5.6 and 5.7, pressures, temperatures and mass flow rates through the valves at rotational speed of 3000 rpm are depicted.

Due to the nature of counter-current heat exchangers, we assume the temperature of the heater walls with an increase in the engine rotational speed and this relation is to reflect the amount of heating fluid delivered, see Table 5.1. In order to simplify the cooling process, standard tap water is predicted as a cooling fluid, so the minimal temperature of the cooler wall is assumed constant and equal to $T_{wCl} = 300\,\mathrm{K}$. The coefficients of heat conduction, dynamic viscosity and specific heats for the working fluid are assumed from the physical properties of air.

Any type of drive of the blowers, either electrical or mechanical, coming directly from the engine, has to be controlled. The rotational speeds of the blowers are approximately constant and their angular velocities are assumed as $\omega_{Bi} = 314\,\mathrm{rad/s}$. The working fluid temperatures and pressures at the inlet to the blowers, i.e., also in the outlet collectors of the heat exchangers, decrease with the rotational speed of the engine, but its density changes insensibly for different deliveries forced by the blowers, thus it is possible to apply them. The mass flow rate $\dot{m}_{Bi} \geq 0.06\,\mathrm{kg/s}$ is the minimal value, for the assumed form of the heat exchangers, for which it is possible to obtain the value of the Reynolds number Re$= 10^4$, during the period when the engine valves are closed. The rotational speed of the engine, the maximal temperature of its heater walls, the averaged densities of the working fluid inside the outlet collectors are presented in Table 5.1.

Other essential data used in the investigations are presented below. The cylinders dimensions are shown in Table 5.2. The valve phases and dimensions are given in Table 5.3. The data assumed for the heat exchangers are given in Table 5.4. T_{bBi} stands for temperatures taken from the outlet of the collectors H_1 and Cl_4 and vary in each simulation cycle. Other essential data set for the blowers are shown in Table 5.5. The values of the above angles, which determine the behaviour of the valve governing system data, are chosen after the preliminary optimization calculations.

A value of the blower pressure step Δp_{H3} depends on the structure of collectors and heat exchangers. Simplifying the investigation process, all values of Δps are assumed to be equal to 10 kPa, when the EHVE works at 3000 rpm.

Table 5.2 Dimensions of the cylinders of the EHVE

Cylinder	Diameter d (m)	Stroke s (m)	Dead height h_0 (m)
Expander	0.083	0.08340	0.0025
Compressor	0.083	0.06255	0.0017

Table 5.3 Control angles and dimensions of the EHVE valves

Valve No.	Opening α_{io}	Closing α_{ic}	Transient $\Delta\alpha_i$	Max. flow area (m^2)
1	$-10°$	80°	35°	0.0010
2	160°	350°	90°	0.0005
3	110°	190°	35°	0.0010
4	210°	360°	50°	0.0005

Table 5.4 Dimensions of the EHVE heat exchangers

Exchanger	Diameter d (m)	Length l (m)	Number of pipes n (−)	Volume V (m^3)
Heater H	0.01	2.0	15	0.00236
Collector H_1				0.00050
Collector H_3				0.00050
Cooler Cl	0.01	2.0	15	0.00236
Collector Cl_2				0.00050
Collector Cl_4				0.00050

Table 5.5 Data of the EHVE blowers

Π_{Bi}	1.03	Input to output pressure ratio in the blower
η_{Bi}	0.70	Assumed efficiency value of the blowers

Some examples of application of the model simulations were already presented in Figs. 5.5, 5.6 and 5.7, where explanations are given in detail in their respective captions. In all cases, the blowers are working with the flow rate of $\dot{m}_{Bi} = 0.1\,\text{kg/s}$. Figure 5.6 needs some attention. The simulation results of the theoretical model for all temperatures are presented. Note the difference caused by the blowers with distinctive values of T_{H3} for the heater and T_{Cl2} for the cooler from their respective temperatures in other parts – T_{H1}, T_H, and, T_{Cl4}, T_{Cl}. The accuracy of the applied approach to the heat exchangers is under continuous control, and, the pressure and the temperature at the outlet from the heater H are always transferred to the pressure and the temperature in the outlet collector H_1.

Let us discuss the results shown in Fig. 5.8 which presents the engine diagram $p - V$, cylinder pressure versus respective volume for both of them, obtained on the assumption of the volume ratio $V_C / V_E = 0.75$. This value is considered as the optimal one for the variant of the engine when we apply a large heater, defined by the volume ratio $V_H \approx 5\,V_E$. The difference in the areas covered by both pressure loops indicates useful work created in the engine.

Another relation of the EHVE pressures, this time as a function of inverted density values, is shown in Fig. 5.9. It is simply the $p-v$ diagram as $v = 1/\rho$ for the complete engine. It shows that the heat can be delivered to the engine under condition

$$p = \text{const},$$

whereas for the early model, see Fig. 2.3, only an isochoric process took place

$$V = \text{const}.$$

This is a very important result of the change in the heat delivery process introduced in this chapter.

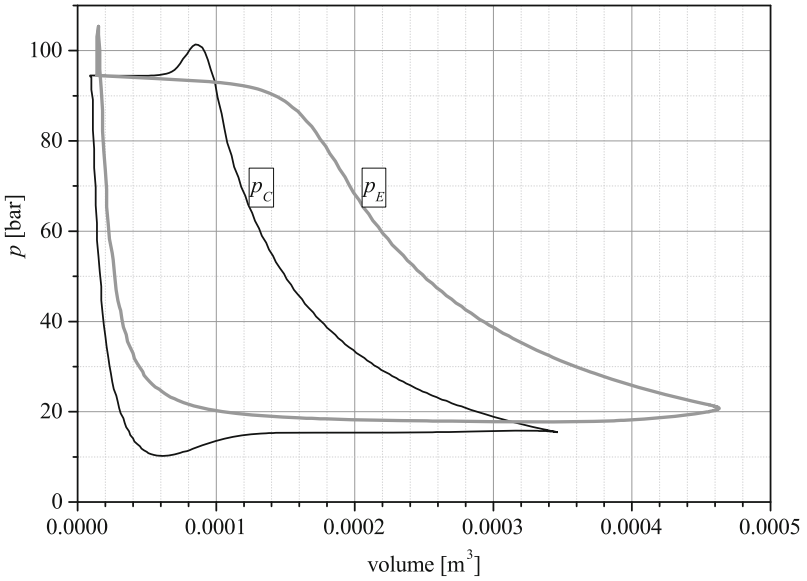

Fig. 5.8 $p - V$ diagram at 3000 rpm for both engine cylinders

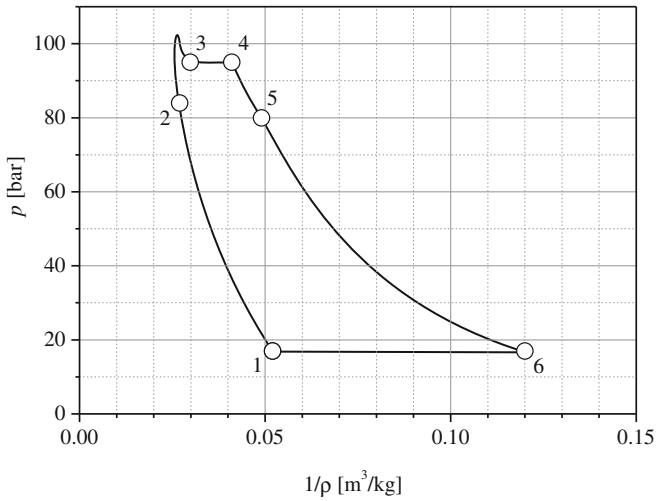

Fig. 5.9 Diagram of the pressure versus inverted density dependence for this variant of the EHVE. *1–2* compression, *2–3* compression and heating, *3–4* heating, *4–5* expanding and heating, *5–6* expanding, *6–1* cooling. See the corresponding discussion in Sect. 2.5

As mentioned above, the cylinders are different. For the ratio of their volumes $V_C / V_E = 0.75$, the power and efficiency are found to be highest. More details of the optimization results and the way of determination of V_C / V_E are presented in [10].

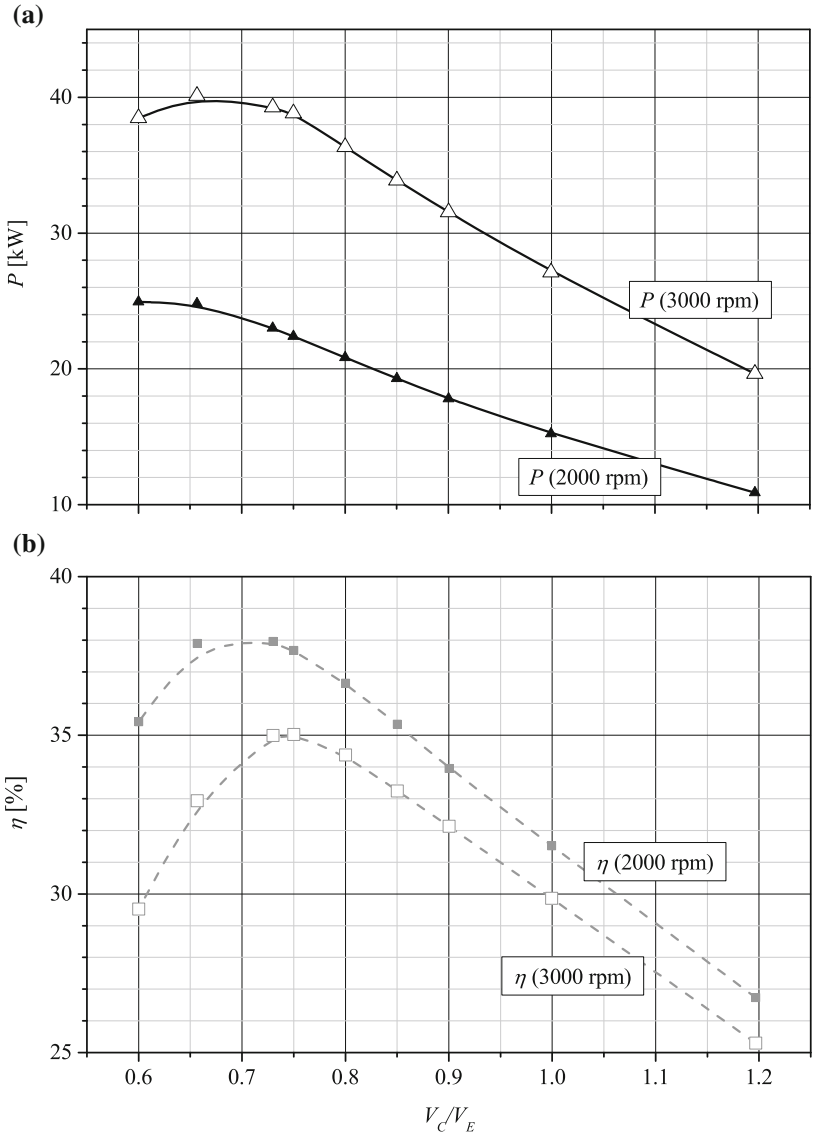

Fig. 5.10 Power (**a**) and efficiency (**b**) of the engine as a function of the ratio of cylinder to expander volumes at 2000 and 3000 rpm, correspondingly

It is important to remind that the ratio is always lower than 1 for the engine with external heating. The representative results are presented in Fig. 5.10.

Another view of the EHVE performance is presented in Fig. 5.11, where values of the power and efficiency of the engine are depicted as functions of its rotational

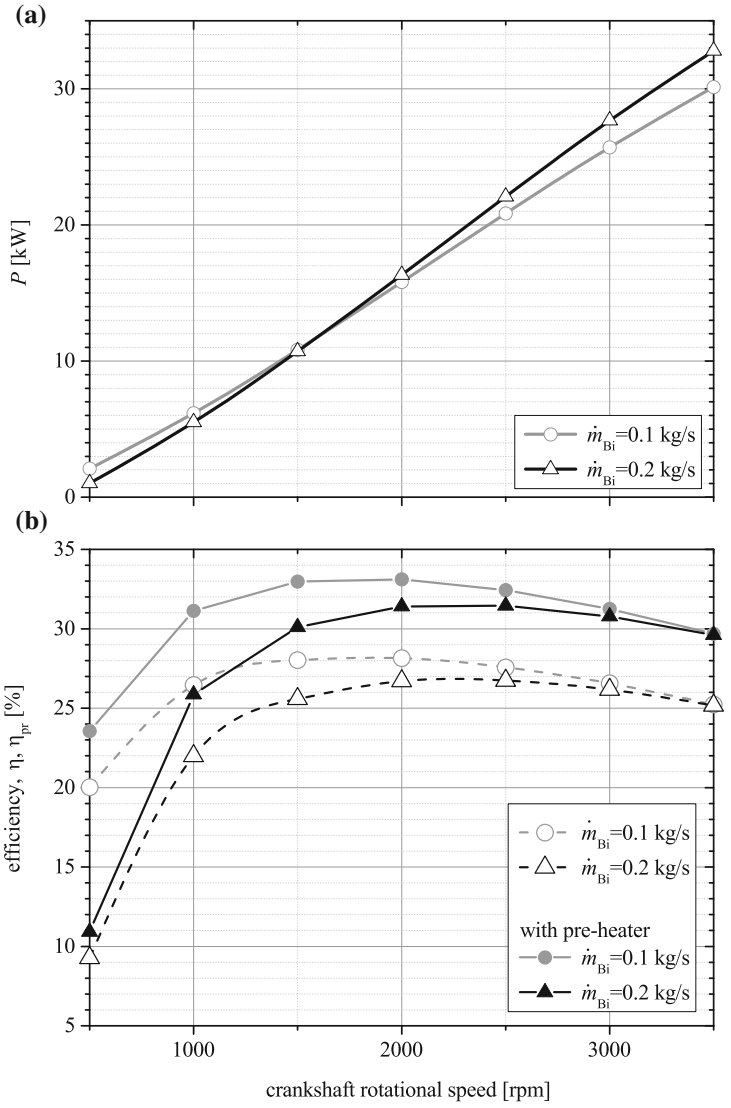

Fig. 5.11 Power (**a**) and efficiency (**b**) of the engine as a function of its rotational speed and blowers delivery for both cases when of a pre-heater is used

speed with the blowers operating at different flow rates, i.e., 0.1 and 0.2 kg/s, correspondingly. The power characteristics shown in part (a) of the figure does not differ too much in both cases of the blowers flow rate and presents only an inconsiderable difference in increasing linear shapes of them. As discussed at the end of the previous section, the heat delivered when a pre-heater is applied has to be lower and here it is

assumed to be equal only to

$$Q_{H-PH} = 0.85 Q_H .$$

This rather modest assumption can be easily met in real installations. In this case, the efficiency of the EHVE is obviously higher than when there is no pre-heater and is presented in Fig. 5.11b as η_{pr}, continuous lines and full symbols. An increase in the obtained values ranges from about 10–12 to 20 %, depending on the rotational speed of the engine. We can safely estimate that a profit from the pre-heater will be about 30 % under the normal working speed of 1500 rpm, at the blowers flow rate of 0.1 kg/s.

5.4 Dynamic Behaviour of the Engine

All previously presented results were attained for stable and constant rotational speeds of the model. It was assumed that the moment of inertia of the crankshaft system was large enough not to cause any visible changes in the rotation during a cycle of the EHVE operation. Now, we are to consider some realistic values of mechanical properties of the model based on the following equation

$$I_{cs} \frac{\mathrm{d}\omega}{\mathrm{d}t} + \frac{1}{2} \frac{\mathrm{d}I_{cs}}{\mathrm{d}t} \omega = M_{pr}(t) - M_r(t). \tag{5.52}$$

The second term on the LHS of Eq. (5.52) can be omitted as, for simplification, we assume that the moment of inertia I_{cs} does not vary in time.

The difference in the driving and friction moments is

$$M_{pr}(t) - M_F(t) = \frac{1}{2} (p_E A_E s_E - p_C A_C s_C) \sin\alpha - (40 + c_R \omega^2). \tag{5.53}$$

The value of the resistance moment M_r depends on the type of an engine, and the coefficient c_R is an important number, usually determined experimentally. In order to show how the angular velocity ω changes as a function of the angle of rotation α during a work cycle with varying values of the moment of inertia I_{cs}, see Fig. 5.12. As a result, the more inertia properties are applied at the crankshaft the flatter behaviour of ω is observed. A common value of the averaged angular velocity is shown as ω_{AV}.

The calculations were made for the data presented in Tables 5.6 and 5.7. The temperatures of the heat exchanger walls were assumed as $T_{wH} = 1200$ K for the heater and $T_{wCL} = 298$ K for the cooler. The value of the coefficient c_R was estimated as 0.005. All valves of the engine were of the governed type with the cross-section values

$$A_1 = A_3 = 0.001\,\mathrm{m}^2 \text{ and } A_2 = A_4 = 0.0005\,\mathrm{m}^2.$$

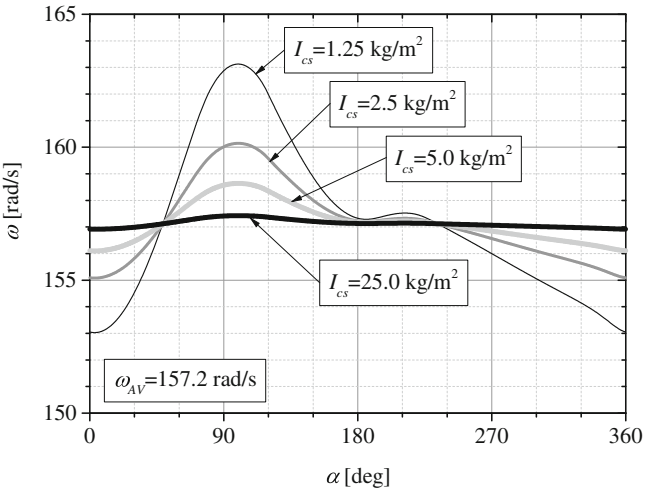

Fig. 5.12 Changes in the rotational speed during a work cycle when the moment of inertia of the flywheel varies between 1.25 and 25.0 kg/m^2

Table 5.6 Physical data of the cylinders

Cylinder	Diameter (m)	Stroke (m)
Expander	0.09	0.0925
Compressor	0.09	0.0694

Table 5.7 Dimensions of the heat exchangers

Exchanger	Diameter d (m)	Length l (m)	Number of pipes n (−)	Exchange area A_H m^2)	Volume V (m^3)
Heater H	0.008	2.0	15	0.754	1.5×10^{-3}
Cooler Cl	0.008	2.0	15	0.754	1.5×10^{-3}

The data for all valve angles were set as in Table 5.3 before. The working fluid was again atmospheric air with its data taken from thermodynamic tables at 1500 rpm.

5.4.1 Control of Rotations

We aim to control the engine speed with a dynamical method in two ways, namely

- by changing temperature of the heater wall,
- by adding/removing mass of the working fluid to/from the cooler volume, or,
- by a combination of the two above-mentioned manners.

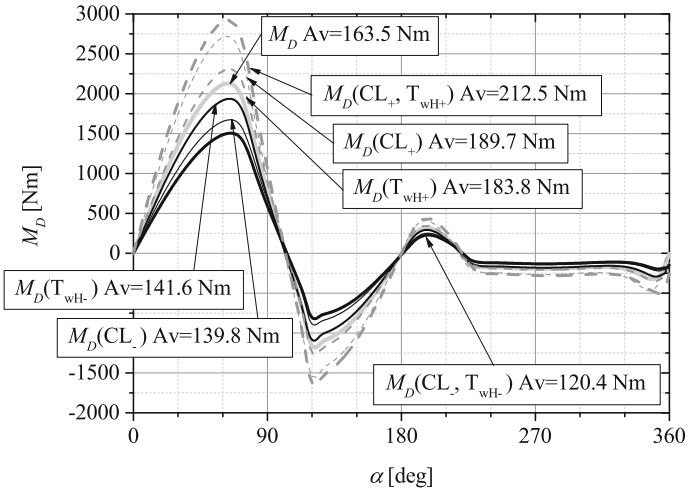

Fig. 5.13 Changes of the driving torque for cases 1–6 showing averaged values

The first of the above methods directly increases energy of the unchanged mass of the working fluid enclosed in all volumes of the engine. The second one increases the mass inside the EHVE and, therefore, influences other variables, resulting thus in a change of performance.

Let us consider some examples. We start from a case when the angular velocity reaches a stable level of 157 rad/s (1500 rpm) and then some alternations in the parameters controlling the velocity are introduced until a new stable state is attained (Fig. 5.13). Duration of linearly changing parameters lasted for 200 simulated cycles, then another stable state of work was achieved. Under such conditions, the torque was equal to 163.5 Nm. The efficiency reaches a level of 30 % and the power output is slightly higher than 20 kW. In all cases, the pressure ratio of maximal to minimal values remains between 5 and 6. The effects of all the above-mentioned control methods on the achieved power and efficiency of the EHVE are presented in Figs. 5.13 and 5.14. A detailed list of the proposed methods is listed below.

1. Removal of some amount of the working fluid from the cooler, simply by opening an additional valve and releasing some air from that volume to the atmosphere. See Fig. 5.15 for the results.
2. Adding some amount of the working fluid to the cooler, for example by opening an additional valve and allowing the flow from the compressed air tank to this volume. This situation is depicted in Fig. 5.16 with almost symmetrical effect when compared to the previous case.
3. Lowering temperature of the heater wall by some amount. This can be done by diminishing the external heating process, depending on its type. If burning is used, then a smaller amount of fuel is delivered. The results are presented in Fig. 5.17. The value of torque is lowest and equal to 120.4 Nm.

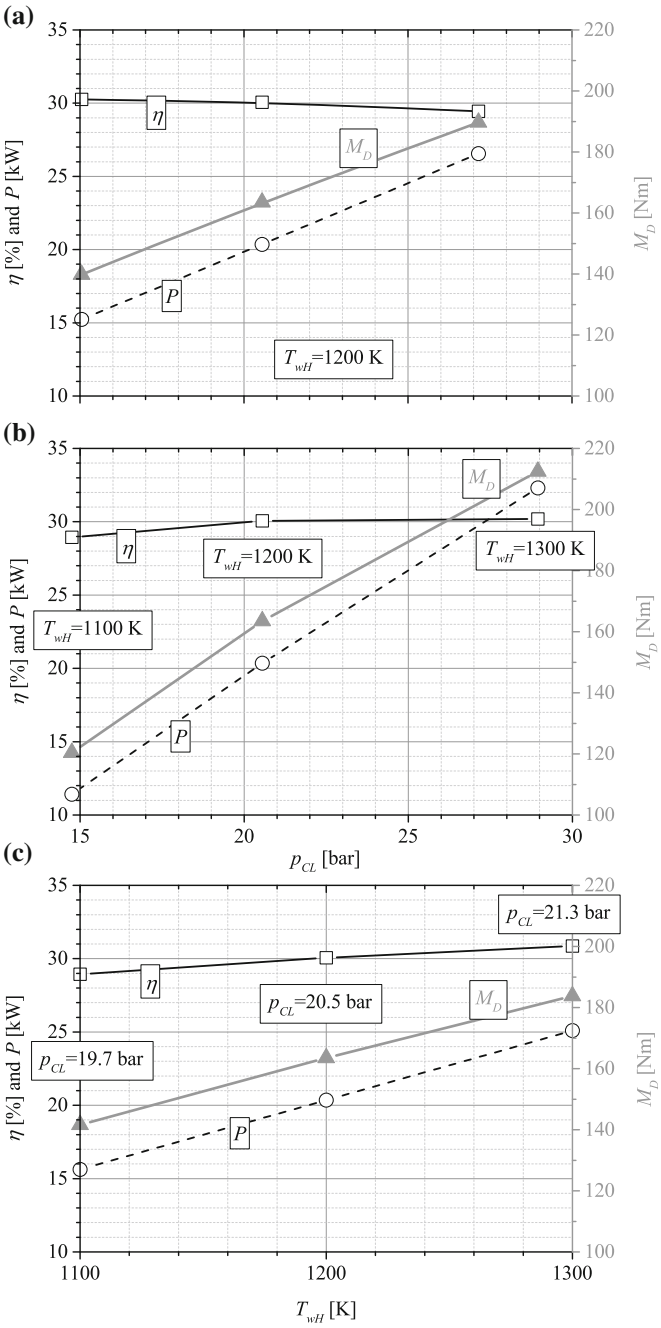

Fig. 5.14 Power P, efficiency η and an average value of the torque M_D as functions of changes of the cooler pressure only (**a**), the cooler pressure combined with the heater wall temperature (**b**), and, the heater wall temperature only (**c**)

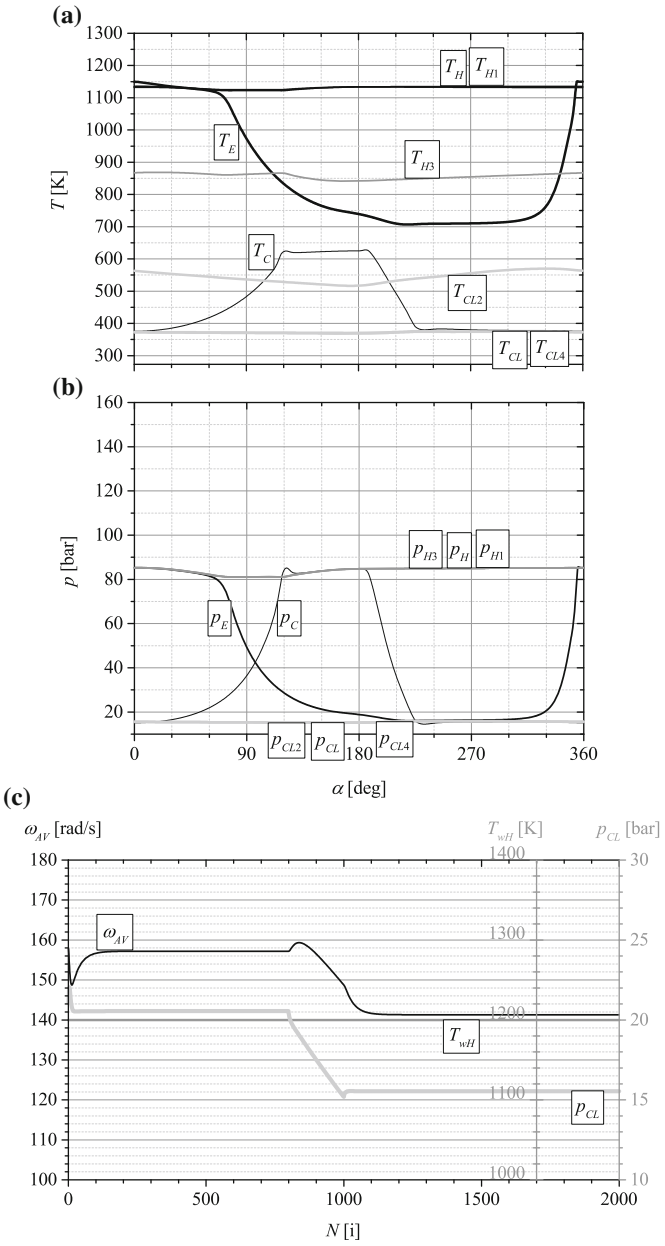

Fig. 5.15 Changes of the rotational speed as a result of the mass removed from the cooler, its pressure p_{CL} drops by about 5.5 bar. The heater wall temperature T_{wH} remains unchanged. The angular velocity drops from 157.2 to 141.3, i.e., by 15.9 rad/s (≈152 rpm). Part **a** temperatures, **b** pressures and **c** average rotational speed, heater wall temperature and cooler pressure versus a number of iterations

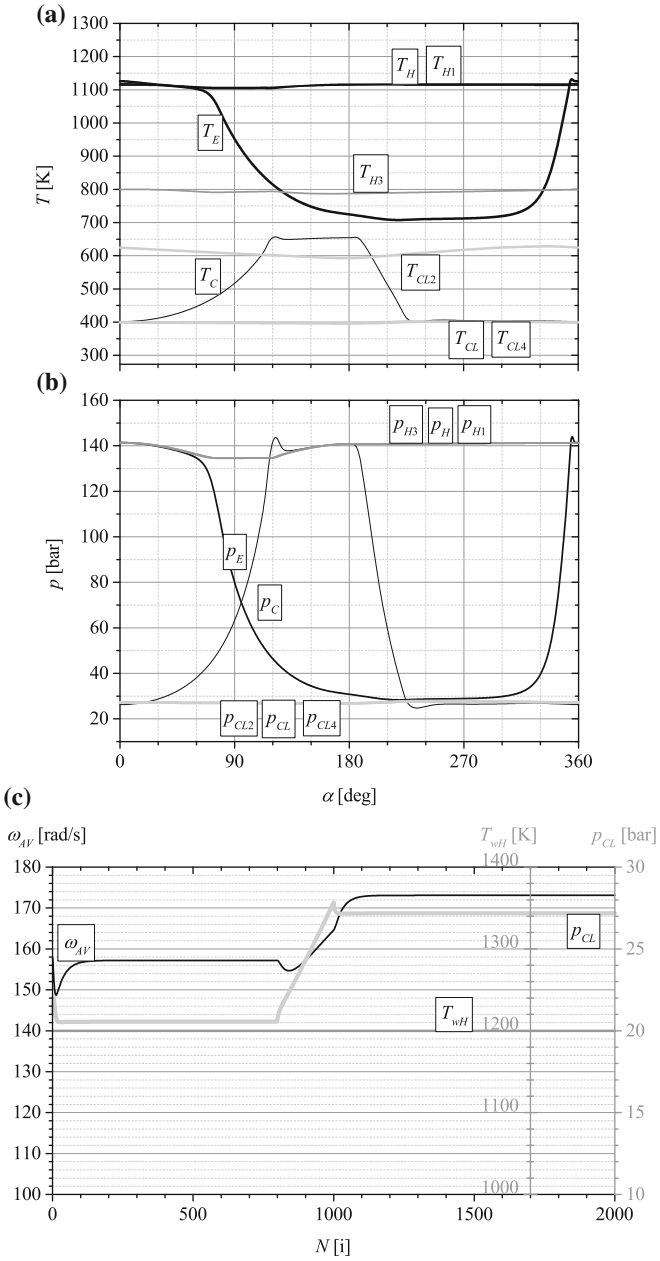

Fig. 5.16 Changes of the rotational speed as a result of the mass added to the cooler, its pressure p_{CL} increases by about 6.6 bar. The heater wall temperature T_{wH} remains unchanged. The angular velocity increases from 157.2 to 173.8, i.e., by 16.6 rad/s (≈158 rpm). Part **a** temperatures, **b** pressures and **c** average rotational speed, heater wall temperature and cooler pressure versus a number of iterations

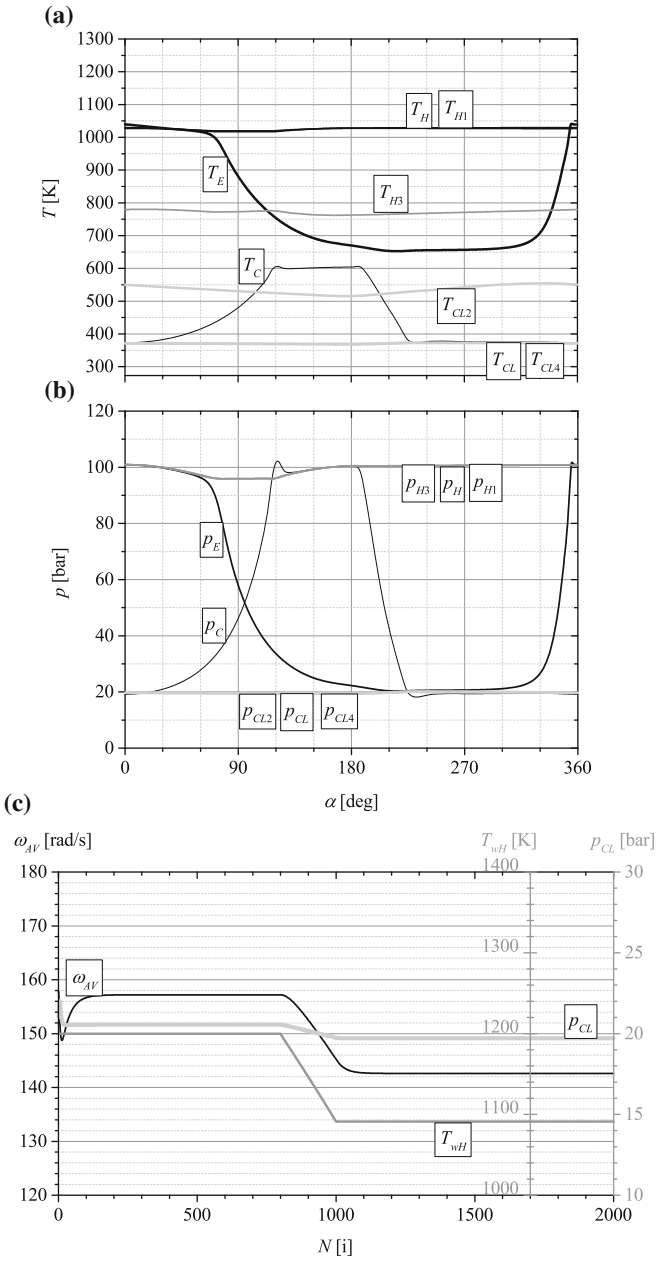

Fig. 5.17 Changes of the rotational speed as a result of a decrease in the heater wall temperature by 100 K, whereas no mass was added to the engine. The cooler pressure decreases by 0.8 bar, the angular velocity drops from 157.2 to 146.6, i.e., by 10.6 rad/s (≈101 rpm). Part **a** temperatures, **b** pressures and **c** average rotational speed, heater wall temperature and cooler pressure versus a number of iterations

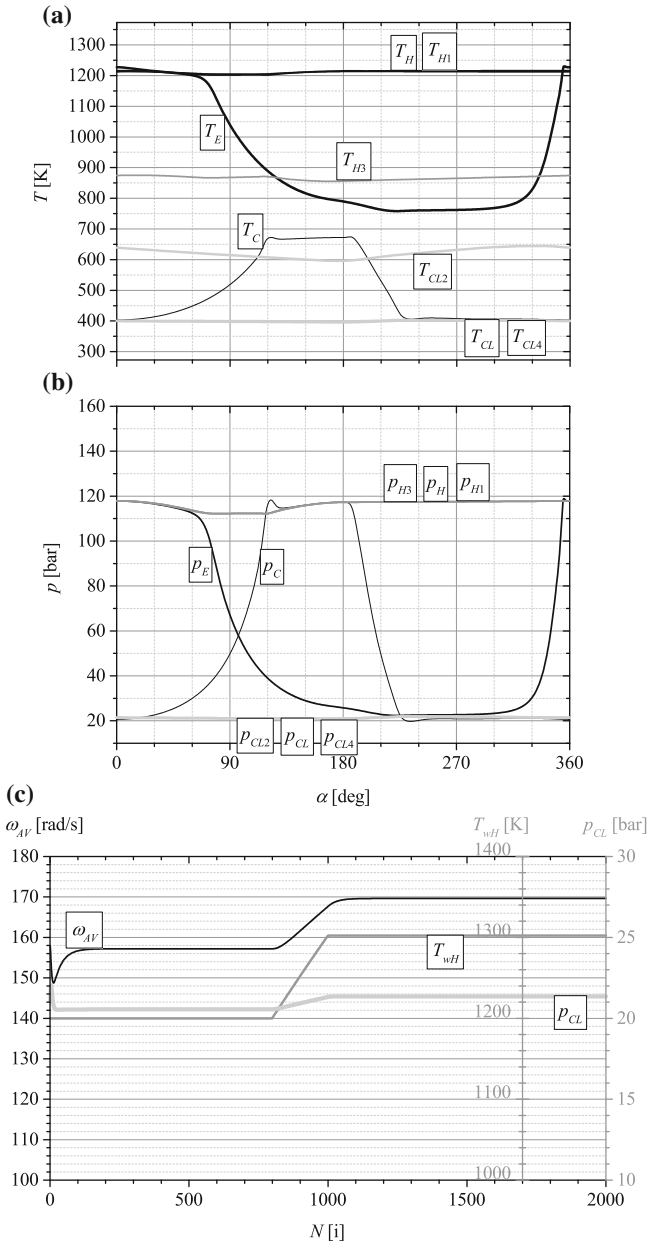

Fig. 5.18 Changes of the rotational speed as a result of an increase in the heater wall temperature by 100 K, whereas no mass was added to the engine. The cooler pressure increases by 0.8 bar, the angular velocity grows from 157.2 to 169.3, i.e., by 12.4 rad/s (≈118 rpm). Part **a** temperatures, **b** pressures and **c** average rotational speed, heater wall temperature and cooler pressure versus a number of iterations

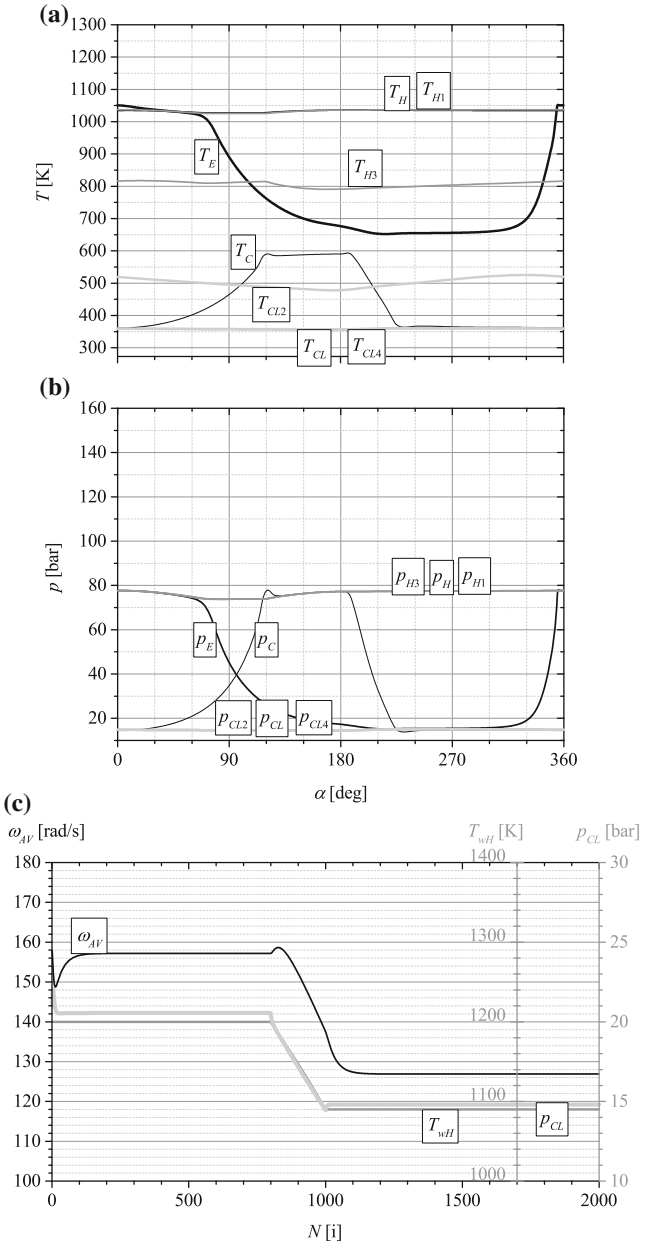

Fig. 5.19 Changes of the rotational speed as a result of a combination of the mass removed from the cooler and a decrease in the heater wall temperature T_{wH} by 100 K. The cooler pressure p_{CL} totally drops by about 5.8 bar. The angular velocity decreases from 157.2 to 126.9, i.e., 30.3 rad/s ($\approx$289 rpm). Part **a** temperatures, **b** pressures and **c** average rotational speed, heater wall temperature and cooler pressure versus a number of iterations

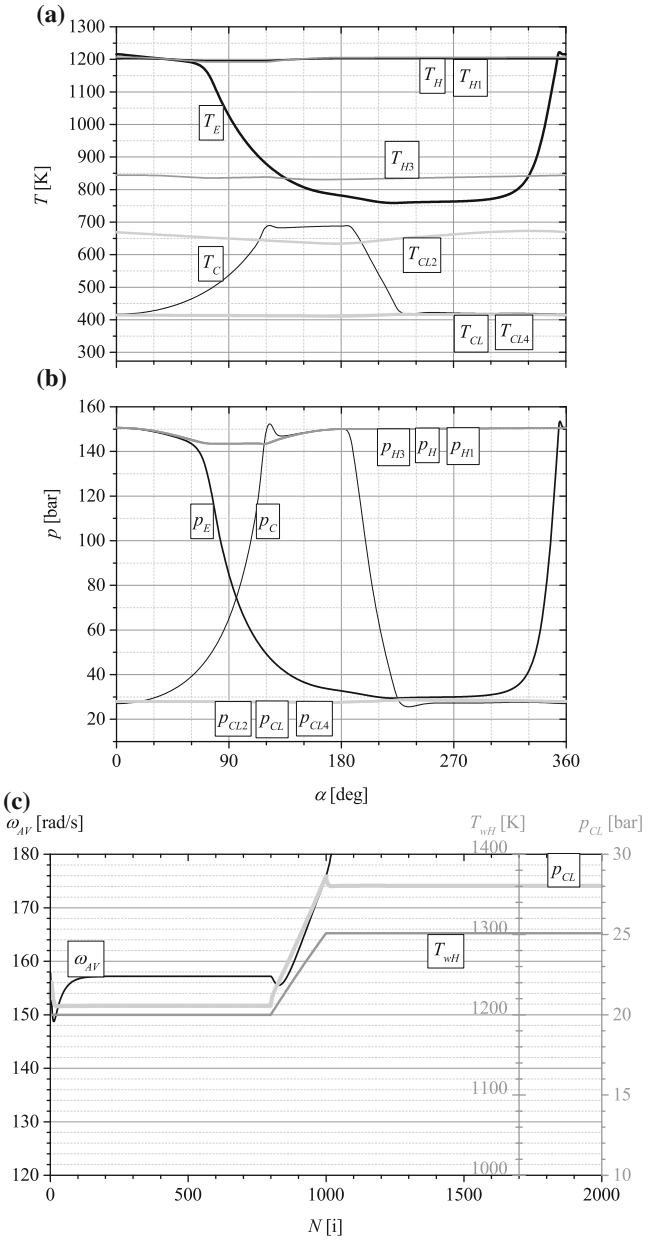

Fig. 5.20 Changes of the rotational speed as a result of combination of the mass added to the cooler and an increase in the heater wall temperature T_{wH} by 100 K. The cooler pressure p_{CL} totally grows by about 8.4 bar. The angular velocity increases from 157.2 to 185.8, i.e., 28.6 rad/s (≈273 rpm). Part **a** temperatures, **b** pressures and **c** average rotation speed, heater wall temperature and cooler pressure versus a number of iterations

4. Increasing the temperature of the heater wall. Any kind of external heating can be applied to achieve this goal. As in above cases 1 and 2, the results look almost symmetrical to case 3 and are depicted in Fig. 5.18.
5. A combination of the two ways to diminish parameters in order to achieve more visible changes in the speed. The rotational speed slows down by about 290 rpm, see Fig. 5.19.
6. Finally, another combination allowing for a larger increase in the rotations by about 270 rpm is presented in Fig. 5.20. Here, the maximal cycle pressure is about 150 bar, with the lowest value just below 30. The highest torque equal to 212.5 Nm is observed.

5.5 Remarks on the Developed 2-Stroke Engine

The two-stroke externally heated valve engine in the version discussed here has moderate exchangers, up to $5V_E$, it works in a closed heat cycle with air as its working fluid, and, additionally, has a conventional crankshaft and an oil lubrication system as in all previous variants. The version of the engine is now supplemented with two blowers aimed to increase the volume of heat exchange when valves connecting the cylinders remain closed.

A disadvantage of the EHVE is a short period of opening of valves delivering a hot fluid to the expander. However, in numerous designs of modern engines with internal heating, proper valve control has already been attained. This fact supplemented with a possibility to use rotary valves is very promising from the viewpoint of the final design of the EHVE.

The mass flow rates transported through so widely discussed valves 1 and 3 should not interfere with the continuous internal flow forced inside the heat exchangers by the blowers B_1 and B_2 in order to increase the amount of heat delivered. This task can be achieved through a specific, custom made design of the collectors.

The essential diagram in this chapter, presented in Fig. 5.11, shows the efficiency and power of the EHVE as functions of the engine rotational speed. Taking into account practical difficulties in installing a blower in the loop of extreme high temperature and pressure, the benefits coming from the application of blowers have to be significant.

What should be emphasized, the EHVE with blowers reaches an efficiency level of the same value as the Stirling engine with a similar cylinder working volume, when a pre-heater is applied. What is even more important, the EHVE uses atmospheric air, whereas the Stirling engine works with helium as the working fluid. Extrapolating the obtained results to the power produced by 1 l volume of the engine at 1500 rpm, we arrive at the following numbers: the Stirling engine yields 28 kW/l, the EHVE with blowers reaches 27 kW/l, whereas the efficiency in both cases is about 32 %. At the rotational speed of 3000 rpm, the EHVE efficiency considered for the blowers rate of 0.1 kg/s and with a pre-heater is to be approx. 31 %, whereas the power reaches

an impressive value of 55 kW/l. More comparisons with Stirling engines are to be presented in Chap. 8.

Figure 5.6 shows diagrams for the temperature of the heater of about 1000 °C. For a solar heat source, so high temperature needs an application of a large set of specifically designed solar concentrators. The calculations of the engine for a lower temperature of the heater and rotational speeds have been performed, but not included here. The engine should operate properly under such conditions as well although the performance will be lower, depending on the heater wall temperature available.

Dynamical behaviour of the model has been investigated in order to demonstrate an ability of the EHVE to control the rotational speed. This aim can be attained in two ways – either by changing an amount of mass of the working fluid enclosed in all volumes (by pumping compressed air or releasing some) or by heating/cooling the heater wall – a change in the temperature influences the energy stored by the fluid. Any combination of the above is possible as well. A summary of the results is presented in Fig. 5.16 as the changes in the EHVE power and efficiency which result from such control.

References

1. Brzeski L, Kazimierski Z (1995) New type of heat engine—externally heated air engine. In: SAE technical papers series paper 950092, International Congress and Exposition, Detroit, Michigan, 27 Feb–2 Mar, 1995. doi:10.4271/950092
2. Brzeski L, Kazimierski Z (1995) Computer simulation of a new type heat engine operation. Comput Assist Methods Eng Sci 2(2):129–139
3. Kazimierski Z, Brzeski L, Wojewoda J (1995) Thermodynamical cycle of a new type of the externally heated engine. Arch Thermodyn 16(3–4):197–215
4. Kazimierski Z, Wojewoda J (2011) Externally heated valve air engine with two small heaters operating alternatively. In: Proceeding of SYMKOM 2011, Turbomachinery, vol. 140, pp 105–114
5. Kovač A (1980) Les moteurs volumétriques á cycle fermé: une vioe peu prospecteé dans le redéploiement énérgetique. Entropie **16**(92):23–30
6. Wisniewski S (1998) The heat exchange. PWN, Warsaw
7. Dejc ME, Zaranin AE (1984) Gasodynamics, Energoizdat Press (In Russian)
8. Watanabe T, et al. (1988) NS30A Stirling engine for heat pump use. In: The 4th International Conferences on Stirling Engines, Tokyo, 1988
9. Press WH (2007) Numerical recipes: the art of scientific computing. Cambridge University Press, Cambridge
10. Kazimierski Z, Wojewoda J (2008) Numerical optimization of externally heated valve air engine with blowers. In: Proceedings of SYMKOM 2008, Turbomachinery, vol. 133, pp 157–164

Chapter 6
Separate Settling Chambers in the Improved 2-Stroke EHVE

Air-powered heat engines like the EHVE, which works in a modified Joule cycle, are still subject to continuous development, both theoretical as shown in [1] and practical, for example [2]. The heat exchange process taking place in such energy generating devices remains under continuous investigations, see [3].

Detailed analyses of flows, covering a wide range of practical applications as sound pipes [4], through cavitation effects in cross-flows [5], nozzle effects with entropy noise [6], or even sound generation [7], are discussed in the book. Many researchers were involved in the investigations of supersonic wind tunnels and turbine devices in order to stabilize internal flows and the results can be applied in the EHVE for similar purposes. For instance, an attempt to predict the pressure characteristics is shown in [8], whereas [9] discusses temperature effects in testing aerodynamic forces. A model for Reynolds number tests is presented in [10]. In [11] a significant role of settling chambers in attaining quiet, low turbulent open jet bursts downstream of the wind tunnel is shown.

The presence of separate settling chambers as described below affects the steady operation of heat exchangers. As a two-stroke engine, the EHVE is equipped with two cylinders, an expander and a compressor, situated between heat exchangers: a heater and a cooler. Similarly to typical internal combustion engines, it has also a conventional crankshaft and an oil lubrication system. The phase angle between the pistons of the expander and compressor is equal to 180°.

The experimental investigations conducted on the EHVE prototype in its early version were presented in Chap. 3. As shown there, the heat exchange could not reach an efficient level when valves 1 and 3 allowing the flows from the heat exchangers were closed. Thus, a new concept arose to use two blowers in the heat exchange internal loops, introduced in Chap. 5 but in a different way. According to this new idea, separate settling chambers are needed to make the heat exchange process steady and, thus, more efficient in charging proper heat exchangers. Consequently, two blowers B_1 and B_2 are included in this new version.

The settling chambers composed of four elements, and additional blowers, also consisting of four devices, are new parts of this version of the EHVE. The separate

Z. Kazimierski and J. Wojewoda, *Externally Heated Valve Engine*,
Springer Tracts in Mechanical Engineering, DOI 10.1007/978-3-319-28355-5_6

settling chambers are additional volumes and so are the blowers, whose task is to obtain a pressure drop in the exchangers. The next section, devoted to the behaviour inside the heater and cooler volumes, describes some other possibilities. Although some solutions with two small heaters operating alternatively were mentioned in Chap. 4, they, however, are not simpler than the ones presented here. Damping properties of the settling chambers were not taken into account in the modelling process.

6.1 Modelling of the Heat Exchanger Operation

As described earlier in Chap. 5 and later in Chap. 8, the collectors of heat exchangers may play a role of settling chambers stabilizing the flow. The highly unsteady working fluid flow incoming from the engine at one side is changed into an almost stationary stream at the other side. As a matter of fact, an unsteady flow can be characterized by some small alternations. The level of changes depends on the applied design and settling chambers volume. However, the algorithm used in the model which is described in Chap. 5 does not take into account any devices stabilizing the working fluid flow and assumes its passage through the collectors to be unsteady.

In this chapter, the behaviour and performance of the proposed engine operating under stationary conditions of its heat exchangers and a comparison to the non-stationary state are subject of detailed investigation. We do not aim at an actual design of the settling chambers, but focus on an explanation why almost stationary work of the exchangers is possible. Figure 6.1 illustrates a separation of collectors and settling chambers in heat exchangers of different types. The manufactured chambers can take other forms, for example, they may be connected to the collectors. It will involve some engineering solutions and, consequently, experimental verification, but is not subject to consideration here.

As far as the idea of the EHVE is concerned, the important issue to be discussed is a pressure increment which appears just upstream of the heater and the cooler, Δp_{H3}, Δp_{Cl2}, respectively, and a decrement, Δp_{H1}, Δp_{Cl4}, respectively, downstream of the exchangers. The values of the above mentioned pressure drops Δps are to be assumed as parameters for the simulation program based on the algorithm described in Chap. 5. The question how to do it, remains a design application. It should be attained by the blowers B_{H3}, B_{H1}, B_{Cl2} and B_{Cl4} and will be discussed below. Nevertheless, other solutions are also possible, although they need to be verified experimentally.

Moreover, the previously presented model included the two blowers B_1 and B_2 making the forced air move from both the collectors H_1 and Cl_4 to H_3 and Cl_2 volumes, correspondingly. Thus, the blowers intensify the heat exchange by increasing the air flow in the exchangers, which is reflected by a value of the Reynolds number calculated in each time step of simulations. Simultaneously, the operation of the blowers B_1 and B_2 is followed by alternations in the temperatures inside both heat exchangers. This includes an increase in the temperature T_{H3} in the heater inlet collector, instead of T_C^{max}, and a decrease in T_{Cl2} in the cooler inlet one, instead of T_E^{min}, respectively (Fig. 6.2).

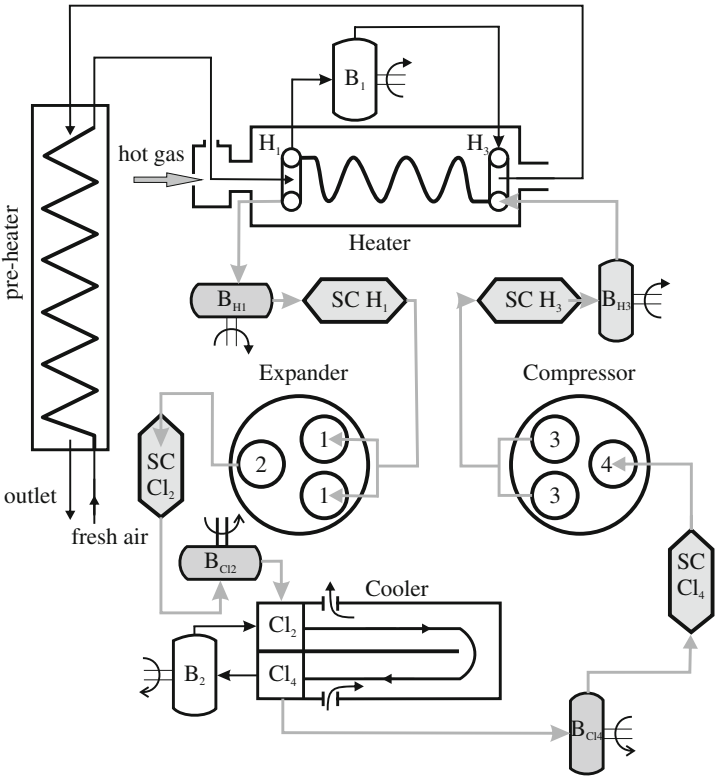

Fig. 6.1 Schematic view of the improved 2-stroke EHVE, B_1, B_2, B_{H1}, B_{H3}, B_{Cl2}, B_{Cl4} – blowers, SC_{H1}, SC_{H3}, SC_{Cl2}, SC_{Cl4} – separate settling chambers, 1, 2, 3, 4 – valves, H_1, H_3 – heater collectors, Cl_2, Cl_4 – cooler collectors. The new elements changing the design with respect to that presented in Chap. 5 are marked in *grey*

An application of the blowers B_1 and B_2 is followed by two benefits, namely:

- an increase in the mass flow rate in the exchangers, and
- an advantageous change in the temperature of the working fluid delivered to the expander.

The disadvantages caused by their application and the necessary blowers B_{H3}, B_{H1}, B_{Cl2} and B_{Cl4} are such that they work with their respective collectors, for example, B_1 and B_{H3} connected to the collector H_3, Fig. 6.1, etc. Hence, the blowers should have similar characteristics to act in parallel.

Both the blowers B_1 and B_2 might be removed if the blowers B_{H1}, B_{H3}, B_{Cl2} and B_{Cl4} are applied. Unfortunately, this causes that the Reynolds number values in the exchangers diminish. Additionally, the heat exchange area significantly increases if the maximal temperature of the heated fluid is close to that one when two blowers B_1 and B_2 are installed. On the other hand, a lack of B_1 and B_2 is attractive because

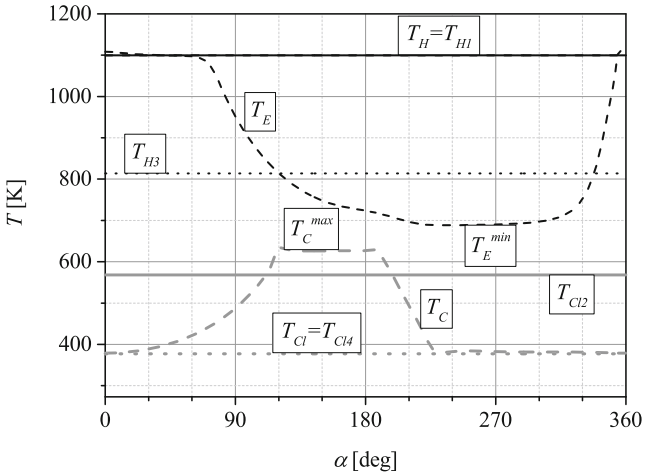

Fig. 6.2 Temperatures in the EHVE with the blowers B_1 and B_2 at the mass flow rate of 0.1 kg/s

only the set of blowers B_{H1}, B_{H3}, B_{Cl2} and B_{Cl4} remains and their characteristics does not need to be related to those of B_1 and B_2.

The set-up of the engine cylinders in the new simulation model remains the same as previously discussed. This version of the EHVE also works in a closed heat cycle. It means that the amount of the working fluid mass remains the same throughout the whole cycle. The value of the engine operation period varies, depending on rotations and is denoted as t_{pe}. An amount of the mass delivered or subtracted by the valve inside a chamber is marked as M_v. At the steady side of a settling chamber, the mass flow rate is assumed constant and equal to

$$\dot{m}_j = \frac{M_v}{t_{pe}} + \dot{m}_{Bi}, \tag{6.1}$$

where $\dot{m}_{Bi}$ $(i = 1, 2)$ are mass flow rates in the blower B_1 and B_2. When either B_1 or B_2 does not exist, the mass flow rates through the heat exchangers $\dot{m}_j$ $(j = \text{H,Cl})$ diminish. The first part of the RHS of Eq. (6.1) is fully described later in Sect. 6.3, where the mass flow rate of additional blowers is denoted in Eq. (6.12) as $\dot{m}_k$.

A turbulent flow of the working fluid through the exchangers is assumed, i.e., the value of the Reynolds number should be $\text{Re} \geq 10^4$. The heat transfer coefficient is calculated for the outlet of the heater in the following steps

$$\text{Re}_H = \frac{4\dot{m}_H}{\pi\, d_H\, \mu_H\, n_H}, \tag{6.2a}$$

$$\text{Nu}_H = 0.022(\text{Re}_H)^{0.8}\,(Pr_H)^{0.6}, \tag{6.2b}$$

and finally

$$\alpha_{AH} = \mathrm{Nu}_H \frac{\lambda_H}{d_H}. \tag{6.3}$$

The constant values of the working fluid heat coefficients μ and λ are taken as averaged values within the temperature range in the exchangers volumes from their inlet to the outlet. The heat stream delivered in the complete heater is

$$\dot{Q}_{AH} = \alpha_{AH} A_H (T_{wH} - T_H). \tag{6.4}$$

Here, the heat exchange area $A_H = \pi d_H l_H n_H$, and $(T_{wH} - T_H)$ is a temperature difference between the heater wall T_{wH} and the working fluid inside its tubes T_H at the end of the period of the engine cycle. The difference $(T_{wH} - T_H)$ does not vary much for the counter-current heat exchangers modelled in the engine. The value of the temperature T_{wH} is assumed at the fluid outlet, similarly to the attempt presented in Chap. 5. For the cooler, we apply a similar procedure as described above for the heater.

In the new model of the heat exchange collectors, the density and the temperature are assumed constant, thus the equations for the unsteady temperature obtained previously transform into simpler formulae determining the constant values of temperatures in these collectors. As the heat exchangers operate in a stationary way, the temperature equation takes the form, e.g., for the heater

$$C_{pH} \dot{m}_H (T_{H1} - T_{H3}) - \dot{Q}_{AH} = 0. \tag{6.5}$$

The above amount of the transferred heat stream $\dot{Q}_{AH}$ has to remain the same as defined in Eq. (6.4). Similarly, in the cooler, the value of $\dot{Q}_{ACl}$ is determined and two equations are obtained for the heater and the cooler. They are used for the calculation of the values of the temperatures T_H and T_{Cl}, according to the new way of modelling. The results, if the two blowers B_1 and B_2 exist, are presented in Fig. 6.2. Having in mind all the above considerations, the heat stream for the heat exchangers of the engine can be determined and it seems to be constant during the period of the crankshaft rotation t_{pe}.

6.2 Power and Efficiency of the EHVE with Separate Settling Chambers

Let us describe the way how the power and the efficiency are estimated for the modelled version of the engine. First, an amount of work attained in the expander and the compressor can be calculated for a full cycle of the crankshaft rotation as

$$L_E = \int_{\alpha=0^\circ}^{\alpha=360^\circ} p_E(\alpha) \frac{dV_E}{d\alpha} d\alpha, \tag{6.6a}$$

$$L_C = \int_{\alpha=0^\circ}^{\alpha=360^\circ} p_C(\alpha) \frac{dV_C}{d\alpha} d\alpha. \tag{6.6b}$$

All the above pressure values are determined when losses in the valves are included into consideration. Thus, the work of the EHVE is

$$L = L_E + L_C - \int_{j=1}^{n} L_{Bj} - L_f - L_{sup}, \tag{6.7}$$

where $\int_{j=1}^{n} L_{Bj}$ is the work consumed by the blowers and L_f is the work lost due to friction between moving parts in the machine. L_{sup} marks an amount of work lost in all additional devices related to the engine. The blowers consume an inconsiderable amount of the power generated. The losses caused by the settling chambers are also included, they are estimated in the range from 80 to 160 J. This way, a total power output of the EHVE can be expressed as

$$P = \frac{L}{t_{pe}}. \tag{6.8}$$

An amount of the heat delivered during the period of work to the engine is

$$Q_H = \dot{Q}_{AH} \frac{2\pi}{\omega}. \tag{6.9}$$

Finally, we can define now the efficiency of the engine as

$$\eta = \frac{L}{Q_H}, \tag{6.10a}$$

$$\eta_{PH} = \frac{L}{Q_{H-PH}}. \tag{6.10b}$$

Here, the value of the heat delivered Q_H is calculated without any additional heat exchanger. Usually, the temperature of the fluid heating the heater pipes at its outlet is very high (Fig. 6.2), so a pre-heater may be applied. This is an additional heat exchanger so it raises the inlet temperature of the heating fluid and brings considerable savings in the heat demand, decreasing the denominator value in Eq. (6.10a) from Q_H to the value shown in Eq. (6.10b) as Q_{H-PH}.

6.3 Computer Calculations

This way of description of the simulated model is a combination of the one previously described in Chap. 5 and the new attempt presented earlier. As assumed, the following data are taken for the model: a constant output rotational speed of 1500 rpm, collector volumes of 10 L, the maximal cycle pressure in the engine of about 100 bar, the temperatures of heat exchangers at their outlet, for the heater $T_{wH} = 1200\,\mathrm{K}$ and for the cooler $T_{wCl} = 298\,\mathrm{K}$, respectively. Tables 6.1 and 6.2 include other important data, except for different values of A_H and A_{Cl} that result from the presence or absence of the blowers B_1 and B_2, correspondingly. Both heat exchange areas were controlled by changing lengths of applied pipes. The values obtained for the data given in the above mentioned tables are averaged, for a full cycle of work for the heater and the cooler and for their collectors, i.e., the pressures p_H, p_{H1}, p_{H3} and p_{Cl}, p_{Cl2}, p_{Cl4} and also the temperatures T_H, T_{H1}, T_{H3} and T_{Cl}, T_{Cl2}, T_{Cl4}.

Then, we calculate the value of the mass of the working fluid, M_v for the expander and valve 1. It describes an amount of mass circulating in the closed heat cycle of the engine. The presence of the settling chambers induces averaged mass flow rates of constant values in both the expander and the compressor, respectively, at a full period of the cycle

$$\dot{m}_{ES} = \dot{m}_{CS} = \frac{M_v}{t_{pe}}. \tag{6.11}$$

The constant mass flow rate through the heat exchangers is

$$\dot{m}_j = \dot{m}_k + \dot{m}_{Bi}, \tag{6.12}$$

where:

1. $k = \mathrm{E}, \mathrm{C}$ – expander and compressor averaged mass flow rates,
2. $j = \mathrm{H}$ – heater with its collectors H_1 and H_3, or
3. $j = \mathrm{Cl}$ – cooler with its collectors Cl_2, Cl_4,
4. $i = 1, 2$ – for the blowers B_1 and B_2, if they are applied in the simulation model.

Table 6.1 Dimensions of the engine cylinders

Cylinder	Diameter (m)	Stroke (m)
Expander	0.09	0.0925
Compressor	0.09	0.0694

Table 6.2 Dimensions of the engine heat exchangers

Heat exchanger	Pipe diameter (m)	Number of pipes (−)	Inlet collector volume (m^3)	Outlet collector volume (m^3)
Heater	0.01	15	0.010	0.010
Cooler	0.01	15	0.010	0.010

6.3.1 EHVE with Separate Settling Chambers and Six Blowers

Let us discuss the heater collectors, i.e., H_1 and H_3. We assume the equality of the mass flow rates $\dot{m}_{H1} = \dot{m}_H$ transferred from the proper heater to the collector H_1. In such a stationary device, the balance of the mass flow rate takes the form

$$\dot{m}_H = \dot{m}_{ES} + \dot{m}_{B1}, \tag{6.13}$$

where $\dot{m}_{ES}$ is the averaged expander mass flow rate defined by Eq. (6.11). Just downstream of the collector H_1, there is a settling chamber SC_{H1} of a constant input mass flow rate. The operation of this chamber causes that the flow becomes non-stationary at its other side close to valve 1.

We derive the equation for the temperature in the collector H_1 from the similar equation used in Chap. 5

$$\dot{m}_H T_H - \dot{m}_{ES} T_{H1} - \dot{m}_{B1} T_{H1} = 0. \tag{6.14}$$

Thus, the following equality occurs

$$T_H = T_{H1},$$

see Fig. 6.3.

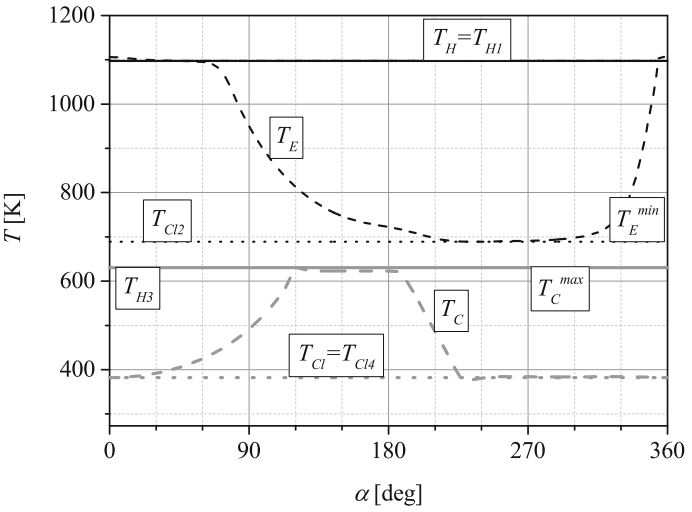

Fig. 6.3 Temperatures in the EHVE without the blowers B_1 and B_2

In the case of the collector H_3, we similarly assume the equality of the mass flow rates $\dot{m}_{H3} = \dot{m}_H$. The balance equation for them for the stationary acting collector H_3 is as follows

$$\dot{m}_H = \dot{m}_{CS} + \dot{m}_{B1}. \tag{6.15}$$

The settling chamber SC_{H3} is situated just downstream of valve 3 of the engine and the temperature at its outlet is assumed constant under stable working conditions, but at the other side of this chamber, valve 3 causes non-stationary flow. The temperature denoted by T_C^{max} occurs when the compressor enforces the working fluid into the heater. In the modelling process, it was based on the results taken from the simulations of the compressor and the heat exchangers.

The equation of energy conservation, owing to which the temperature in the collector H_3 can be determined, also comes from the procedure described in Chap. 5 and is expressed by

$$\dot{m}_{CS} T_C^{max} + \dot{m}_{B1} T_{H1} - \dot{m}_H T_{H3} = 0. \tag{6.16}$$

Here, the value of the temperature $T_H = T_{H1}$ is taken from Eq. (6.20).

To arrive at the solution for the collectors of the cooler, a similar attempt is undertaken. This time, the values of the index $j = \mathrm{Cl}$, with Cl equal to Cl_2 or Cl_4. For the outlet collector Cl_4, we take the equality of the mass flow rates $\dot{m}_{Cl} = \dot{m}_{Cl4}$. The cooler mass flow rate balance yields

$$\dot{m}_{Cl} = \dot{m}_{CS} + \dot{m}_{B2}. \tag{6.17}$$

From the energy conservation equation for the collector Cl_4, it is indicated that

$$T_{Cl} = T_{Cl4}.$$

For the collector Cl_2, we take a similar dependence of the equality of the mass flow rates $\dot{m}_{Cl} = \dot{m}_{Cl2}$. Hence, the balance equation is a sum of

$$\dot{m}_{Cl} = \dot{m}_{ES} + \dot{m}_{B2}. \tag{6.18}$$

The temperature in the inlet collector T_{Cl2} is determined from the following equation

$$\dot{m}_{ES} T_E^{min} + \dot{m}_{B2} T_{Cl4} - \dot{m}_{Cl} T_{Cl2} = 0. \tag{6.19}$$

We can obtain the value of the temperature T_{Cl2} from Eq. (6.19) but in the case of the temperature T_E^{min}, some explanation is needed. It is to be understood as the temperature defining the output from the expander to the cooler. We determine its current value on the basis of simulations carried out for the expander and both heat exchangers. It stands for the temperature at the stationary side in the volume of the

chamber SC_{Cl2}. The value of the temperature

$$T_{Cl} = T_{Cl4}$$

comes from Eq. (6.21). Thus, the calculations of temperatures in the collectors of the engine based on the equations for all the collectors H_1, H_3, Cl_2 and Cl_4 are completed.

Now, let us consider the values of temperatures for the heater and the cooler, i.e., T_H and T_{Cl}, which are defined at their outlets. The heat streams that follow from different temperatures in the exchangers have to be the equal to the streams that come from the calculations of the amount of heat exchanged inside the whole volume of the exchanger pipes. For the heater, Eqs. (6.4) and (6.5) should be equalized, i.e.,

$$\alpha_{AH} A_H \left(T_{wH} - T_H\right) = C_{pH} \dot{m}_H \left(T_H - T_{H3}\right). \tag{6.20}$$

One can calculate a formula for the heater temperature T_H from the above equation. The working fluid coefficients C_{pH}, μ_H, λ_H are assumed as averaged values in the volume between the heater collectors. Moreover, the value of the heat exchange area is assumed as $A_H = 1.2\,\mathrm{m}^2$. Figure 6.2 includes the calculation results for the heater.

Now, if we focus on the cooler, we have to consider the equation

$$\alpha_{ACl} A_{Cl} \left(T_{wCl} - T_{Cl}\right) = C_{pCl} \dot{m}_{Cl} \left(T_{Cl} - T_{Cl2}\right). \tag{6.21}$$

The current value of the temperature T_{Cl} is calculated from Eq. (6.21). The working fluid coefficients C_{pCl}, μ_{Cl}, λ_{Cl} are, as for the heater, taken as averaged values in the volume between the cooler collectors. In this part, the value of the heat exchange area is $A_{Cl} = 1.0\,\mathrm{m}^2$. The numerical simulation results for the cooler are also presented in Fig. 6.2.

6.3.2 *EHVE with Separate Settling Chambers and without the Blowers B_1 and B_2*

The operation of the settling chambers has been already described earlier in this chapter. All the assumptions mentioned at the beginning of this section are to be kept in mind during the modelling. In the case under analysis, there is no mass flow caused by the blowers $\dot{m}_{Bi} = 0$ and the value of the Reynolds number in the exchangers decreases significantly as the mass flow rate $\dot{m}_j$, $j = \mathrm{H}, \mathrm{Cl}$ is simply lower for both of them. According to Eqs. (6.1) and (6.11)–(6.12), the following equality of averaged mass flow rates exists

$$\dot{m}_{ES} = \dot{m}_{CS}.$$

Thanks to this modelling design, the blowers B_{H1}, B_{H3}, B_{Cl2}, B_{Cl4} characteristics can be chosen as much easier. The role of the blowers B_1 and B_2 is played now by the blowers B_{H1}, B_{H3}, B_{Cl2} and B_{Cl4} and the separate settling chambers together.

To obtain a similar power generated in the engine as it was with the two blowers B_1 and B_2, the heat exchange area has to be enlarged. Due to the presence of the collectors in the heater and in the cooler, the results are obvious, i.e., the following equalities take place

$$T_H = T_{H1},$$

$$T_{H3} = T_C^{max},$$

$$T_{Cl} = T_{Cl4}$$

and

$$T_{Cl2} = T_E^{min}.$$

Now, the current values of the temperatures T_H and T_{Cl} have to be calculated when the heat streams obtained on the basis of changes in temperatures from the inlet to the exchanger to its outlet and the stream delivered in the whole volume of the exchanger pipes are equal.

For the heater, we build the following dependence

$$\alpha_{AH} A_H \left(T_{wH} - T_H\right) = C_{pH} \dot{m}_H \left(T_H - T_C^{max}\right), \tag{6.22}$$

which allows us to determine the current value of the temperature T_H. The working fluid coefficients C_{pH}, μ_H, λ_H are taken as averaged values for the volume of the heater between its collectors. Besides, the assumed heat exchange area inside it is $A_H = 1.74\,\mathrm{m}^2$. Figure 6.3 depicts changes of these temperatures.

For the cooler, a similar equality is derived

$$\alpha_{ACl} A_{Cl} \left(T_{wCl} - T_{Cl}\right) = C_{pCl} \dot{m}_{Cl} \left(T_{Cl} - T_E^{min}\right). \tag{6.23}$$

This allows one to calculate a current value of the temperature T_{Cl}. The working fluid coefficients in this volume, C_{pCl}, μ_{Cl}, λ_{Cl}, are also assumed as averaged values inside the volume of the cooler between its collectors. In this case, the heat exchange area is assumed as $A_{Cl} = 1.46\,\mathrm{m}^2$. Together with temperatures for other parts of the engine, the values for the cooler are shown in Fig. 6.3.

6.3.3 Calculations of the Generated Power and Efficiency

As mentioned earlier in Sects. 6.1 and 6.2, losses were included in the simulation process for all additional devices and the settling chambers. Due to the fact that the

working fluid temperature leaving the expander is high enough, a pre-heater can be included in the model at the stage of efficiency estimation. This way the heat stream value should be decreased by 15 %. When the two blowers B_1 and B_2 are applied, the working fluid flow rate is assumed as $\dot{m}_{Bi} = 0.1$ kg/s. On the other hand, when they are not present, then we simply change it to $\dot{m}_{Bi} = 0.0$ kg/s, and the results of the simulations in both cases are presented in Fig. 6.4.

The settling chambers and their additional blowers obviously cause some losses estimated to be in the range from 80 to 160 J. They were taken into account in the simulations of the engine model with settling chambers. In the calculation algorithm, the initial phase was conducted in a similar way as in the procedure described in Chap. 8 until the steady state was attained typically, as shown in Fig. 6.4, after minimum 250 cycles and next, a new procedure replaces the action of the heat exchangers, whereas the main part of the engine works normally, as in Sect. 6.3.

In order to extend the discussion of possible losses, we present Fig. 6.5 which shows relationships between the EHVE power and efficiency as functions of the losses caused by the settling chambers and the blowers.

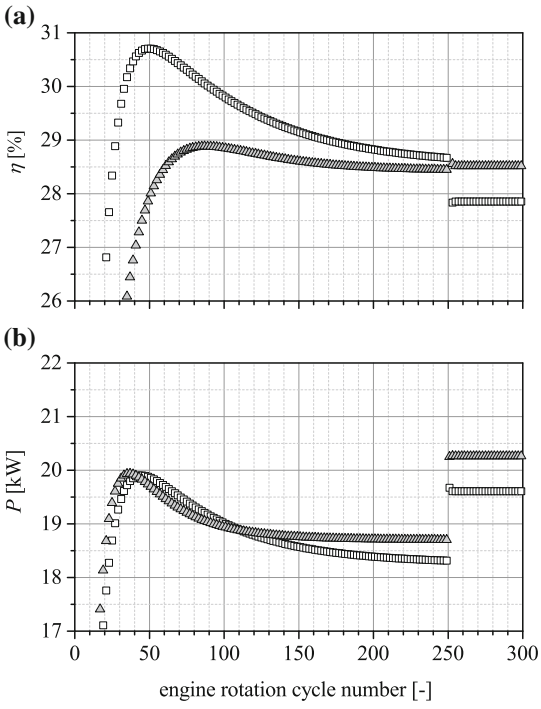

Fig. 6.4 Efficiency (**a**) and power (**b**) of the EHVE at 1500 rpm when losses in the settling chambers are assumed at the level of 3000 W. *White rectangles* – without the blowers B_1 and B_2 and *greyed triangles* – with the blowers. The simulation results of the new model after 300 cycles. The mass flow rate through the blowers B_1 and B_2 is 0.1 kg/s

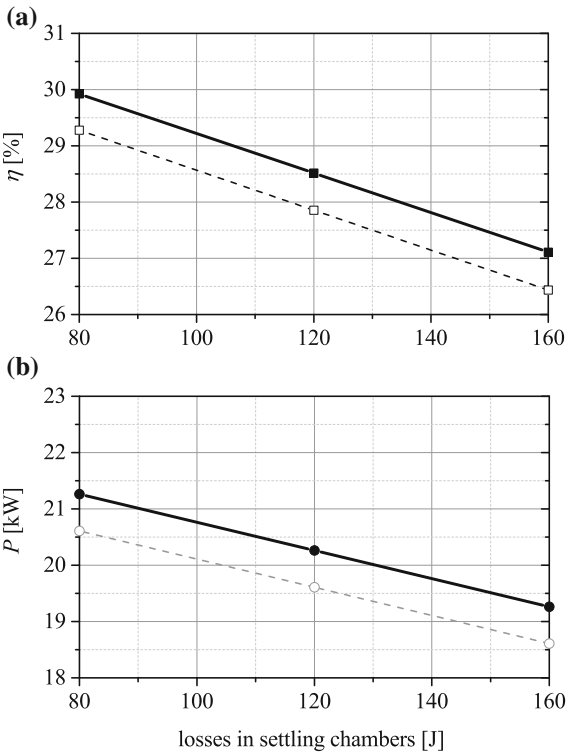

Fig. 6.5 Efficiency (**a**) and power (**b**) of the EHVE as functions of losses in the settling chambers. *Rectangles* – efficiency in (%) and *circles* – power in (kW); *Dashed lines* and *open symbols* – without the blowers B_1 and B_2; *continuous lines* and *filled symbols* – with the blowers. The mass flow rates through the blowers B_1 and B_2 at 0.1 kg/s

6.4 Remarks on the EHVE with Separate Settling Chambers

The air engine with external heating and with separate settling chambers, whose scheme is shown in Fig. 6.1, is more complicated when compared to the previous solutions, but provides steady operation for both the heat exchangers. The model applied in the simulations is a combination of the one presented for unsteady flows and a new idea described in Sects. 6.1 and 6.3. The used solutions although obvious, appear to be reliable. Of course, other solutions are possible as well, but they should be subject to expensive experiments.

The advantages coming from the application of the blowers B_1 and B_2 are as follows

- the velocity of the working fluid flow through the heat exchangers is significantly increased, and,
- the temperature changes inside the collectors H_3 and Cl_2 are more beneficial.

On the other hand, the shortcomings consist in a specific choice of their properties, which has to comply with the power characteristics of the blowers B_{H1}, B_{H3}, B_{Cl2}

and B_{Cl4}. The latter complication can be simplified when the blowers B_1 and B_2 are removed from the design but the settling chambers have still to be applied.

However, it will be followed by a considerable decrease in the working fluid velocity inside the heat exchangers. In order to reach a similar amount of the created power and efficiency as that one obtained with two blowers, the heat exchange area in the heater and the cooler should be considerably increased.

Furthermore, if settling chambers and blowers are employed, further losses in the working fluid energy will occur. They are assumed to vary from 80 to 160 J and are related to other parameters of the engine, depending on the design of settling chambers. The power and the efficiency of the engine with separate settling chambers for different levels of losses inside them, with and without the blowers B_1 and B_2, reach a reasonable level when compared to the applied cylinder volumes.

The results of simulations of this new solution of the EHVE with separate settling chambers for the parameter values described in Tables 6.1 and 6.2 show **similar levels of power and efficiency generated, not less than the averaged values in the non-steady modelling process**, but now the heat exchange becomes stationary. This new idea may be worth consideration when a new prototype is built.

References

1. Lontsi F, Hamandjoda O, Fozao K, Stouffs P, Nganhou J (2013) Dynamic simulation of a small modified Joule cycle reciprocating Ericsson engine for microcogeneration systems. Energy 63:309–316. doi:10.1016/j.energy.2013.10.061
2. Xu Q, Cai M, Shi Y (2014) Dynamic heat transfer model for temperature drop analysis and heat exchange system design of the air-powered engine system. Energy 68:877–885. doi:10.1016/j.energy.2014.02.102
3. Guo J, Huai X, Li X, Cai J, Wang Y (2013) Multi-objective optimization of heat exchanger based on entransy dissipation theory in an irreversible Brayton cycle system. Energy 63:95–102. doi:10.1016/j.energy.2013.10.058
4. Erdem D, Rockwell D, Oshkai P, Pollack M (2003) Flow tones in a pipeline-cavity system: effect of pipe asymmetry. J Fluids Struct. 17(4):511–523. doi:10.1016/S0889-9746(02)00159-7
5. Chemloul NS (2012) Experimental study of cavitation and hydraulic flip effects on liquid jet characteristics into crossflows. J Appl Fluid Mech 5(4):33–43. http://jafmonline.net/JournalArchive/download?file_ID=26908&issue_ID=210
6. Leyko M, Moreau S, Nicoud F, Poinsot M (2011) Numerical and analytical modelling of entropy noise in a supersonic nozzle with a shock. J Sound Vib 330(16):3944–3958. doi:10.1016/j.jsv.2011.01.025
7. Kings N, Enghardt L, Bake F (2012) Indirect combustion noise: experimental investigation of the vortex sound generation in a choked convergent-divergent nozzle. In: Proceedings of the Acoustics 2012 Nantes Conference, Nantes, France, 23–27 April 2012. HAL Id: hal-00811052. https://hal.archives-ouvertes.fr/hal-00811052
8. Bhoi SR, Suryanarayana GK (2011) Prediction of total pressure characteristics in the settling chamber of a supersonic blowdown wind tunnel, Aeronaut J New Ser 115(1171):557–566. http://nal-ir.nal.res.in/5021/1/INCAST_2008-105.pdf
9. Rajani SH, Bindu MK, Usha N (2012) Stability analysis and temperature effect on the settling chamber pressure of a hypersonic wind tunnel. In: IEEE International Conference on Compu-

tational Intelligence and Computing Research, pp 1–5. http://dx.doi.org/10.1109/ICCIC.2012.6510283

10. Silva MG, Gamarra VOR, Koldaev V (2009) Control of Reynolds number in high speed wind tunnel. J. Aerosp. Technol. Manag. 21(1):69–77. http://www.jatm.com.br/ojs/index.php/jatm/article/download/9/148
11. Chong TP, Joseph PF, Davies POAL (2014) Design and performance of an open jet wind tunnel for aero-acoustic measurement. Appl. Acoust. 70(4):605–614. doi:10.1016/j.apacoust.2008.06.011

Chapter 7
Further Development of the EHVE – a 4-Stroke Engine

Now, we will discuss the next improved version of the EHVE – a 4-stroke engine and the alternations introduced to eliminate the so-called "hot cylinder" of the expander being a part of the 2-stroke engine model.

In order to enhance the heat transfer, a working fluid circulation forced by a small blower installed in a closed, internal loop of the large volume heater, $V_H > 4\,V_{Cyl}$, is applied. Moreover, some modifications in the valve system are employed to attain the demanded high compression ratio of the engine (more than 10) when such a heat exchanger is used. Furthermore, self-acting valves are eliminated and governed valves are used instead.

A theoretical model of the 4-stroke engine is based on the time-dependent equations of mass and energy conservation, formulated for each engine part separately. The calculation method described in detail in Chap. 5 is adopted here. The dynamic properties of the model are described in Sect. 7.3.

7.1 Principle of the 4-Stroke Engine Operation

This engine is composed of three essential parts, namely: a cylinder and two heat exchangers, a heater, and a cooler presented on the engine schematic view shown in Fig. 7.1. The operation regime of the 4-stroke EHVE cycle contains the consecutive strokes, namely

1. the engine piston moves downwards from its upper position and the working fluid from the cooler flows into the cylinder through valve 2;
2. in this stroke, the piston starts moving up from its lower position and compresses the fluid in the cylinder. At the crankshaft angle of approximately 60°, before the piston achieves its upper position, valve 3 from valve set 1–3 opens and the compressed fluid is pushed out to the heater. The fluid circulation in the internal heater loop is here forced by the blower that determines the flow direction in such a way that the delivered fluid aims the heater inlet collector H_{InC};

Z. Kazimierski and J. Wojewoda, *Externally Heated Valve Engine*,
Springer Tracts in Mechanical Engineering, DOI 10.1007/978-3-319-28355-5_7

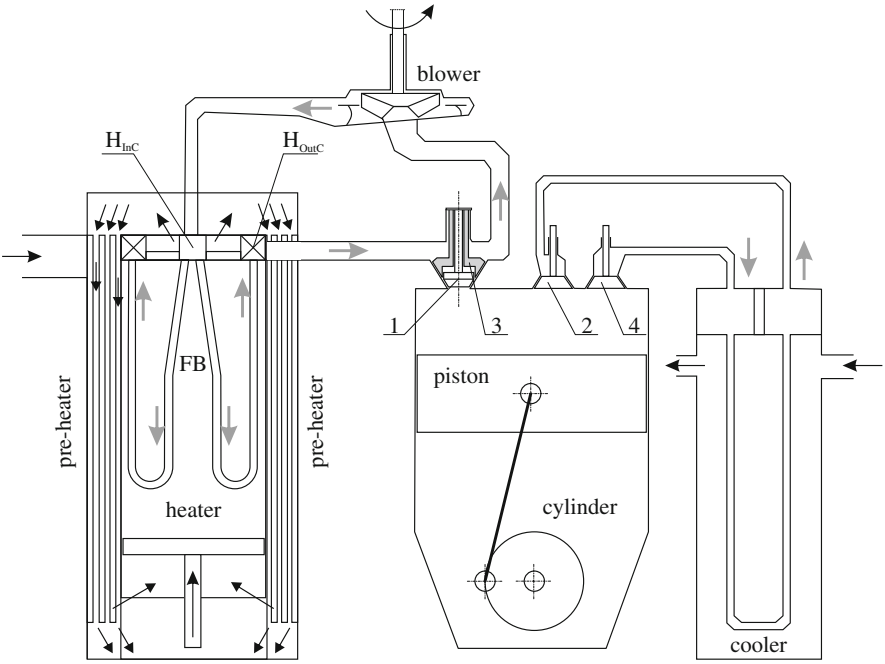

Fig. 7.1 Example of a schematic diagram of the engine with both heat exchangers: *1*, *2*, *3*, *4* – governed valves, H_{InC} – inlet collector to the heater, H_{OutC} – outlet collector to the heater, *FB* – fluidized bed. The heater set-up together with an embedded pre-heater on the left

3. the piston moves downwards from its upper position and sucks the hot fluid from the heater into the cylinder through open valve 3. The blower operation causes that the fluid delivered to the cylinder during this stroke comes directly from the heater outlet collector H_{OutC}. At approximately 80° of the crankshaft angle from the piston upper position, valve set 1–3 closes and then the hot fluid in the cylinder expands until the piston reaches its lowest position;
4. the piston pushes out the expanded fluid from the cylinder to the cooler through valve 4.

Valve set 1–3 is thought to be rather complex and represents modern technology as this is an advanced element in the engine due to the task it is to perform. Therefore, the present version of the 4-stroke EHVE can be considered as an externally heated engine of the future. As expected, it will be possible to manufacture the above-mentioned elements thanks to upcoming technological progress. Nevertheless, a theoretical model of the engine operation and the results of the calculations are presented here to support the method given in Chap. 5. The heater used in this example of the engine is different from those used in other versions. It can be of a fluidized-bed type, see, e.g., [1].

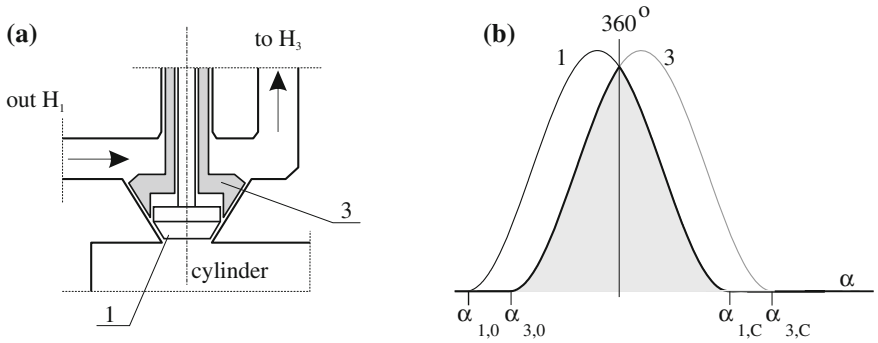

Fig. 7.2 **a** Idea of the valve *1–3* set-up, **b** timing of valve *1–3*

A new element is valve set 1–3 of original design, cf. Fig. 7.2a. The valve and its timing are depicted in Fig. 7.2. Valve set 1–3 can be used when its opening time is very short. It is a double valve composed of separate valves marked 1 and 3. The movements of these valves are shifted and their operation is explained in Fig. 7.2b. The darken area stands for a fully opened range between two volumes located on each side of the valve.

This valve set, especially its propulsion, may be complex and it can fail because it is not sure that the direction of the mass flow into the blower and from the heater will comply with the designed one without any additional devices. These auxiliary devices can have the form of two cut-off valves operating alternatively. When, for instance, the mass stream flows from the cylinder to the blower, the cut-off valve situated downstream of the inlet collector should be closed. On the contrary, if the flow is directed to the cylinder from the outlet collector, the cut-off valves located upstream of the blower should be closed.

Another solution proposed to achieve the proper flow direction is to introduce separate valves 1 and 3 of different structure, e.g., rotary valves, shown schematically in Fig. 7.3, instead of valve set 1–3. Their rotational speed has to correspond to the desired time of the working fluid flow.

A new scheme of the engine heater loop is presented now in Fig. 7.4. In this case, the operation of a 4-stroke engine is as follows: the upward movement of the piston compresses the cool air and delivers it through separate valve 3 to the heater. The downward movement causes that the hot air leaves the heater and flows to the expanding cylinder through separate valve 1. The non-stationary operation of such valves should not disturb the almost steady flow generated by the blower B in the sequence H–H_1–B–H_3–H. The collectors H_1 and H_3 have to be of special design, difficult to attain but feasible from the engineer's point of view.

A similar situation takes place in the case of the blower B_1 as described in Chap. 5 and illustrated in Fig. 5.3, respectively.

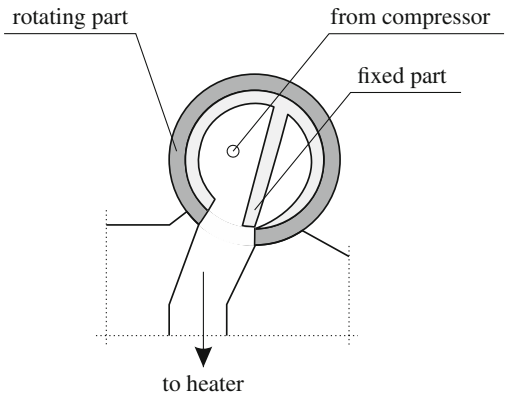

Fig. 7.3 Idea of rotary valves

7.2 Numerical Investigations of the 4-Stroke EHVE

The method applied for calculations uses the simplified attempt already presented in Chap. 5. Both heat exchangers, the heater and the cooler, are modelled again as counter-current devices although their dimensions are different. No collectors are employed also for simplification purposes but this attempt can be used. A scheme of the heater operation is shown in Fig. 7.4. The cooler is treated as a stationary heat exchanger characterized by constant thermodynamic parameters T_{Cl} and p_{Cl}, and, what should be obvious, its dimensions are large even when compared to the heater, for example $V_{Cl} > 10\,V_H$. The experience gathered in earlier phases of the investigations carried out by the authors allowed for avoiding any return flows or

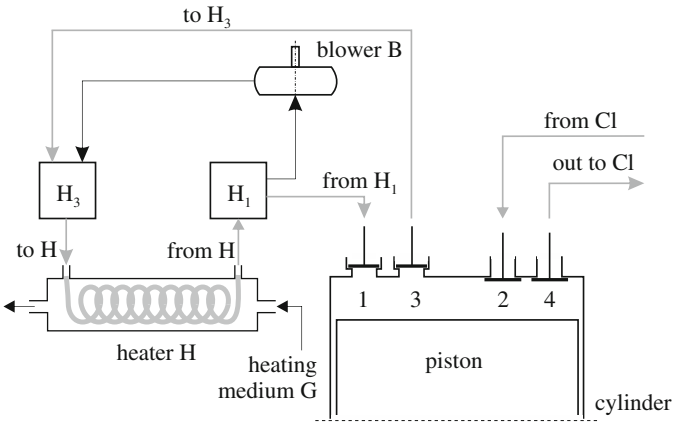

Fig. 7.4 Idea of the EHVE with separate valves *1* and *3* and the blower operating between the collectors H_1 and H_3

Table 7.1 Control angles, dimensions and loss coefficients of the 4-stroke EHVE valves

Valve No.	Opening α_{io}	Closing α_{ic}	Transient $\Delta\alpha_i$	Max. flow area (m^2)	Loss coeff. ζ_j
1	355° *	440°	15°	0.00120	0.85
2	0°	180°	50°	0.00075	0.85
3	295° *	360°	15°	0.00120	0.85
4	540°	720°	50°	0.00075	0.85

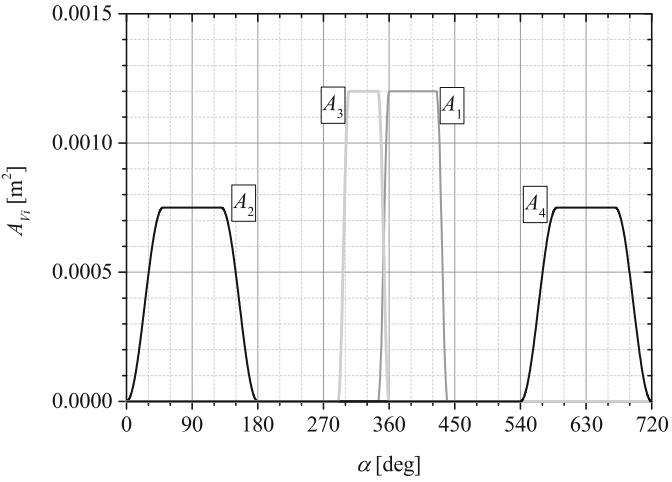

Fig. 7.5 4-stroke EHVE valve characteristics

overshooting the assumptions of initial conditions, which was followed by quick and easy simulations of the investigated model.

Valves in this version of the EHVE are of two kinds. Firstly, those numbered 2 and 4 are typical, cam-governed devices as in any 4-stroke internal combustion engine. Their dimensions and control parameters are given in Table 7.1. Both valves numbered 1 and 3 have to be of specific design, as discussed earlier. They can be, for example, **separate rotary valves**. We present here only an idea, whereas the solution is an engineering task which needs practical testing. This way, we propose a demanded characteristics of valves 1 and 3 together with 2 and 4, as shown in Fig. 7.5.

The values of the above angles, which determine the behaviour of the valve governing system data, are chosen after the preliminary process of optimization. The current cross-section areas are calculated as in Chap. 5, formulae (5.5)–(5.6). The mass flow rates $\dot{m}_j$, $j = 1, 2, 3, 4$ are given by Eqs. (5.7)–(5.9) with the exceptions – the values marked with the * symbol are minimal numbers after which the program slightly adjusts their opening angle when pressure conditions are met in the following way

- the flow $\dot{m}_1$ leaves the heater through valve 1 and loads the cylinder with slight adjusting of the fixed opening angle α_{1o} only after the following condition is met

$$p_H \geq p_{Cyl}.$$

- similarly, for valve 3 after the fixed value of α_{3o}, the condition required for its opening is

$$p_{Cyl} \geq p_H.$$

As a result, smooth transition in operation of valves 3 and 1 occurs with no overlap and quick opening in the proper moment allows the working fluid to flow into the cylinder without any overshooting of its pressure over the heater one. Additional profit of using of the above conditions is no incidence of reverse flows through the valves.

The 4-stroke EHVE has only one cylinder playing a role of both the compressor and the expander, correspondingly, in different phases of its working cycle. Varying values of the volumes V_{Cyl} and its derivative $\mathrm{d}V_{Cyl}/\mathrm{d}t$ are calculated as in Eqs. (5.1) and (5.2). The mass flow rates flowing towards the engine cylinder take positive values and those leaving its volume – negative values. All dependencies of the $\dot{m}_j$ on pressures, temperatures and current cross-sections values are given in the above-mentioned equations. We assume the cylinders do not play any role in the heat exchange process. The equations are written in the way which does not include any so-called reverse flows, which has been achieved because of the pressure conditions shown above.

The equation of mass conservation for the cylinder takes the form

$$\frac{\mathrm{d}\rho_{Cyl}}{\mathrm{d}t} = \frac{1}{V_{Cyl}}\left(\dot{m}_2 - \dot{m}_3 + \dot{m}_1 - \dot{m}_4 - \rho_{Cyl}\frac{\mathrm{d}V_{Cyl}}{\mathrm{d}t}\right). \tag{7.1}$$

The equation of energy conservation for the cylinder is

$$\begin{aligned}\frac{\mathrm{d}T_{Cyl}}{\mathrm{d}t} = \frac{1}{\rho_{Cyl}V_{Cyl}}\Big(&-T_{Cyl}\left(\dot{m}_2 - \dot{m}_3 + \dot{m}_1 - \dot{m}_4\right)\\ &+\kappa\left(\dot{m}_2 T_{Cl} - \dot{m}_3 T_{Cyl} + \dot{m}_1 T_H - \dot{m}_4 T_{Cyl}\right) - \frac{p_{Cyl}}{c_v}\frac{\mathrm{d}V_{Cyl}}{\mathrm{d}t}\Big).\end{aligned} \tag{7.2}$$

Finally, the equation of state allowing calculations of the pressure inside its volume is

$$p_{Cyl} = \rho_{Cyl} T_{Cyl} R. \tag{7.3}$$

All the above equations are written for a cycle of the engine operation, i.e., for $0 \leq \alpha \leq 720^\circ$ or $0 \leq t \leq 4\pi/\omega$.

Now, let us consider modelling of processes which take part inside the heat exchanger and allow for calculation of an amount of the heat delivered to the engine. The blower B is located in its internal working fluid flow loop (see Fig. 7.4) and we

assume the blower flow rate to be $\dot{m}_B \geq 0.1$, causing the Reynolds number value Re_H not less than 10^4. The flow rate through valve 3, $\dot{m}_3$, loads the heater volume so it is $\dot{m}_3 > 0$ but, on the other hand, the flow equals $\dot{m}_1 < 0$ as it leaves it. If valves 1 and 3 remain closed, then due to the blower operation, we have the Reynolds number value calculated as

$$\mathrm{Re}_B = \frac{4\dot{m}_B}{\pi d_H \mu_H n_H}, \tag{7.4}$$

but when the mass flow rate $\dot{m}_1$ or $\dot{m}_3$ is greater than zero, the Reynolds numbers Re_H are usually larger. The Nusselt number for Re_H is defined by

$$\mathrm{Nu}_H = 0.022\,\mathrm{Re}^{0.8}\mathrm{Pr}^{0.6}. \tag{7.5}$$

The heat transfer coefficient is calculated as

$$\alpha_{AH} = \frac{\mathrm{Nu}_H \lambda_H}{d_H}. \tag{7.6}$$

For the complete heater with the heat exchange area of $A_H = \pi d_H l_H n_H$, the heat stream is determined by

$$\dot{Q}_{AH} = \alpha_{AH} A_H (T_{wH} - T_H), \tag{7.7}$$

where T_{wH} is the temperature of the heater wall.

The equation of continuity for the heater is

$$\frac{\mathrm{d}\rho_H}{\mathrm{d}t} = \frac{1}{V_H}\left(\dot{m}_3 - \dot{m}_1\right). \tag{7.8}$$

The equation of energy for the heater takes the form

$$\frac{\mathrm{d}T_H}{\mathrm{d}t} = \frac{1}{\rho_H V_H}\left(-T_H\left(\dot{m}_3 - \dot{m}_1\right) + \kappa\left(\dot{m}_3 T_{Cyl} - \dot{m}_1 T_H\right) + \frac{\dot{Q}_{AH}}{c_v}\right). \tag{7.9}$$

The equation of state for the heater inside its volume is

$$p_H = \rho_H T_H R. \tag{7.10}$$

As mentioned earlier, the cooler in the model of the 4-stroke EHVE is assumed to be of a large volume when compared to the cylinder or the heater, which allows us to state it has assumed the constant temperature $T_{Cl} = 390\,\mathrm{K}$ and the pressure $p_{Cl} = 18\,\mathrm{bar}$ inside its volume. The rotational speed is equal to 3000 rpm. The heater wall temperature T_{wH} is set to 1270 K. The dimensions of the cylinder and the heater are shown in Tables 7.2 and 7.3, respectively.

Table 7.2 Dimensions of the cylinder of the 4-stroke engine

Diameter d_{Cyl} (m)	Stroke s_{Cyl} (m)	Dead height $h_{0\,Cyl}$ (m)
0.0700	0.0600	0.0017

Table 7.3 Dimensions of the heater for this version of the EHVE

Tubes diameter (m)	Tubes length (m)	Number of tubes (−)	Heat exchange area (m^2)	Volume (m^3)
0.01	1.27	10	0.399	0.000997

The results are presented in Figs. 7.6 and 7.7. The cylinder pressure (Fig. 7.6a) travels between a low level of the cooler and a high level of the heater. It influences changes in the heater only due to the model applied when valves 1 or 3 are open. The overall character is smooth, with no rapid passages. The heater wall temperature is represented with a high limit in part (b) of this figure. Pressure changes, controlled by the above-mentioned conditions for openings, cause almost smooth transition between closing of valve 3 and opening of valve 1. No return flows or rapid changes are observed in any flow.

When Fig. 7.7 is compared to Fig. 5.8, one can notice a similarity in the shape of the loop which represents the useful work generated in the EHVE. The differences lie in shapes of line-like parts in the bottom and top parts of the diagram and are mostly due to constant cooler parameters and no overshooting of p_C over p_H, respectively. The above results may indicate a prediction of longer durability of the EHVE when compared to the life of the typical internal combustion engine due to a lack of explosions (and rapid jumps of thermodynamic parameters) and clean, table conditions of the working fluid inside. Solving the problem of overshooting is a case of subtle pressure control of opening times of valves 1 and 3. Such self-adjusting, added to strictly mechanical control improved here, is an important advantage over the method described in Chap. 5 and seems to be a practically solvable engineering task nowadays.

The engine internal work and power without a pre-heater is

$$L_i = \int_{t=0}^{t=\frac{4\pi}{\omega}} p_{Cyl}(t) \frac{\mathrm{d}V_{Cyl}}{\mathrm{d}t}\,\mathrm{d}t \tag{7.11}$$

and

$$P_i = L_i \frac{\omega}{2 \cdot 2\pi}. \tag{7.12}$$

The efficiency without any pre-heater can be calculated as

$$\eta_i = \frac{P_i}{\dot{Q}_{AH}}. \tag{7.13}$$

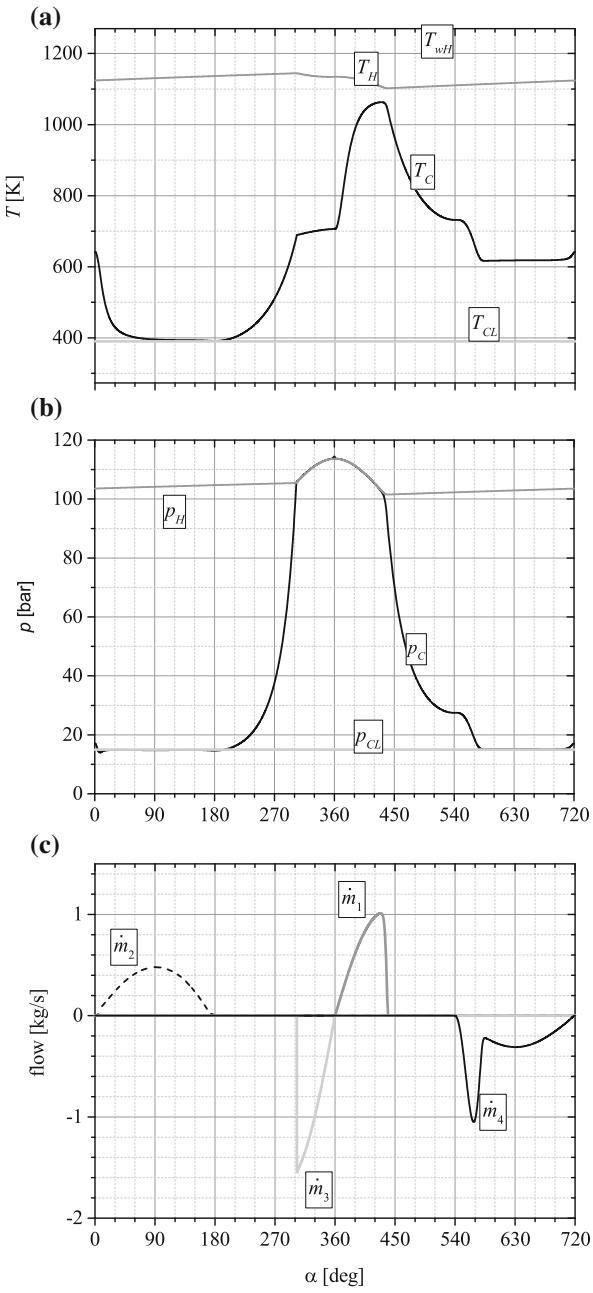

Fig. 7.6 4-stroke EHVE work cycle, pressures (**a**); temperatures (**b**) and mass flow rates (**c**) when a large cooler is applied

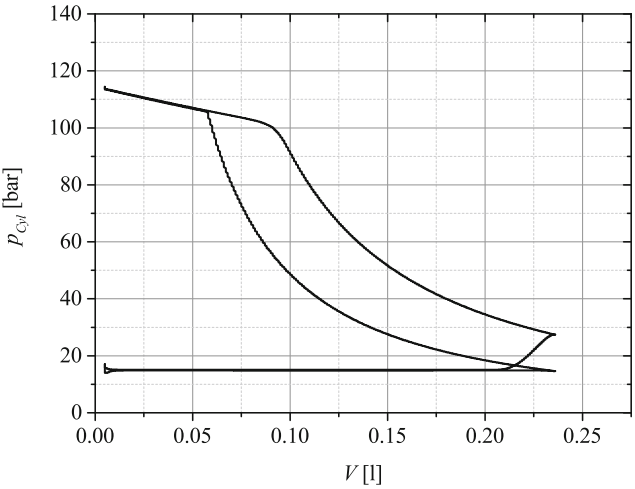

Fig. 7.7 $p - V$ diagram of the 4-stroke EHVE work cycle with a large cooler

Performing the calculations for the simulation model, we obtain its internal power $P_i = 11.7\,\text{kW}$ and the efficiency $\eta_i = 34.77\,\%$. Recalculating it to a volume of 1 litre of the working capacity of the EHVE, we get an impressive value of 50.7 kW.

7.3 Inequality of Rotations of the 4-Stroke Engine Model

In modelling the dynamic behaviour, we recall Eq. (5.53). The driving torque resulting from expansion and compression of the working fluid inside the engine is described by the simplified equation

$$M_{dr} = A_{Cyl}\, p_{Cyl} \frac{s}{2} \sin(\alpha). \tag{7.14}$$

Additionally, we define the resistance torque caused by friction and other forces as

$$M_R = M_0 - c_R \omega^2. \tag{7.15}$$

After applying a variable cooler model to the 4-stroke version of the EHVE in a similar way to that for the heater, we arrive at similar results as shown for the cooler treated as having constant volume parameters. In Fig. 7.8, a $p - V$ diagram of the engine is presented. Figure 7.9 shows the most important representation of a work cycle of the model with a variable cooler.

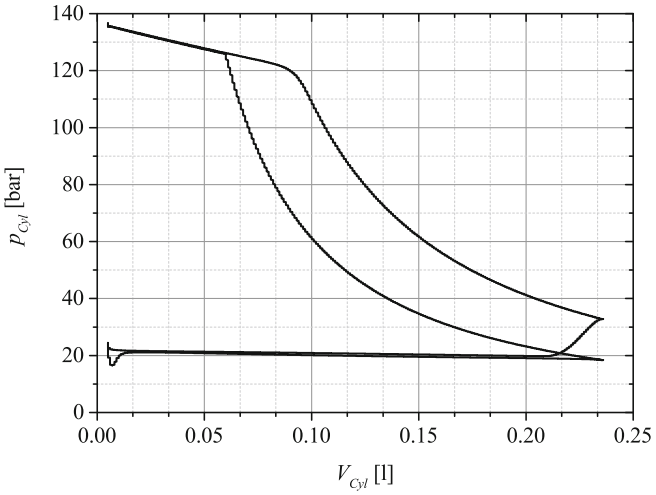

Fig. 7.8 $p - V$ diagram of the 4-stroke EHVE work cycle with the cooler of a similar size to the heater

If we are able to avoid any return flows by careful setting of valve opening/closing moments, then stable work of the model depends only on the external load. The results of calculations of the 4-stroke EHVE model are presented below. Figure 7.10a shows dependences of the driving torque M_D and its part (b) – the rotational speed ω as functions of the angle of rotation α when the moment of inertia I_{cs} is taken as the control parameter. All driving moments present almost the same shape during the cycle, whereas the rotational speed varies and its changes are most visible for the lower values of the moment of inertia. The span of irregularities can be diminished by a larger flywheel or when the multicylinder design is used. In the simulations, the following values in Eq. (7.15) were applied: $M_0 = 34\,\mathrm{kgm}^2$, $c_R = 2 \cdot 10^{-5}\,\mathrm{kgm}^2\mathrm{s}^2$, $T_{wH} = 1270\,\mathrm{K}$ and $T_{wCL} = 353\,\mathrm{K}$. The basis value of the I_{CS} was $2.5\,\mathrm{kgm}^2$. It can be seen that for $I_{cs} \geq 25$ the angular velocity ω is almost stable at the value 314 rad/s for which the previous thermodynamic calculations were performed.

7.4 Control of Rotations

We propose to control the rotational speed of the 4-stroke engine in a similar way to that discussed earlier in Sect. 5.4.1 for the 2-stroke version. The control can be attained in two ways

1. by adding/removing the mass of the working fluid to/from the cooler volume where pressure is lowest, or,
2. by changing the temperature of the heater wall, and, additionally,
3. by a combination of the two above-mentioned manners.

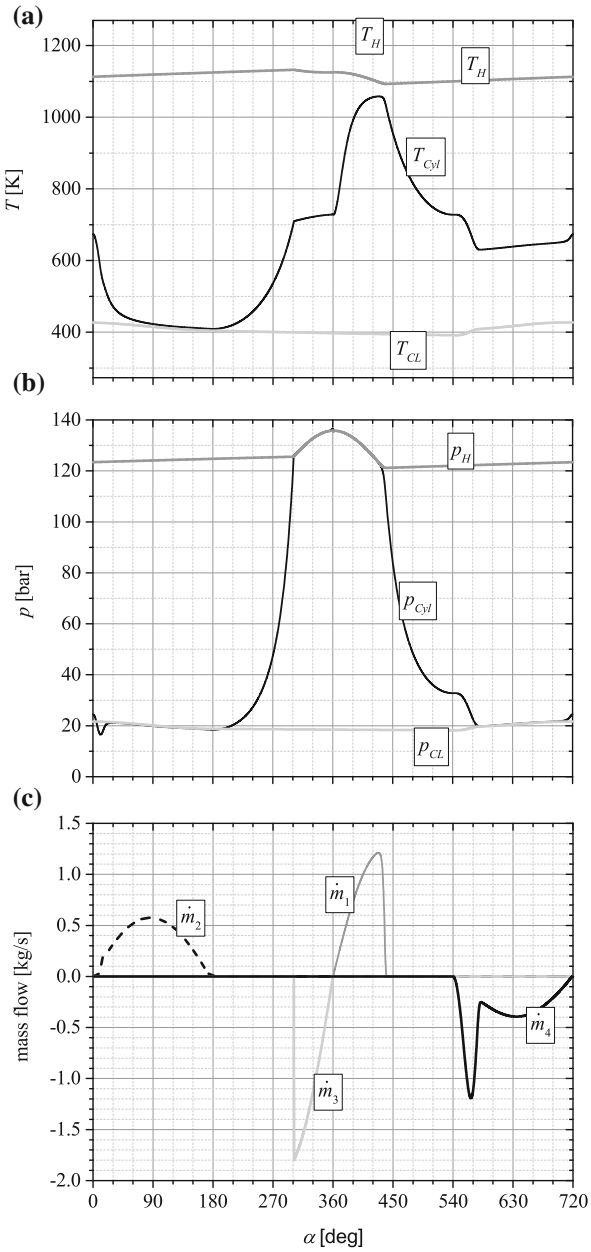

Fig. 7.9 4-stroke EHVE work cycle, pressures (**a**); temperatures (**b**) and mass flow rates (**c**) in the case when the cooler is similar in size to the heater

Some examples of individual attempts of control are presented in Fig. 7.11a – by changing the mass in the system (item 1), and (b) – by changing the heater wall temperature (item 2), respectively. The simulation results are shown for $I_{cs} = 0.625\,\mathrm{kgm}^2$ with the same other parameters as those in the previous section. Similar

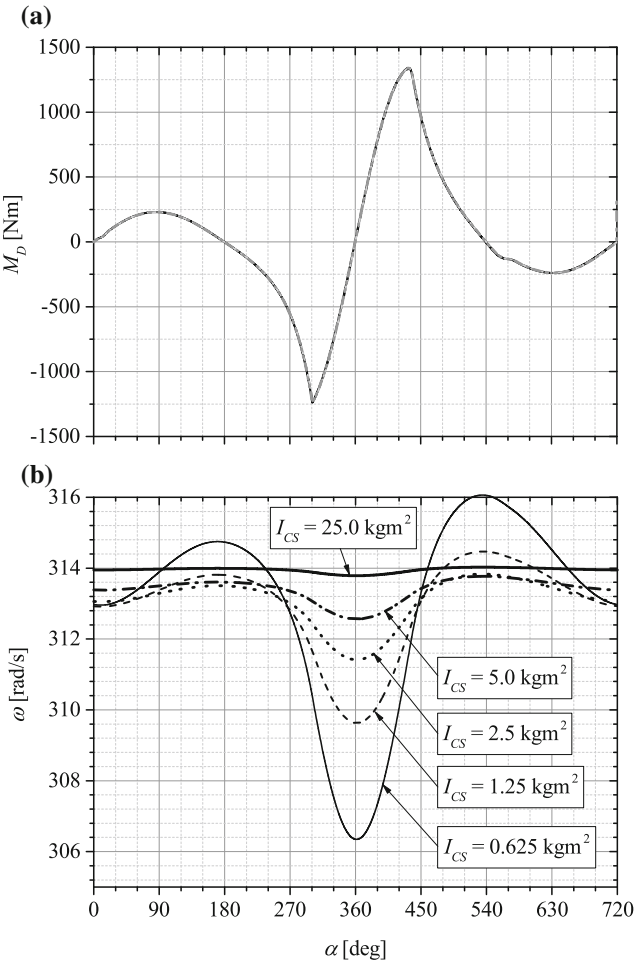

Fig. 7.10 Driving torque (**a**) and rotational speed (**b**) during a cycle of work for the 4-stroke EHVE with a variable cooler

results when both control parameters are modified are shown in Fig. 7.12, where a wider range of the obtained changes in the rotational speed is observed.

An addition of about 20 % of the working fluid mass causes approx. an 18 % increase, whereas a decrease by about 18 % of the mass results in a 26 % decrease in the rotational speed. The generated power changes from 8 to 13.6 kW and the efficiency diminishes from 35 to 33.2 %, correspondingly. Control via changes in the heater wall temperature gives the following values – an increase by 78 K (≈6 %)

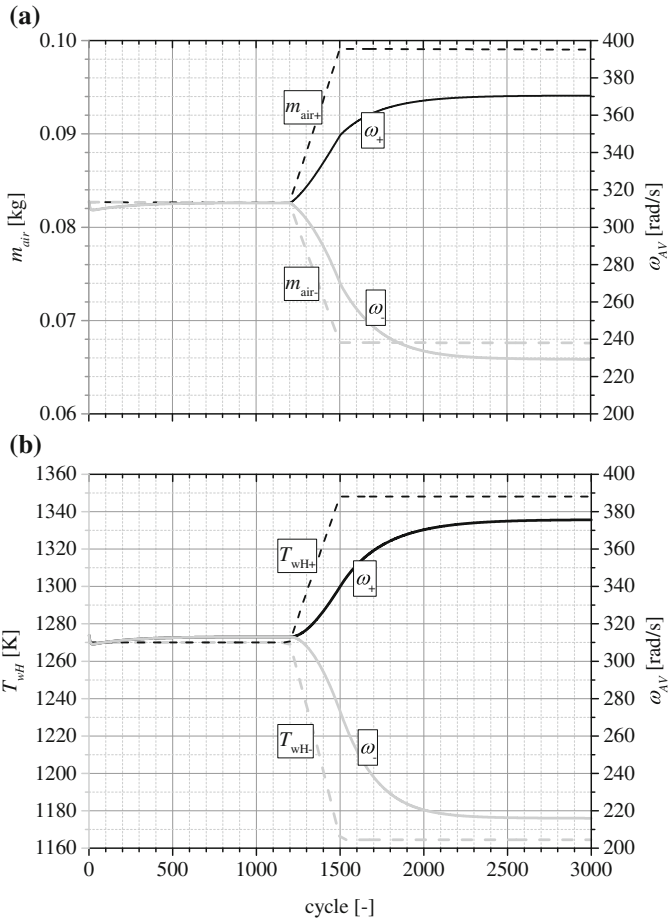

Fig. 7.11 Control of the angular velocity ω_{AV} as a result of a combination of the simultaneous increase/decrease mass in the system and the temperature of the heater wall. An influence on the mass changes shown in part (**a**) and on the temperature in part (**b**), respectively

speeds up by 20 % and a decrease by 106 K slows down by about 31 % the initial value of 157 rad/s. In these cases, the power grows from 7.5 to 13.8 kW and the efficiency changes from 34.4 down to 33.8 %. These results are summarized in Fig. 7.13.

When a combination of both ways is applied, the extreme results are presented in Fig. 7.12 together with the changes in the lowest pressure in the cooler, part (a). In the case when both control parameters increase, i.e., the mass by 19 % and the temperature of the heater wall by 6 %, then the rotational speed grows up by 35 %. When both parameters decrease, the mass by 19 % and the temperature by 7 %, as a result the engine slows down by 58 %. The values of the generated power vary

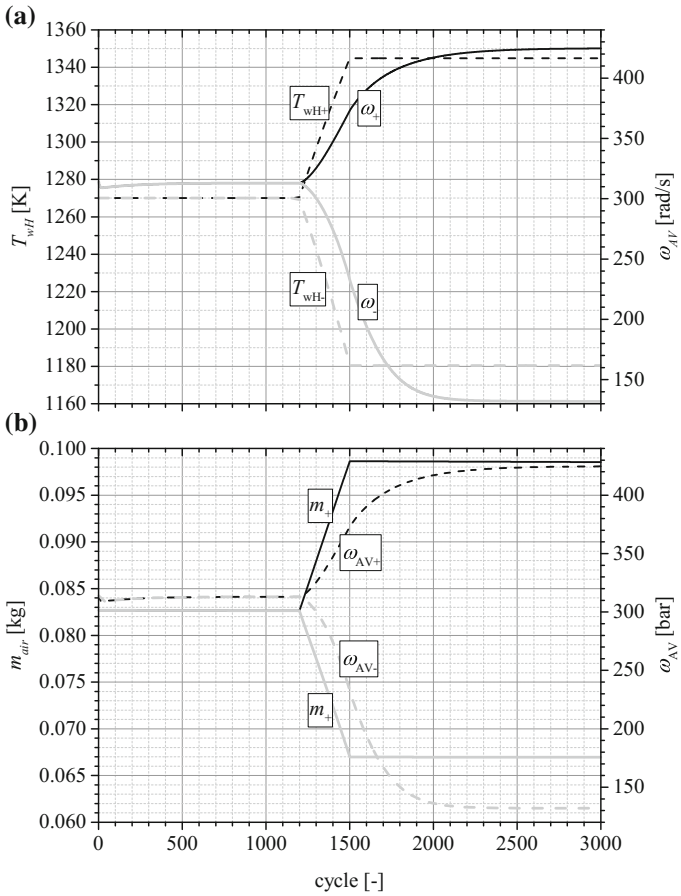

Fig. 7.12 Control of the angular velocity ω_{AV} as a result of an increase/decrease temperature in the heater wall (**a**) and an increase/decrease of the mass in the system – part (**b**)

between 4.5 and 16 kW, whereas the efficiency diminishes from 35 down to 32.9 %, see Fig. 7.14.

In all of the discussed examples, the rotational speed stabilization is 3–5 times longer than the time of applied changes in the input parameters. Low levels of the delivered power can be compensated by adding some mass to the working fluid in order to reach the desired value of the rotational speed. A proper combination of control parameters seems to be feasible, which can take a similar form to mapping of fuel injection in internal combustion engines.

We should emphasize that extreme values of the rotational speed of 4500 rpm would be rather impossible to be reached in a real installation due to critically low

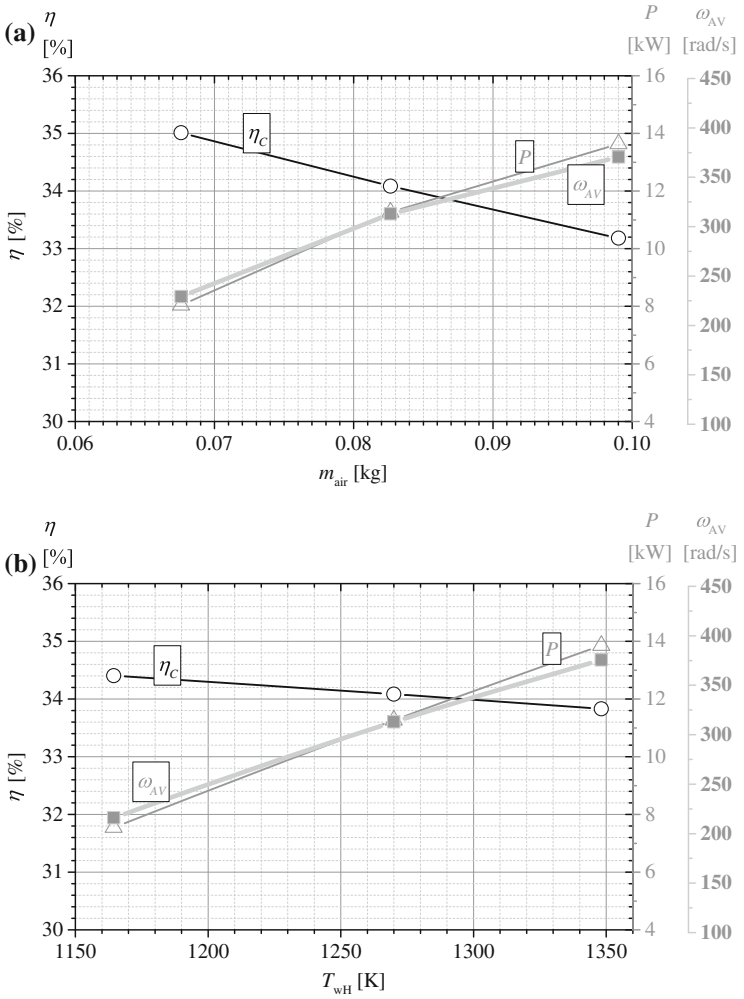

Fig. 7.13 Efficiency η_C, power P and the rotational speed ω_{AV} as functions of the working fluid mass enclosed in the system (**a**) and the temperature of the heater wall – part (**b**), when both parameters change simultaneously

time for the heat exchange. The same limitation relates to the heater wall temperature, $T_{wH} = 1350\,\mathrm{K}$, which would require costly materials and extremely high demand for the delivery of heat. A reasonable limit should be attained just after the central point of the above presented diagrams, where the values of parameters represent available measures.

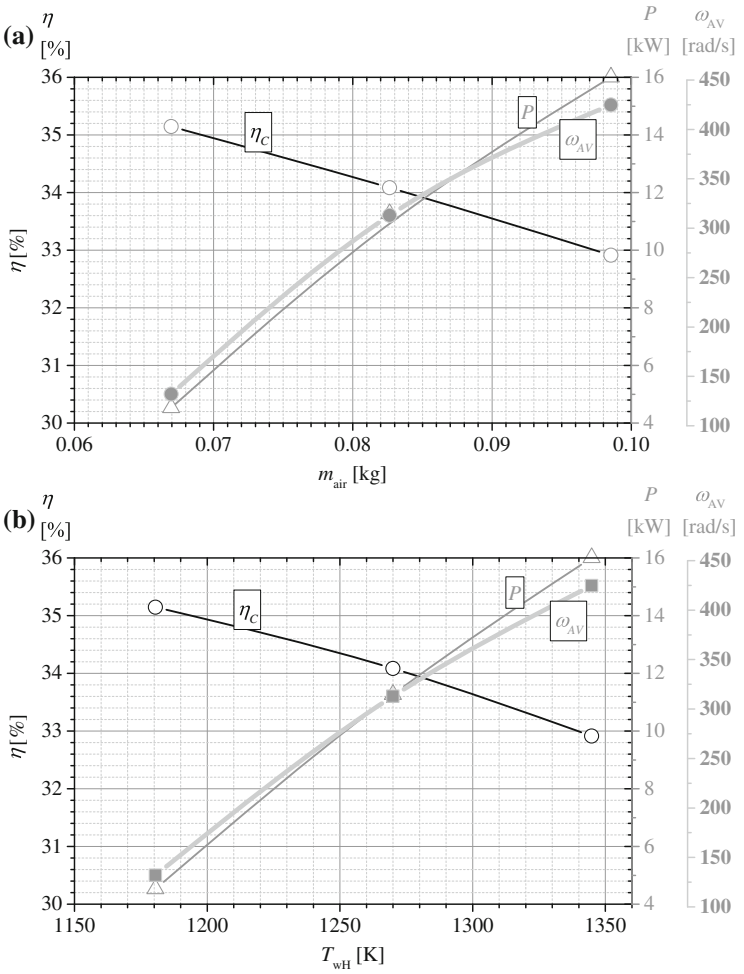

Fig. 7.14 Efficiency η_C, the power P and the angular velocity ω_{AV} as functions of the working fluid mass enclosed in the system (**a**) and the temperature of the heater wall—part (**b**), when both parameters change simultaneously

7.5 Remarks on this Model of the EHVE

In this chapter, a 4-stroke EHVE that operates according to the presented principle was investigated numerically with the method described in the previous chapter. Separate rotary valves 1 and 3 can be used (see Fig. 7.3) instead of the valve set 1–3 shown in Fig. 7.1. This alternation is introduced due to some manufacturing difficulties. A blower working in the heater space is employed in order to increase the heat exchange.

The conducted numerical simulations of the developed engine operation prove that it can deliver the internal power of approximately 50 kW/l for a single cylinder volume at the rotational speed of 3000 rpm and moderate heater temperature. For the obtained temperatures and the compression ratio of about 10, the internal efficiency can attain the level of almost 35 % without a pre-heater.

The dynamic behaviour of the 4-stroke EHVE discussed in Sects. 7.3 and 7.4 presents combined effects of thermodynamic and dynamic characteristics of the engine. Its driving torque is different than that for the 2-stroke version. The irregularity of runs depends on the inertia of the flywheel applied. An ability to control the rotational speed is achieved as for the 2-stroke version.

The 4-stroke variant of the engine is a very important case for the idea presented in the book. Assuming that the present disadvantages found in the design and manufacturing of valves 1 and 3 will be solved soon, the 4-stroke idea seems to be very promising. The additional devices such as a blower in the heater loop and the heater itself may use well-known technology (counter-current exchangers). The presence of a fluidized bed like the one in Fig. 7.1 allows for applying such a solution here. Hence, the proposed engine is considered to be a prospective solution in the field of externally heated valve air engines.

Reference

1. Ramzy A, Kadoli R (2015) Modified PGC model and its validation by experiments for heat and moisture transfer analysis in a vertical fluidized desiccant bed. Appl Therm Eng 81:83–91. doi:10.1016/j.applthermaleng.2015.02.018

Chapter 8
EHVE versus Stirling Engines – a Comparison

In this chapter, the version of the 2-stroke EHVE having two blowers applied in internal heat exchanger loops, described in detail in Chap. 5, is investigated and quantitative results of its performance are compared to chosen examples of Stirling engines. The related devices are well-known, still developed externally heated machines and continue to be subject to numerous current investigations [1–5]. The similarities shared with the EHVE are as follows

- external heating,
- high thermal efficiency,
- multi-fuel capability,
- low noise generation, and finally,
- low pollution when a combustion process is used as the heat source.

A very attractive common feature of the EHVE and Stirling engines is a broad range of possible heat sources. When a combustion process is used, burning can be optimized for a particular fuel. However, applicable heat sources are not limited to combustion processes only, but they can involve any type of externally supplied energy able to reach the temperature required for efficient work.

The numerical simulations of the EHVE operation are compared with the experimental results presented for the Stirling engines [1, 2], which were chosen from not a broad set of available reports on the subject. The representative example of fully described engine has a compact mechanical form and comparatively high power and efficiency at the total volume of 588 cm^3 enclosed in four double-action cylinders with four piston rods. It uses helium as the working fluid. The later presented test data for developed versions of the above mentioned Stirling engines [3–5], have analogous or even lower effectiveness at very close design parameters. An initial comparison of the early version of the EHVE and an example of the Stirling engine was already presented in our paper [6], but considering experience gathered during its evolution as shown in the previous chapters of the book, such evaluation has to be critically revised with a conclusion that the results presented were overevaluated. A more realistic and extended judgement is completed below.

Z. Kazimierski and J. Wojewoda, *Externally Heated Valve Engine*,
Springer Tracts in Mechanical Engineering, DOI 10.1007/978-3-319-28355-5_8

8.1 Some Aspects of the Design

The EHVE prototype and its laboratory investigations in their early form are presented in Chap. 3. The conclusion coming from the results obtained fully supported the concept. In the prototype, two electric heating devices were used as a source of energy delivered to the engine heaters. However, the amount of heat transferred from them to the working fluid during the period when the engine valves were closed and no internal flow existed was not sufficient. Therefore, in order to improve the heat exchange rate, two centrifugal blowers B_1 and B_2 were added to each of the heat exchangers. The power requirements for driving them are rather low but they should significantly enhance the heat exchange during the mentioned critical phase of the work cycle. It is assumed that the working fluid flow inside the exchangers is turbulent even when the engine valves are closed. The volumes of the exchangers are large, at least 3–5 times higher than the volumes of the cylinders. Both heat exchangers contain in their design volumes called collectors at their respective inlet and outlet ends. These volumes can play a role of settling chambers to equalize pressure and temperature values in the main part of the exchanger.

The EHVE version used for comparison purposes is a two-stroke engine which operates in a closed heat cycle. It is equipped with two cylinders of different role, as shown in Figs. 8.1 and 8.2 and the other main parts are two external heat exchangers. The phase angle between the expander and the compressor is equal to 180°. Its valves are equipped with a standard camshaft mechanism. Furthermore, the EHVE features a conventional oil lubrication system, which is extremely advantageous from the viewpoint of manufacturing as it is the same as in all typical internal combustion engines. An increase in performance due to possible multi-cylinder arrangement of the engine is to be expected [7].

Similarly to all other versions of the EHVE presented in the book, an important advantage of this configuration consists in the fact that the most easily available working fluid – atmospheric air – is employed. Reviewing the existing Stirling installations which use helium as the working fluid, much better performance is expected when such a fluid is used instead of air. Also, the EHVE can use any source of heat able to deliver appropriate temperature inside the heater, starting from solar energy, through combustion of other fuels, to the heat recovered from nuclear processes. This makes the EHVE a beneficial solution when available resources of presently accessible fuels like oil and gas run out. Moreover, due to the high temperature of the working fluid leaving the expander, an additional heat exchanger, i.e., a pre-heater, can be installed to improve the overall efficiency of the engine, as shown in Fig. 8.1 and Sect. 8.1. The design of the early version of the EHVE, described in Chap. 2, did not include such a device.

Due to different working principles of both compared types of engines, the pressure ratio p_{max}/p_{min} of the EHVE and the Stirling engines are obviously different. For the EHVE, this value is higher than 5, whereas for both Stirling engines, it is lower than 2. Thus, the comparisons cannot be conducted at equivalent minimal pressures. For the Stirling engines, the lowest applied pressures remain in the range from

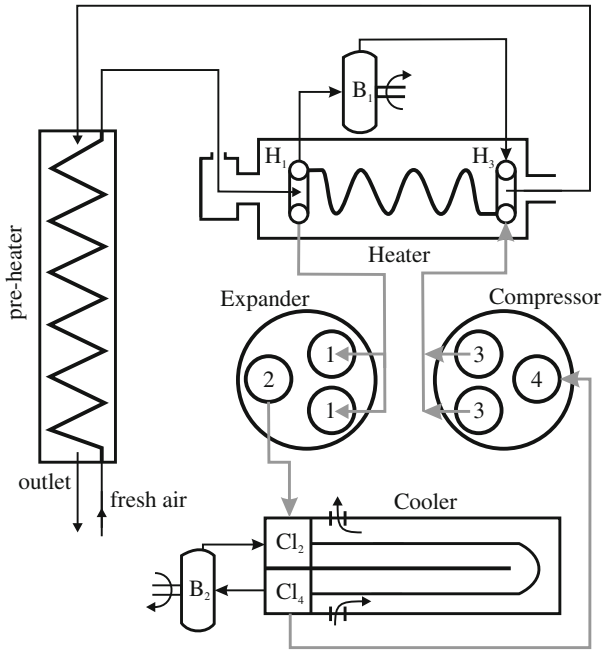

Fig. 8.1 Scheme of the transversal cross-section of the engine with two blowers B_1, and B_2. Other important elements are: *1*, *2*, *3*, *4* valves, H_1, H_3 heater collectors, Cl_2, Cl_4 cooler collectors

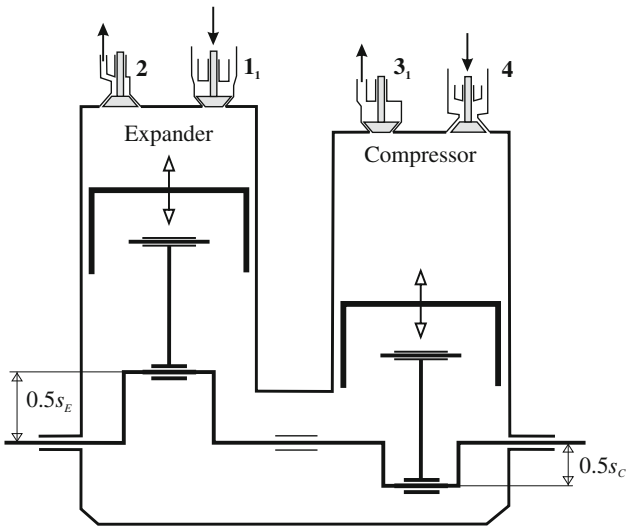

Fig. 8.2 Scheme of the longitudinal cross-section of the engine

60 to 110 bar. In the case of the EHVE, such minimal values would imply unrealistically high respective maximal pressures, which can be totally unacceptable from an engineering point of view. The new form of the proposed engine with blowers applied is therefore compared with the Stirling engines at the same maximal working pressures. A full description of the considered version of the EHVE is presented in Chap. 5.

8.2 Comparison of the EHVE and the AISIN Stirling Engines

In the numerical simulations of the EHVE model, a set of 19 non-linear ordinary differential equations with appropriate switching conditions for the internal flows between engine elements, together with a set of non-linear algebraic equations describing the behaviour of particular parts, was solved. Stationary, periodic solutions to the engine operation at a given, constant angular velocity of the engine are subject of further discussion. The custom written simulation program standard libraries of procedures and solvers, here the Runge-Kutta fourth-order method, was applied [8]. Every calculation started from identical initial conditions which determined an amount and parameters of the working fluid enclosed in the model and continued until the solution reached the state where the integrated values during a cycle of work differed by no more than 0.01 % from those obtained during the previous one. Such a state, related to a stable solution, which simply repeated the previous results, was usually reached after 150–250 cycles of simulated crankshaft rotations and the presented engine behaviour at the chosen rotational speed.

The calculations were performed for the cylinders which were not identical. The value of ratio of the cylinders volumes $V_C / V_E = 0.75$ results from a series of simulations where the mentioned ratio was a parameter and was found to be optimal in the case when a large heater was used, $V_H \approx 5\, V_E$, see [9]. The considered version of the EHVE has the same expander volume V_E as the Stirling engines presented in [1, 2], which are double-action systems. Other essential data representing dimensions in the volumes of both cylinders, different than those presented in Chap. 5, are shown in Tables 8.1 and 8.2. The data for heat exchangers are similar although not all of them are the same.

Table 8.1 Dimensions of the cylinders used for comparison

Cylinder	Diameter d (m)	Stroke s (m)	Dead height h_0 (m)	Volume V (m^3)
Expander	0.0900	0.0925	0.0025	0.604×10^{-3}
Compressor	0.0900	0.0694	0.0017	0.423×10^{-3}

Table 8.2 Dimensions of the heat exchangers

Exchanger	Diameter d (m)	Length l (m)	Number of pipes n (−)	Volume V (m^3)
Heater H	0.01	2.0	15	2.36×10^{-3}
Collector H_1				1.00×10^{-3}
Collector H_3				1.00×10^{-3}
Cooler Cl	0.01	2.0	15	2.36×10^{-3}
Collector Cl_2				1.00×10^{-3}
Collector Cl_4				1.00×10^{-3}

The value of the pressure step Δp_{H3} forced by a blower depends on the structure of the collectors and the heat exchangers. Here, all those values are fixed at 10 kPa assuming the blowers are not to consume too much of the generated power in the engine. The mass flow rates of the blowers are for the same reason estimated as $\dot{m}_{Bi} = 0.1$ and 0.2 kg/s. Other important blower parameters are the input to output pressure ratio $\Pi_{Bi} = 1.01$ and the efficiency $\eta_{Bi} = 0.7$.

The amount of work lost due to friction during the cycle derived and adapted from [10–12] is estimated to be equal to

$$L_f = 40 + 0.8\frac{\omega}{2\pi}.$$

The power consumed by all auxiliary devices, L_{sup}, supplied by an electric motor rotating at 3000 rpm, independently of the EHVE rotations, is also included in modelling. All the above losses translate to the power consumption assumed as a value of 1000 W.

In order to reflect real conditions like in the Stirling installations under comparison, we suppose that the source of external heat is able to make the temperature of the heater walls T_{wH} increase with the engine rotational speed n_{EHVE} in the range from 752 to 1220 K related to the amount of heat delivered. For the data, see Table 8.3. This temperature values are to create similar conditions to those included in [1, 2] for the Stirling engines. The minimal temperature of the cooler wall is assumed constant and equal to $T_{wCl} = 298$ K on the basis of standard parameters of the cooling water supply and the data shown in [1, 2]. The coefficients of heat conduction, dynamic viscosity and specific heats for the working fluid are taken from tables of physical properties of air. Finally, selected rotational speeds from 500 to 2000 rpm were set

Table 8.3 Heater wall maximal temperature in the comparison process as a function of the model rotational speed

n_{EHVE}	(rpm)	500	1000	1500	2000
T_{wH}	(K)	752	1000	1200	1220

The mean temperature of the wall is the same for all compared engines and equal to 1043 K

as parameters for the simulation program to fully reconstruct the available data for the compared Stirling engines.

Let us start the discussion of the results obtained for the model of the EHVE from two diagrams characterising its capabilities in Figs. 8.3 and 8.4. Figure 8.3 shows pressures in both cylinders as functions of their respective volumes. One can interpret a difference in the area enclosed by the $p - V$ curves as the useful work of the engine. Figure 8.4 presents the temperature versus entropy diagram $T - s$ for the EHVE operation cycle. The heat cycle shown is a new type of the heat exchange cycle, similar to the Joule one.

A pre-heater reduces evidently the energy requirements of the heater. All details presented for the Stirling engine in [1], earlier than [2], and even the pre-heater described, are different when compared to [1]. Comparing with older results presented in [2], they are improved, with efficiency values about 6 % higher than those quoted in [1]. Therefore, it was assumed that the amounts of heat profits were $Q_{H-PH} = 0.80\, Q_H$ for [2] and $Q_{H-PH} = 0.85\, Q_H$ for [1]. These suppositions are rather modest and can be met easily in real devices. Thus, the calculated efficiency of the EHVE is obviously higher than without a pre-heater and the results with superimposed data for the Stirling engines are presented in Figs. 8.5, 8.6 and 8.7. It should be underlined that all Stirling engines employ pre-heaters [1, 2].

The comparisons presented in the above-mentioned figures show the effects of simulations of the EHVE working with air versus the experimental results of the helium Stirling engines for the same engine parameters as far as volume, rotational speed and maximal cycle pressures are concerned. Those pressures reported as 102, 140 and 190 bar can be easily available for the EHVE.

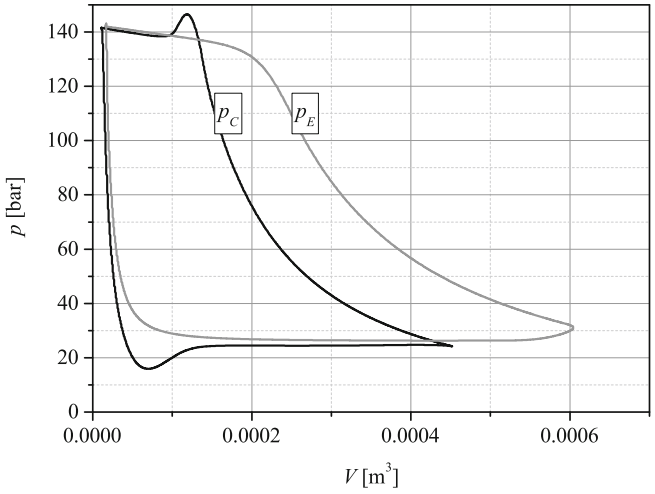

Fig. 8.3 $p - V$ diagram for the EHVE at 1500 rpm, $p_{max} = 140$ bar and $\dot{m}_{Bi} = 0.1$ kg/s. Data in Sect. 8.2

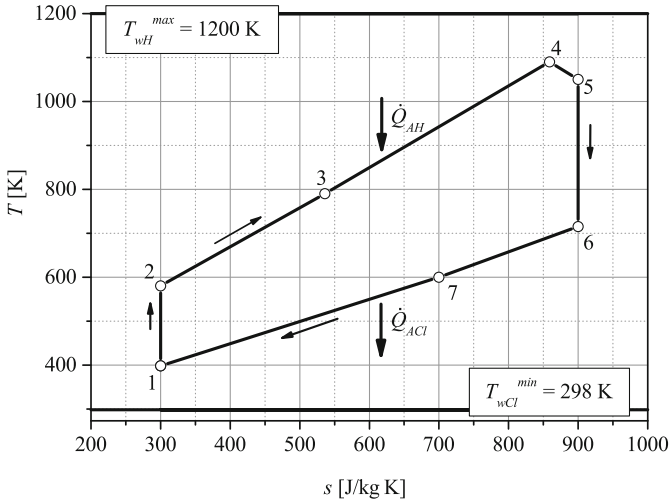

Fig. 8.4 Approximate $T - s$ diagram for the EHVE at 1500 rpm, $p_{max} = 140$ bar and $\dot{m}_{Bi} = 0.1$ kg/s. *1–2* isentropic compression inside the closed C volume, *2–3* compression by C, heating by H and mixing in the collector H_3 by the blower B_1, *3–4* heating inside the H volume, *4–5* expansion in E with heating at opened valve 1 until its closing, *5–6* isentropic expansion inside the closed E volume, *6–7* flow to the collector Cl_2, expansion and mixing with the collector Cl_2 by the blower B_2, *7–1* cooling inside the Cl volume

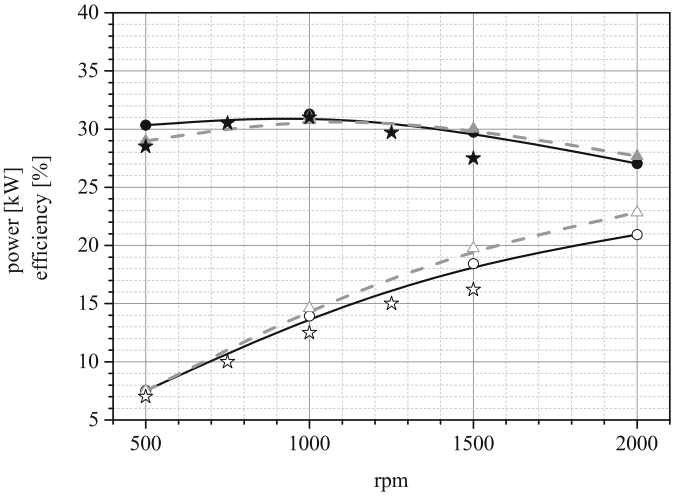

Fig. 8.5 Comparison of the EHVE and AISIN Stirling engines at the maximal working pressure $p_{max} = 102$ bar. Power values are presented with empty markers and efficiency with the filled ones. *Circles* on *solid lines* represent the EHVE with its blowers working at $\dot{m}_{Bi} = 0.1$ kg/s, *top-triangles* in *grey*, *dashed line* with blowers at $\dot{m}_{Bi} = 0.2$ kg/s, whereas *star symbols* stand for the AISIN engine [2]

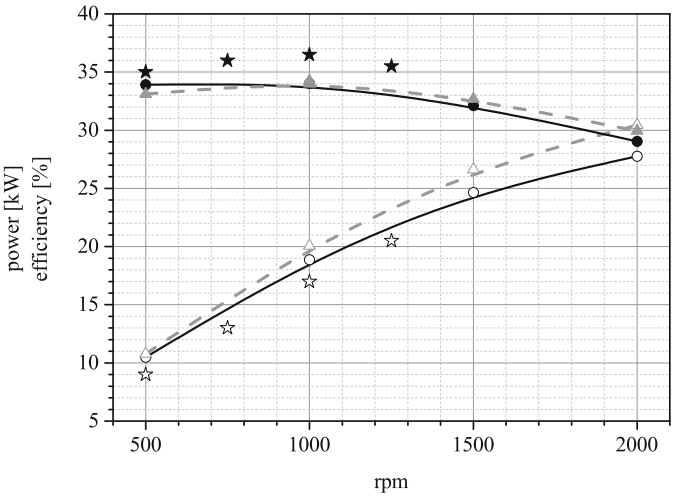

Fig. 8.6 Comparison of the EHVE and the AISIN Stirling engines at the maximal working pressure $p_{max} = 140$ bar. Power values are presented with empty markers and efficiency with the filled ones. *Circles* on *solid lines* represent the EHVE with its blowers working at $\dot{m}_{Bi} = 0.1$ kg/s, *top-triangles* in *grey*, *dashed line* with blowers at $\dot{m}_{Bi} = 0.2$ kg/s, whereas *star symbols* stand for the AISIN engine [1]

As has been concluded from earlier considerations in the previous chapters, the blowers B_1 and B_2 are necessary for the EHVE to operate efficiently. Their flow rates are assumed on an average level of $\dot{m}_{Bi} = 0.1$ kg/s. A further increase in the blower flow rate appears to be not practical, see Figs. 8.5, 8.6 and 8.7, due to an increase in the power consumed by the blowers and a relatively low increase of the engine performance. The results also show that the EHVE can deliver almost the same amount of power as the equivalent helium Stirling engine for all values of maximal pressures with blowers working at the mass flow rate of only $\dot{m}_{Bi} = 0.1$ kg/s, but using air as the working fluid.

The examination of the efficiency levels of both the engines needs more discussion. The maximal efficiency of the Stirling type engine shows a distinct peak at 1000 rpm, whereas the efficiency plot for the EHVE is flatter. In Fig. 8.5, where heat exchangers of basic type of pre-heaters in the case of Stirling engines are very similar, the EHVE presents very close performance. In Figs. 8.6 and 8.7, where heat exchangers in the Stirling engine are improved, the EHVE efficiency remains equal as well.

We have to mention some disadvantages that result from the presence of valves in the design of the EHVE:

- rather short time of opening/closing phases of valve 1 and 3 actions while connecting the cylinders and the heat exchangers, which is reflected by the following values $\Delta\alpha_1 = 90°$ and $\Delta\alpha_3 = 80°$;
- the blower B_1 has to work under extreme conditions of temperature and pressure, see Fig. 5.1. Similar applications can be found in turbo-charging systems of internal

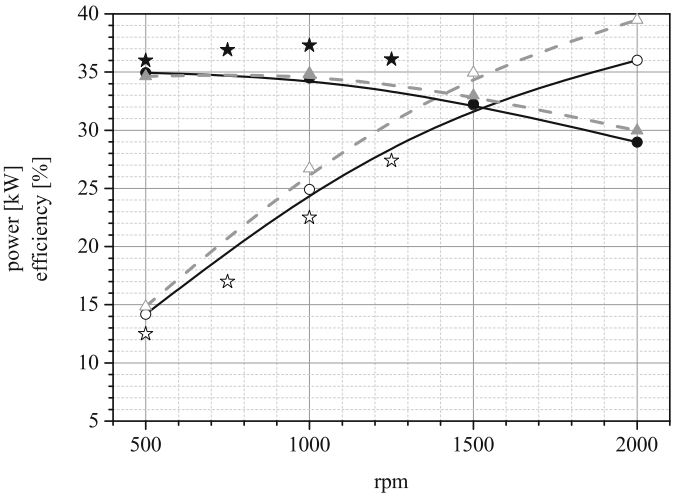

Fig. 8.7 Comparison of the EHVE and the AISIN Stirling engines at the maximal working pressure $p_{max} = 190$ bar. Power values are presented with empty markers and efficiency with the filled ones. *Circles* on *solid lines* represent the EHVE with its blowers working at $\dot{m}_{Bi} = 0.1$ kg/s, *top-triangles* in *grey*, *dashed line* with blowers at $\dot{m}_{Bi} = 0.2$ kg/s, whereas *star symbols* stand for the AISIN engine

combustion engines and we hope that such a solution can be adopted in the EHVE as well.

A quick action of the valve system remains a challenging but solvable engineering problem. In the light of the above-mentioned circumstances, it may be worth taking into account an application of rotary valves. Other solutions related to the valve timing are still in progress [13], automotive designs are promising due to new technologies applied. The heater, whose design is not discussed here in detail, creates also an engineering challenge. High working pressure and temperature are the demanding conditions which have to be carefully considered during its construction. Continuous improvements in heat exchangers used in the Stirling engines allow us to expect they can be easily applied and improve the heat exchange in the EHVE.

8.3 Remarks on the Results of the Comparison

The choice of maximal cycle pressures made the comparison of two ideas of externally heated engines the only reasonable procedure. The same physical properties as engine capacities, heater wall temperatures and working frequencies were assumed. Significant differences in pressure ratios p_{max}/p_{min} of the compared engines (i.e., 5:2) have their reasons in the presence of valves and different values of dead space. In the Stirling engine, there are no valves and dead space is large, totally opposite to the EHVE.

The proposed engine can reach almost the same level of generated power as the Stirling engines under comparison. It is worth repeating that the most important advantage of the new idea is the fact that these results are possible to obtain using working fluid being simply atmospheric air. The EHVE entails also less complicated manufacturing technology, well known and widely used for internal combustion engines. Owing to modern manufacturing solutions, already applied to the mass production of piston engines, it will be possible to build an efficiently working EHVE.

A lack of valves is an important favour of the Stirling engine, nevertheless the advantages of the EHVE are numerous, namely:

- the working fluid is air, whereas Stirling engines have to use helium to attain comparable performance values;
- the EHVE uses a simple, well developed crankshaft system widely applied in most modern internal combustion engines;
- the EHVE does not need any heat regenerator which usually is an additional heat exchanger, an essential part of any Stirling engine. This way, the heat exchange is simpler;
- due to the fact that a regenerator, usually manufactured of steel wires, is needed, the EHVE can be lubricated with the same, well known oil lubrication system as normally used in internal combustion engines.

The maximal pressures applied to the EHVE are in ranges normally used in Stirling installations. We want to point out that the sealing system in the EHVE can be similar to those used in modern internal combustion engines which sometimes work at higher absolute pressures. The above statements allow us to expect that the proposed engine can perform even better at higher values of pressures. The comparison under typical conditions shows the conformity of power and efficiency for the air EHVE and helium Stirling engines.

References

1. Nogawa M et al (1987) Development of NS30A Stirling engine. SAE Technical Paper, Series 879155
2. Watanabe T et al. (1988) NS30A Stirling engine for heat pump use. In: The 4th International Conference on Stirling Engines, Tokyo
3. Iwamoto S, Hirata K, Toda F (2001) Performance of Stirling engines, JSME Int J Ser B 44(1):140–147. https://www.nmri.go.jp/eng/khirata/list/ecoboy/jsmepaper_eng2001.pdf
4. Biedermann B, Carlsen H, Schoch M, Obernberger I (2003) Operating experiences with a small-scale CHP pilot plant based on a 35 kW(EL) hermetic four cylinder Stirling engine for biomass fuel. In: Proceedings of the 11th International Stirling Engine Conference (ISEC), Rome
5. Çinar C, Karabulut H (2005) Manufacturing and testing of a gamma type stirling engine. Renew Energy 30(1):57–66. doi:10.1016/j.renene.2004.04.007
6. Brzeski, L, Kazimierski, Z (1996) A new concept of externally heated engine—comparisons with the Stirling engine. Proc Inst Mech Eng Part A J Power Energy 210(51):363–371. doi:10.1243/PIME_PROC_1996_210_060_02

7. Hirata K, Kawada M (2005) Development of a multi-cylinder Stirling engine. In: Proceedings of 12th International Stirling Engine Conference, (September 2005), pp. 315–324
8. Press WH (2007) Numerical recipes: the art of scientific computing. Cambridge University Press, Cambridge
9. Kazimierski, Z, Wojewoda, J (2008) Numerical optimization of externally heated valve air engine with blowers. In: Proceedings of the SYMKOM 2008, Turbomachinery, 133:157–164
10. Heywood JB (1988) Internal combustion engine fundamentals. McGraw Hill, New York
11. Ciulli E (1992) A review of internal combustion engine losses part 1: specific studies on the motion of pistons. Valves Bear Proc Inst Mech Eng Part D J Automob Eng 206(44):223–236. doi:10.1243/PIME_PROC_1992_206_183_02
12. Ciulli E (1993) A review of internal combustion engine losses part 2: studies for global evaluations proceedings of the institution of mechanical engineers, part D: J Automob Eng 207(34):229–240. doi:10.1243/PIME_PROC_1993_207_184_02
13. Holt DJ (ed) (2003) Design of racing and high performance engines 1998–2003. SEA Publication, Warrendale (Pa)

Conclusion

One of the most important factors indicating the technological progress in every civilization is an amount of energy consumed by its members. Different kinds of energy are needed, from heat through electrical to nuclear, including mechanical, which still remains extremely important among them. This kind of energy is presently generated mostly by heat engines. They need fuels to run. Nowadays, the most important and widely used are mineral fuels, i.e., oil and gas. Resources of them are large although limited and continuously diminishing until one day they disappear. What then will become a source of heat needed for running combustion engines? We can exploit some other resources, like solar energy, heat regained from cooling systems of nuclear reactors, wastes collected in many places in vast quantities can be burnt, etc. Bio-fuels coming from plants can be applied as well.

Nowadays, all piston heat engines are intended to provide mechanical energy in a limited and local amount. There are many mobile applications employed to drive different vehicles on land (cars or trucks), at sea (ships of different size) or in air (small aeroplanes). They are also used as stationary devices producing energy to drive other machines performing different useful jobs or just as generators delivering electrical energy.

Definitively, almost all of the above listed tasks are fulfilled by internal combustion engines utilizing derivatives of oil and gas and burning these fuels under variable combustion conditions involving sophisticated continuous control systems. They strongly depend on availability of the fuel and each design is very limited as far as use of any alternative fuel is concerned. The limitation of energy resources can spell an end of the majority of such engines.

External heating creates a chance for another way of development in piston engines with an advantage of combustion process being stable and having optimal parameters. This can result in less pollution from exhaust gases, including zero value in the case of delivering energy different than burning of fuels. The EHVE is also an alternative for existing externally heated engines like the Stirling ones, mostly due to much simpler technology and use of a cheaper working fluid. Potentially lower manufacturing and running costs may become a decisive factor sooner rather than later.

Z. Kazimierski and J. Wojewoda, *Externally Heated Valve Engine*,
Springer Tracts in Mechanical Engineering, DOI 10.1007/978-3-319-28355-5

The book discusses some ideas for further analysis of externally heated engines and presents their main advantages, namely:

- the working fluid is cheap air, not expensive helium, whereas a level of power and efficiency is comparable to Stirling engines;
- the EHVE uses well-known technology of the conventional crankshaft and piston system met in most modern internal combustion engines;
- no heat regenerator is needed, which also enables standard lubrication as in all IC engines.

Chapter 2 of the book presents an early solution of the EHVE with the computational algorithm and the thermodynamic cycle obtained at that stage. The solution covered a long period of the engine cycle operation, at which simple isochoric heating took place. The amount of heat delivered during such a period appeared to be insufficient for effective work of the engine prototype, which is documented in Chap. 3 In order to solve the problem, some additional devices increasing velocity of the working fluid inside the heat exchanger tubes, which, in consequence, increased the level of heat exchange, are proposed in Chap. 4. Another approach is discussed in [1] together with the most important results obtained. Such a solution can be applied only to the early version of the EHVE. The results of all numerical simulations are based on the algorithm presented in Chap. 2, where the heat transfer coefficient α_A can be iteratively calculated on the assumption of uninterrupted work of the EHVE.

A totally different method is presented in Chap. 5. Blowers were applied to achieve a high flow velocity of the fluid inside the heat exchangers in both heat exchange circuits, the heater and the cooler, respectively. A single, large heat exchanger was applied with additional collectors, whose volumes were included in the simulations. Such a design was simulated and solved numerically in the closed heat cycle of the working fluid – the atmospheric air – under non-stationary conditions of the EHVE.

All the modelling processes supported by methods developed in Chap. 5 have to include the collectors in the heat exchange design. They should have such a construction which does not allow any interfering of their continuous, stationary internal flows forced by the blowers with those in the main circuit of the engine having interrupted behaviour caused by the valves. This is presented as an idea here and entails a demanding engineering task.

The engine described in Chap. 5 is a two-stroke EHVE. The solution still needs experimental verification, which has not been performed yet due to high costs and a lack of financial support. A set of devices added in Chap. 5, which is assumed to work in order to stabilize the flows in the heat exchangers, can be treated as stationary. Settling chambers typically fulfilling such tasks were applied. The results of the numerical simulations performed in such a case comply with the earlier solution for non-stationary, averaged parameters. The results presented in Chap. 6 led also to a conclusion on a possibility of removing the blowers introduced in the development stage of the EHVE shown in Chap. 5

A four-stroke version of the EHVE is described in Chap. 7. The calculation method presented in Chap. 5 is used again but with some improvements. The fast acting valves, which make the cylinder and the heater contact, are controlled in such a way

that they equalize quickly the pressure in contacting volumes, without overshooting, typically observed for slow valves. Here, the classically designed valves of short opening time can be replaced with another solution, e.g., a rotary type valve or any other, on the basis of the suggestions presented in the book. The model, at 3000 rpm, reaches the internal power level of 50 kW/l at the efficiency of about 35 % without any pre-heater. These results yield a possibility for the 4-stroke version of the EHVE to be a working solution in the near future. If a pre-heater is applied, the internal efficiency grows even up to 41 %.

The next advantage of the four-stroke version of the engine is such that it uses only one cylinder to attain a full thermodynamic cycle of operation. This point has its equivalent, as recalled in the book many times, with internal combustion engines which operate according to the same rule. And, following this relation, benefits of the same scale can be expected in multi-cylinder arrangements in real installations.

Chapters 2 and 4 show the early versions of the EHVE in which heat is delivered from relatively small heat exchangers, $V_H < V_E$. The results achieved prove that heat is delivered at a constant volume. Different attempts are presented in Chaps. 7, 5 and 6, where heaters are much greater and $V_H > V_E$ are not less than 2. In these cases, heat is delivered to the engine at a constant pressure, which constitutes the essential alternation to the EHVE design.

Finally, in Chap. 8, a comparison to the data from the existing Stirling engines is presented. The data came from the experiments and those for the EHVE are from the simulations corrected with real factors lowering the performance. The comparison shows that a similar level of power and efficiency can be reached in the EHVE with air as the working fluid as in the Stirling engine using helium. This is a huge potential advantage of the design. Being based on the well-known technology, it provides a bridge to new applications of piston engines generating mechanical energy from different sources of heat.

The dynamic behaviour with attachments to the driving shaft having inertial properties of both 2- and 4-stroke versions were investigated. It has been shown for large flywheel applied the dynamic properties do not influence the thermodynamic behaviour. When the flywheel is smaller, the thermodynamic behaviour fully reflects changes in rotation speed of the simulated model.

Such engines could be installed close to oil plants used to produce bio-fuels or any other places where such bio-fuels are easily available. Due to the fact that for these fuels, external combustion can take place under optimal conditions, which are not possible to attain in internal combustion, the level of pollution generated in the burning process can be significantly lower. Generally, the EHVE can mechanically drive an electric generator which transmits energy to where it is necessary.

The EHVE can employ solar heat – ships or yachts of the future may be propelled by winds driving electronically controlled new-generation sails and if they fail in the case there is no wind, intensive sun heat can be used to generate mechanical energy to drive a propeller or an electric generator. The described EHVE is then the only

source of mechanical energy on board. During the night, such ships can use batteries charged by the EHVE during the time when the wind blows. Also, the EHVE can use the heat produced by cooling systems of nuclear plants, therefore it can be installed on stationary basis or on submarines as well.

Reference

1. Kazimierski Z, Wojewoda J (2011) Externally heated valve air engine with two small heaters operating alternatively. In: Proceedings of the SYMKOM 2011, Turbomachinery, vol 140, pp 105–114

Author Index

Z. Kazimierski and J. Wojewoda, *Externally Heated Valve Engine*,
Springer Tracts in Mechanical Engineering, DOI 10.1007/978-3-319-28355-5